

PPM

Bi-Annual Report

2017 & 2018

The Bi-Annual Report for the PPM Research Centre

DEPARTMENT OF GEOLOGY

UNIVERSITY OF JOHANNESBURG



The Bi-annual Report of the PPM Research Centre for the two years 2017 and 2018, compiled by Jan Kramers. Layout and design by UJ Graphic Studio

Special thanks/Acknowledgements

We wish to extend a special word of thanks to all our corporate and governmental financial and logistical supporters (in alphabetical order):

African Rainbow Minerals
Anglo American
Anglo Coal
Anglo Gold Ashanti
Anglo Platinum
Anglo Research
Assmang
Assore
Coaltech
Council of Geoscience
Cradle of Humankind Trust of Gauteng
De Beers Consolidated Mines
Department of Science and Technology (DST)
Deutsche Akademische Austauschdienst (DAAD)
Golder Associates
Impala Platinum
Kumba Iron Ore
Lonmin
National Research Foundation (NRF)
Nkomati Joint Venture
Rand Uranium (Gold One)
Sibanye Stillwater
South 32
Two Rivers Platinum Mine
Vale
Vedanta Resources

Please direct all enquiries and proposals for research to:

Dr Bertus Smith, Prof. Jan Kramers or Prof. Fanus Viljoen or
PPM, Department of Geology
University of Johannesburg
Auckland Park Kingsway Campus
PO Box 524, Auckland Park 2006
Johannesburg, South Africa
E-mail: bertuss@uj.ac.za, jkramers@uj.ac.za or fanusv@uj.ac.za
Tel: +27(0)11 559 4701
Fax: +27(0)11 559 4702

Cover photo: Product being poured at the ferrochrome smelter near Machadodorp. Photo B. Cairncross

Header photo: The landscape at Aggeneys, Northern Cape. Photo: Trishya Owen-Smith

Footer photo: Stalagmite Phalanx at Cango Caves. Photo: Trishya Owen-Smith Both footer and header photos were taken on the Honours field trip, September 2018.

INTRODUCTION

The present report on activities of the Palaeoproterozoic Mineralization (PPM) research Centre of the UJ Geology Department differs from the norm, in that it covers two years: 2017 and 2018. This does not reflect a lessened activity over these two years than before, nor is it the new norm: it is a once-off anomaly resulting from budgetary constraints in 2018, caused by unexpected salary obligations. In contrast, the move of the PPM colloquium to early in the year is hoped to be a lasting change, which will also show the PPM Centre as a separate (although peacefully coexisting) entity from the interuniversity Centre of Excellence for Integrated Mineral and Energy Resource Analysis (CIMERA), and better demonstrate the diversification of PPM. The years reported on here are the first two of the current funding cycle of Research Centres at UJ. In the current year, 2019, the UJ Research Centres will be again reviewed. Also, during this year, Jan Kramers will stand down as Director of PPM and Dr Bertus Smith will take on this responsibility.

While in the previous review process (2016) the continuation of the PPM Centre for 2017-2019 was 'highly recommended', one criticism was that (while the number of graduate students in the Centre was high) the rate at which they completed their projects and graduated was sluggish. We can now report that in 2017, eight MSc and four PhD candidates graduated, and in 2018, five MSc candidates. Overall the trend is upwards. It must be

noted that PPM has a relatively large percentage of part-time MSc and PhD candidates. It is important to continue offering this opportunity to graduates that are employed, and it is further an attractive option for the University, as no bursaries need to be sought. However, completing an MSc and particularly a PhD project on a part-time basis is a daunting challenge. Some part-time students have been promoted, even to director level, in the organizations where they work and this comes with a greater responsibility and work load. In such cases it is the duty of supervisors within PPM to make sure that these candidates do not become the victims of their own success, in terms of graduating, and it has been good to see that the Faculty and University academic instances have shown understanding.

PPM's multidisciplinary diversification of research, initiated in 2014 and 2015 to coexist optimally with the CIMERA Centre of Excellence (as a University Research Centre, PPM has inherently more freedom of movement in its scientific endeavours than an NRF-funded one), has five main focus clusters (see Organigram): (i) the core discipline of ore deposit geology (now combined with coal and hydrocarbon geology), (ii) geometallurgy and kimberlite research, (iii) Precambrian environments, Geochronology and Tectonics, (iv) Palaeomagnetism and Sediment Provenance, and (v) Subrecent, Environmental and Medical Geology. For 2017, 55

refereed journal publications and book chapters and 54 conference presentations in the ambit of PPM were counted. For 2018, the numbers are 68 (of which 3 in the 'Nature' stable) and 89, respectively.

The fields of Economic Geology and Geometallurgy remain a strong research focus, now shared with and clearly strengthened by CIMERA as well as the SARChI Chair in Geometallurgy. In 2018 this Chair was extended for a further five-year period, and upgraded to Tier one, with Prof. Fanus Viljoen being confirmed as the incumbent. Meanwhile CIMERA has been reviewed in 2018 and is set to continue for another five years. The basis for continued Economic Geology and Geometallurgy research can thus be considered very stable. Further, due to Prof. Sebastian Tappe joining UJ, a strong component of kimberlite and related deep mantle research has been added. The projects and cooperations, both nationally and internationally, are too numerous to list in this introduction and an impression can be gleaned from the section "selected Research Projects and Progress" and the publications lists.

Internationalization within Africa itself has a number of facets. In 2017, three junior Staff members of the University of Ghana registered at UJ for the PhD programme, with research projects centered on Ghanaian geology. In 2016, PPM had specifically endorsed their applications for TWAS-NRF PhD bursaries with placement at UJ. Accordingly, the Centre supplied them with research





infrastructure (such as computers) and supported their analytical work at SPECTRUM. To a large extent, their field work and that of their supervisors was also funded through PPM. The progress of their research is sketched out in the section 'Selected Research Projects and Progress'. Generally, the number of graduate students from other African countries is increasing, and this is particularly visible in Coal Petrology and Medical Geology.

The establishment of coal petrography as a research focus has become consolidated within PPM in the reporting years, as shown by the large number of graduate students in this subject (see organigram and listing of graduate students). Dr Ofentse Marvin Moroeng, previously an Assistant Lecturer, has been appointed as a Lecturer following the completion of his PhD degree, thus greatly strengthening the subject at UJ: since Prof. Wagner has been appointed as the new Director of CIMERA, with new strategic and administrative duties, it is fortunate that there is a second-in-command in this discipline. The demand for the coal petrographic facility has continued in 2017 and 2018. The specialized coal petrographic microscope, originally purchased with substantial PPM support, continues to be used on a daily basis by UJ staff and students, as well as by (and on behalf of) external postgraduates. The latter are from Wits (Geology and Mining), University of Limpopo, Botswana International University of Science and Technology, North-west

University, University of Fort Hare, and the Council for Geosciences. The study under CIMERA's KAREN project of samples of Karoo shales with gas potential continued in the project years. So did the participation in the international ERA-MIN consortium project on "Charphite".

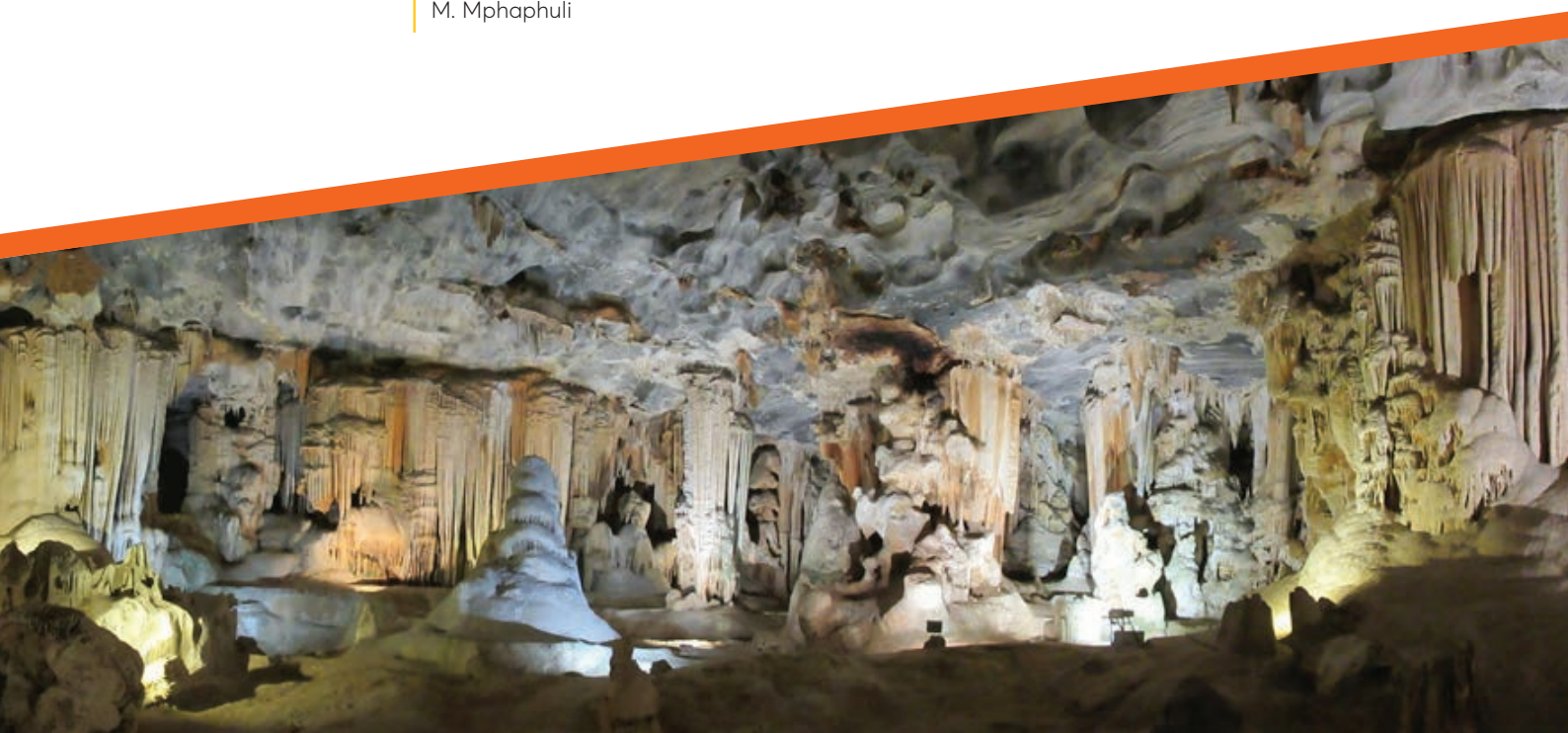
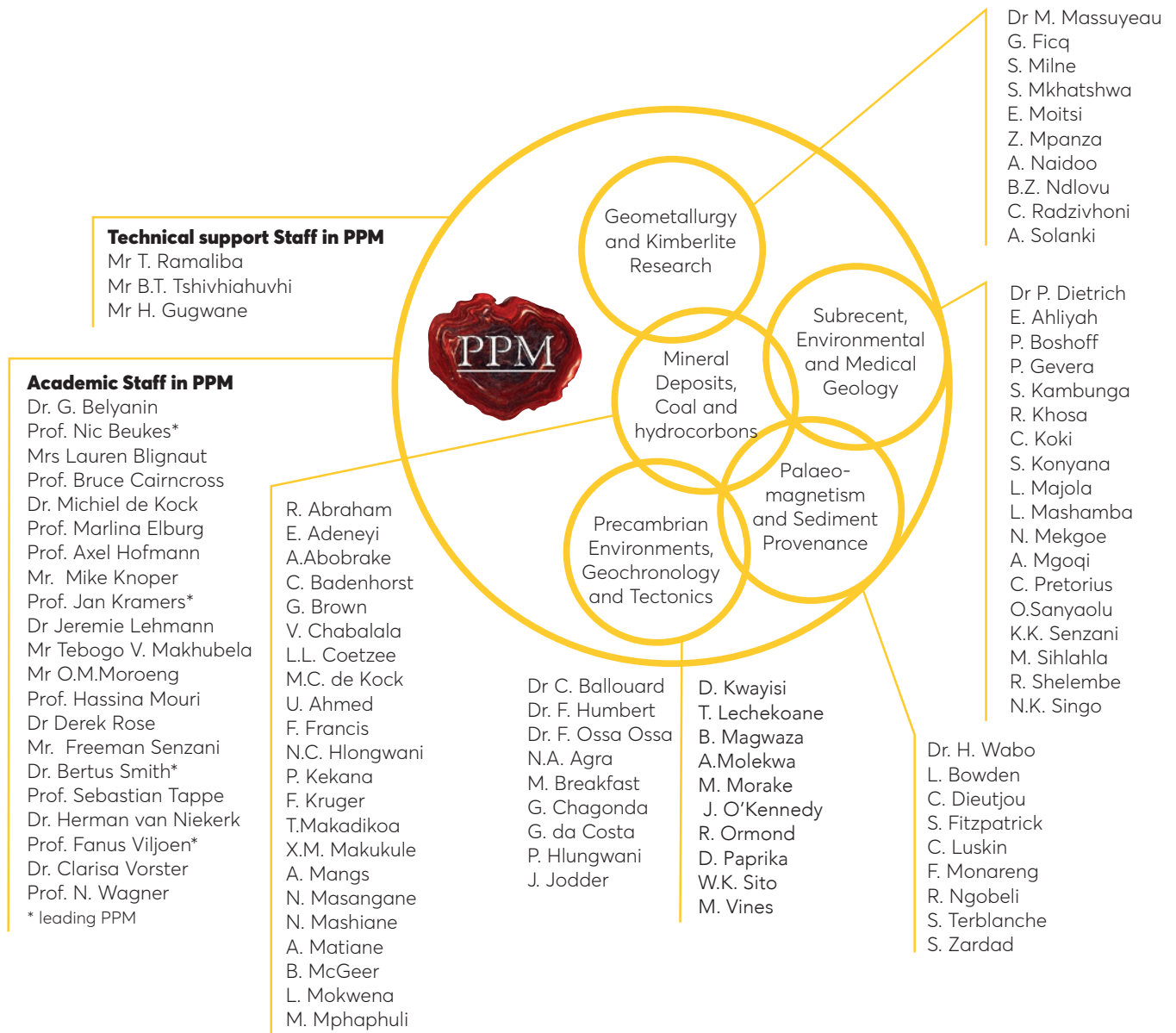
The Medical Geology research group headed by Prof. Hassina Mouri comprised 8 Msc and 2 PhD students through 2017 and 2018. A major event in 2018 was their participation in the European Geosciences Union conference held in Vienna from April 8 to 13, with nine mainly poster presentations (see the collection of abstracts in the Selected Research Projects and Progress). Among these projects, two involve cooperation with Kenya, and one each with Ghana, Namibia and Nigeria. Further, three of the projects are carried out with the Department of Applied Chemistry at UJ. Thus the Medical Geology initiative highlights both internationalization within Africa, and interdisciplinary research.

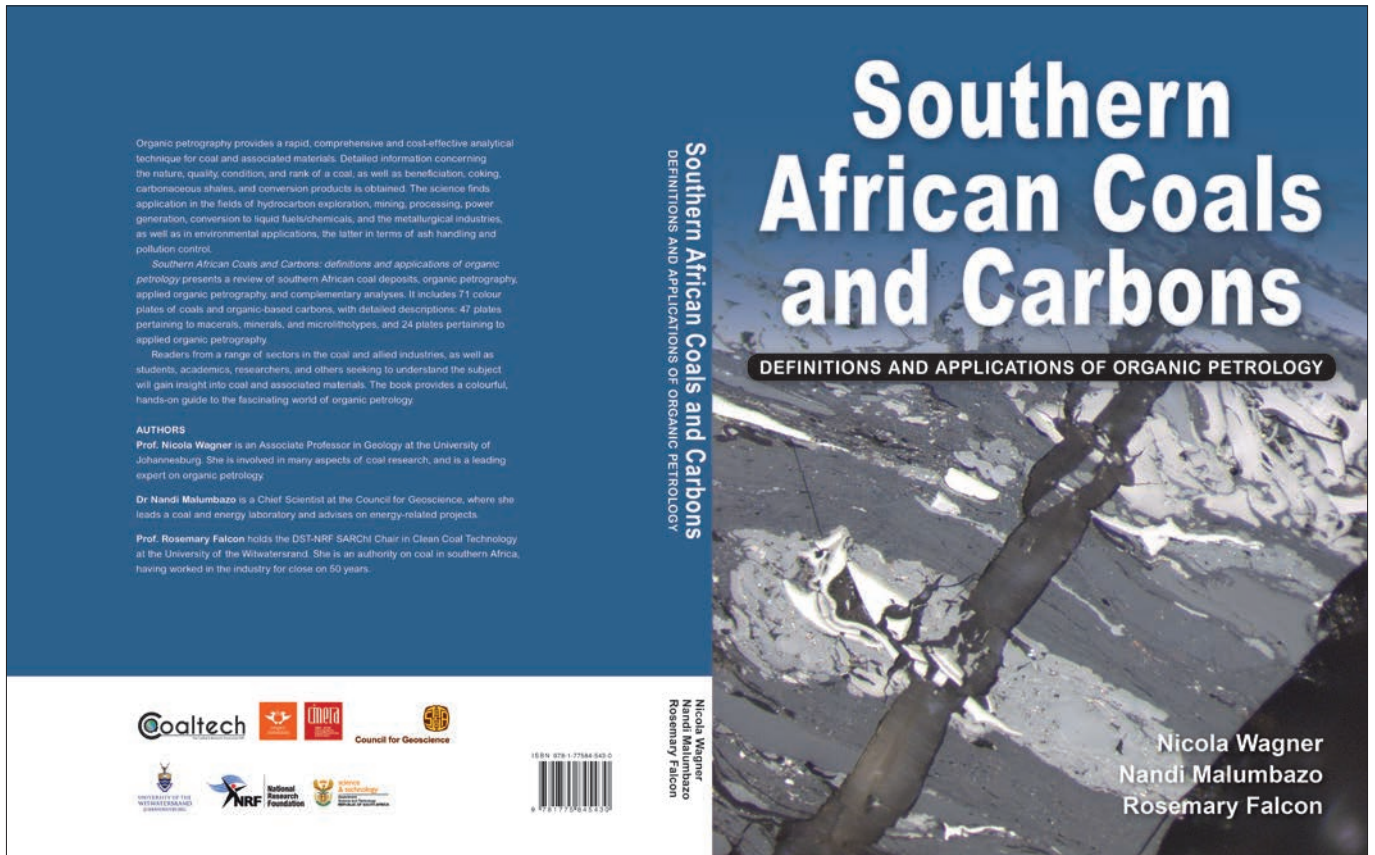
Research on cave deposits related to hominin evolution has involved cooperation with Profs. Lee Berger and his research group at Wits, Prof. John Hawks of the University of Wisconsin, USA as well as research groups in Australia, coordinated by Prof. Paul Dirks of James Cook University, Townsville, Queensland. This has led to co-authorship of PPM members in two important papers in eLIFE on the age of Homo naledi (Dirks et al. 2017) and the discovery of a second H. naledi site in the Rising Star cave (Hawks

et al., 2017); see publications list. In another development, cooperation with physicists Dr Stephan Woodborne, Dr Stephan Winkler and Dr Vela Mbele at iThemba Labs Johannesburg has led to the first analytical work on cosmogenic nuclides ^{10}Be and ^{26}Al to determine erosion rates and surface exposure ages, to be carried out on the African continent, which is a breakthrough in the study of landscape evolution in South Africa. In a related development, PPM together with the Centre for Anthropological Studies (CfAR) in the Faculty of Humanities, Prof. Shahed Nalla of the Faculty of Health Sciences and participants from the Faculty of Engineering, have worked towards an interfaculty Institute of Palaeo-Science at UJ, which was approved by the UJ Senate in 2018.

Last but not least, early in 2018 PPM members published a detailed petrographic study of the diamond-bearing extraterrestrial stone named "Hypatia", which showed that the parent body of this carbonaceous, silicate-free object had never been significantly heated before its encounter with the Earth, probably originated outside the orbit of Jupiter or possibly even Neptune, and should ultimately provide information on the chemistry of interstellar clouds (Belyanin et al. in the 2018 list). Thanks to Ms Therese van Wyk of the UJ strategic partnerships unit, this research reached an audience of at least 20 million people worldwide.

ORGANIGRAM OF THE PPM RESEARCH CENTRE 2017-18





The book *Southern African Coals and Carbons: Definitions and Applications of Organic Petrology* by Nicola Wagner, Nandi Malumbazo and Rosemary Falcon was launched in August 2018.

This is an impressive and highly useful compendium of petrology not only of coal in the strictest sense, but broadened in its scope as the subtitle indicates. It covers methodology used in the petrographic study of organic rocks and complementary analyses in detail, and also reviews southern African coal deposits in detail, richly illustrated with 71 colour plates, providing examples of macerals, minerals, and microlithotypes, and the highly varied organic petrography. The timely publication of this book will assist the application of coal petrology not only in exploration, mining, processing, power generation and the petrochemical and metallurgical industry, but also in environmental applications. The PPM Centre is proud to be associated with the publication of this important work.

RESEARCH PROJECTS AND PROGRESS

Ore deposit, Coal and Hydrocarbon Geology

CHARACTERIZATION OF THE UPPER MANGANESE ORE BED OF THE HOTAZEL FORMATION AT KMR MINE, KALAHARI MANGANESE FIELD, NORTHERN CAPE PROVINCE

Nkhensani Caroline Hlongwani

Three manganese (Mn) ore beds are interbedded with banded iron formation of the Paleoproterozoic Hotazel Formation in the Main Deposit of the Kalahari Manganese Field (KMF) in the area between Mamatwan and Black Rock in the Northern Cape Province. Virtually all the ore produced from the deposit comes from the lower Mn bed because it is very well developed, with thickness varying between 45 m at Mamatwan (the locality for typical well-preserved sedimentary Mamatwan-type ore) in the south to 5-8 m at Black Rock in the north, where it is often hydrothermally altered to high-grade Wessels type ore (Gutzmer and Beukes, 1996; Cairncross and Beukes, 2013). Most of the studies in the KMF have thus focused on the

composition and grade of the upper Mn bed. The middle Mn bed is poorly developed and seldom more than 1m thick and thus not exploited at all. This study focused on the upper Mn bed at KMR Mine (located on the farm York 279 and owned by Kudumane Manganese Resources), which has not been investigated in detail previously because it was deemed to be too thin and uneconomic (Nel et al, 1986). However, in the York area as well as further to the southwest near Middelplaats this bed reach thicknesses in excess of 20 m (Cairncross and Beukes, 2013) and may thus be considered a potential future resource for manganese ore.

Based on macroscopic to mesoscopic features observed during core logging,

the upper Mn bed is subdivided into nine lithostratigraphic zones (Figs. 1 and 2), which are grouped into four lithofacies based on features such as lamination type and the distribution and nature of early diagenetic Mn-carbonate lenticles and ovoids. Facies 1 defines zones A, C and H which display more ovoids (up to 5mm in size) than lenticles and mesobands (Fig. 2). Facies 2 comprises zone F which displays ovoids (up to 2mm in size) only (Fig.2). Facies 3 consists of zones B, D and G, which contain more abundant lenticular carbonate laminae and small ovoids less than 1mm in diameter (Fig. 2). Facies 4 comprises zones E and I which have a massive lutitic appearance (Fig. 2).

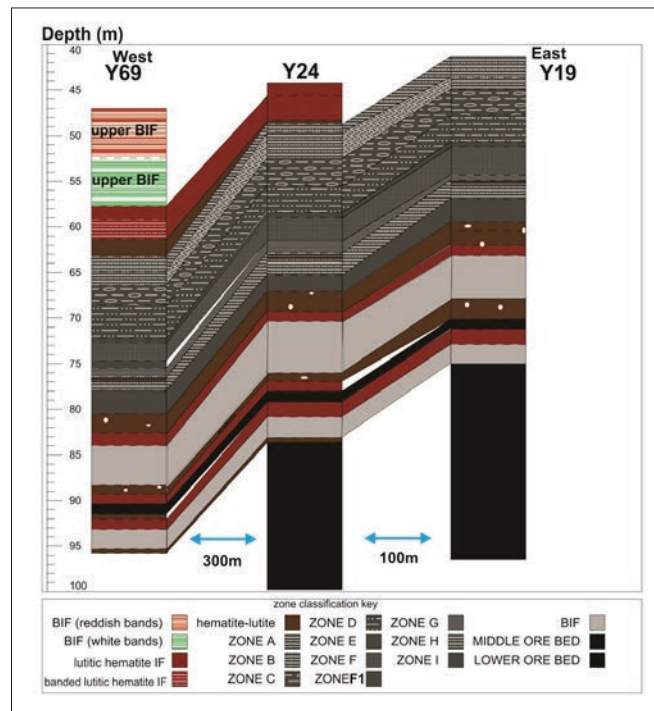
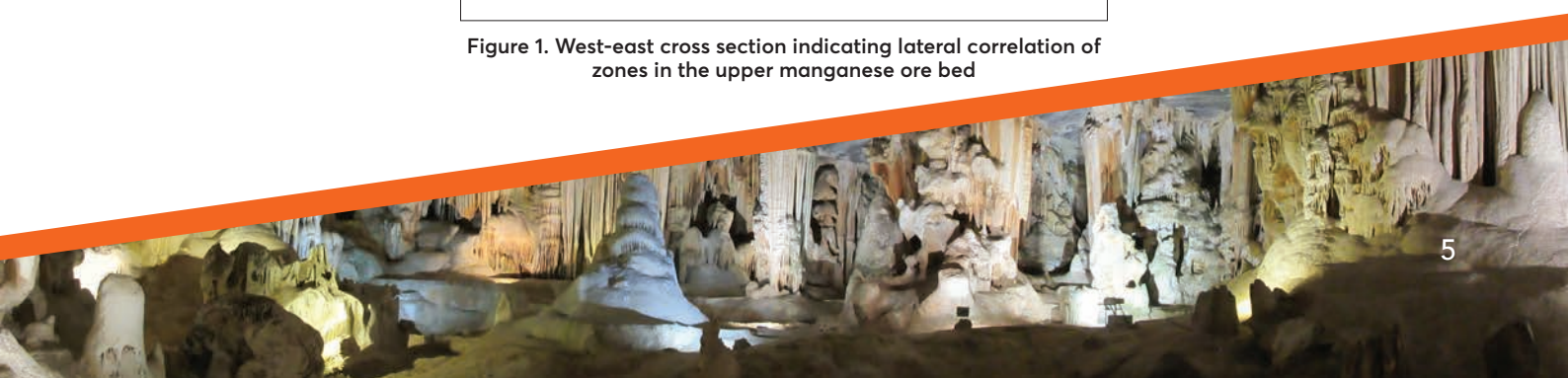


Figure 1. West-east cross section indicating lateral correlation of zones in the upper manganese ore bed



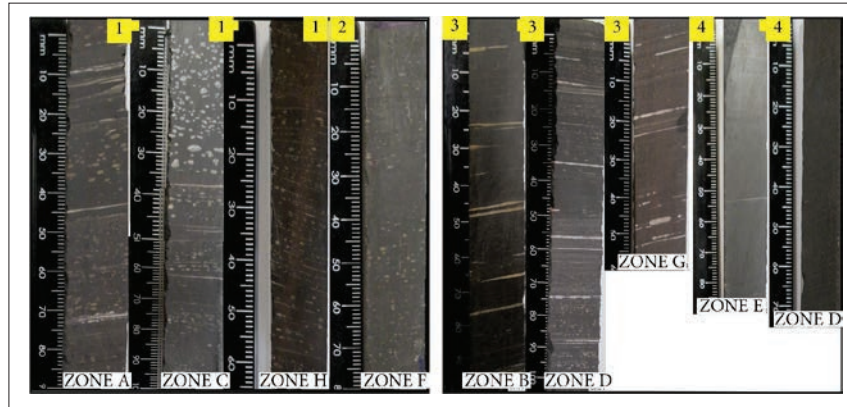


Figure 2. Typical character of lithostratigraphic zones in the upper manganese ore bed composed of black braunite lutite with different styles of light-coloured manganese carbonate ovoids and stringers. Numbers (in yellow) 1 to 4 refer to the four lithofacies as described in the text above.

Optical and scanning electron microscopy indicated that the upper Mn bed is similar to Mamatwan-type ore and has a microcrystalline texture that shows little to no signs of recrystallization. The fine ore, that has a dark grey to black colour, is composed of a microcrystalline intergrowth of braunite and kutnohorite with traces of fine hematite. The two most common early diagenetic features observed in the dark grey ore are white ovoids (Fig 3A); and lenticles (Fig 3B) composed of kutnohorite and Mn-calcite. In some zones the carbonate ovoids are partly replaced by hausmannite. In some samples late cross-cutting veinlets, filled with hausmannite and Mn-carbonate, are present. Some of these veinlets may also contain subordinate amounts of barite, tephroite (Fig 3C) and/or specularitic hematite (Fig 3D). The presence of the high-temperature mineral tephroite indicates that the veins formed during

a later event of localized hydrothermal fluid flow.

Geochemical analyses indicate that zones C, E and F have the highest Mn metal concentrations of just over 30 wt percent. Mn concentrations rapidly decline in both the upper and lower transition zones of the ore bed into adjacent hematite lutite and eventually iron formation (Fig. 4). REY data normalized to PAAS display negative Ce anomalies, positive Y anomalies and generally no Eu anomaly (Fig. 5). Mn-carbonate in the ore displays negative $\delta^{13}\text{CPDB}$ values with a wide range of -14.21 to -6.36 ‰. The $\delta^{18}\text{OPDB}$ values of the carbonates show a compositional range of -14.08 to -11.06 ‰ (Fig. 4).

The mode of deposition for the upper Mn bed supports the previously proposed depositional model by Cairncross and Beukes (2013). Iron, silica and manganese precipitated out of a hydrothermal plume, where iron precipitated at close proximity and

manganese at a distal proximity to the hydrothermal source. This order of precipitation for the three elements (Si, Fe and Mn) is supported by the cyclicity (developed from the waxing and waning of the plume) of the banded iron formation, hematite lutite and braunite lutite (Mn ores) units of the Hotazel Formation. Negative ^{13}C isotopes of the carbonates in the ore suggest that they formed through reduction of Mn^{3+} or Mn^{4+} phases by organic matter during early diagenesis (Okita et al., 1988). Shale-normalized enrichment of heavy rare earth elements (HREE) and positive Y anomalies suggest the upper Mn bed precipitated in a marine environment whereas negative Ce anomalies indicate that deposition took place under oxidizing conditions. The absence of Eu anomalies could imply that the plume water was derived from low-temperature (< 250°C) hydrothermal systems (Bau and Dulski, 1996).

References

- Bau, M. and Dulski, P. (1996). Distribution of yttrium and rare earth elements in the Penge and Kuruman iron-formations, Transvaal Supergroup, South Africa. *Precambrian Research*, **79**, 37–55
- Cairncross, B. and Beukes, N.J. (2013). The Kalahari Manganese Field: the adventure continues. *Struik Nature, Cape Town*.
- Gutzmer, J. and Beukes, N.J. (1996). Mineral Paragenesis of the Kalahari Manganese Field, South Africa, *Ore Geology Reviews*, **11**, 405–428
- Nel, C.J., Beukes N.J. and de Villiers, J.P.R (1986). The Mamatwan manganese mine of the Kalahari Manganese Field. In: Anhaeusser, C.R and Maske, S. (Eds) Mineral Deposits of Southern Africa. *Geological Society of Southern Africa*. Johannesburg, 963–978.
- Okita, P.M., Maynard, J.B., Spiker, E.C. and Force, E.R. (1988). Isotopic evidence for organic matter oxidation by manganese reduction in the form of stratiform manganese carbonate ore. *Geochim. Cosmochim. Acta*, **52**, 2679–2685

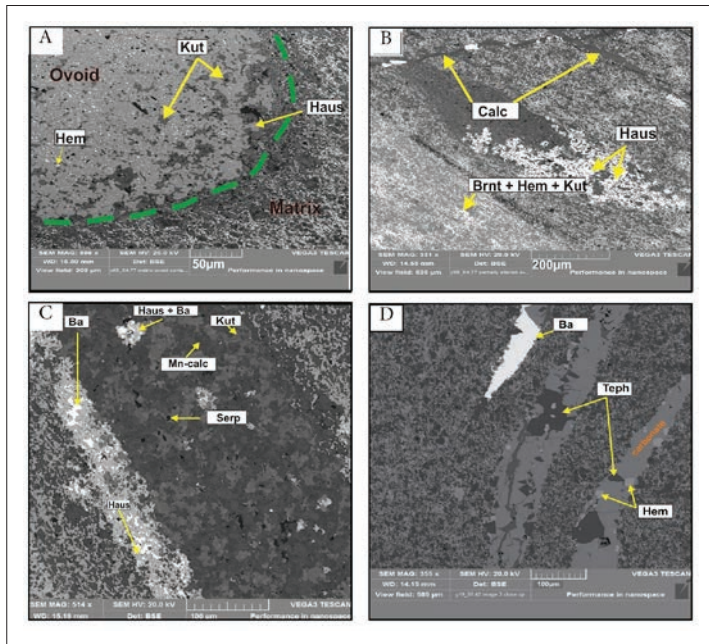


Figure 3. BSE SEM images of (A) ovoid (randomly selected) with surrounding microcrystalline groundmass, ovoid comprises the following compositions; kutnohorite (Kut), hematite (Hem) and hausmannite (Haus). (B) Slightly deformed ovoid and veinlet filled with calcite (Calc) and hausmannite (Haus). (C) Example of barite developed in association with hausmannite along the margin of a veinlet filled with Mn-calcite (Mn-calc) and kutnohorite(Kut) with subordinate concentrations of serpentine (serp), hausmannite (haus) and barite (Ba); the latter associated with Hausmannite. (D) Fine microcrystalline lutitic ore with crosscutting veinlets filled by recrystallized hematite (Hem), tephroite (Teph) and barite (Ba) inclusions.

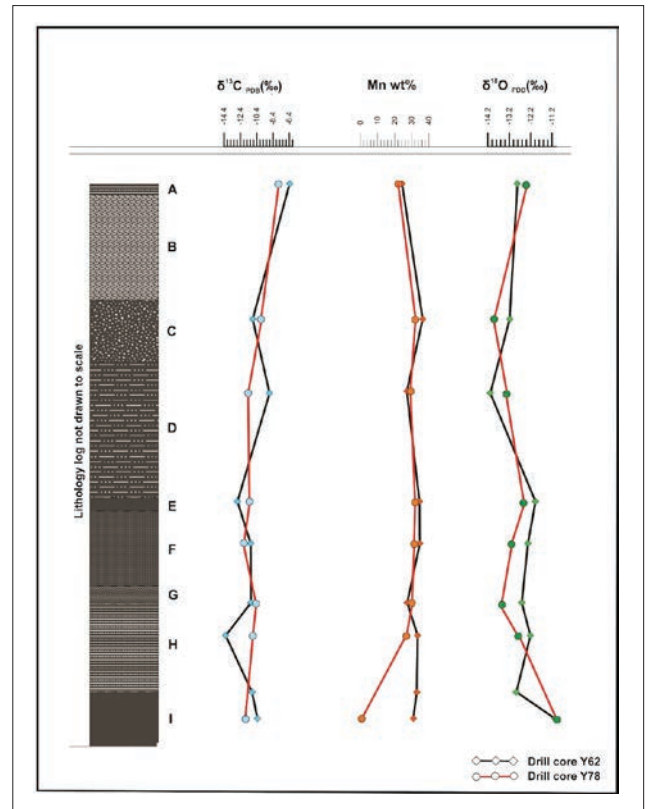


Figure 4. $\delta^{13}C_{PDB}(\text{‰})$, $\delta^{18}O_{PDB}(\text{‰})$ and Mn (wt%) whole rock signatures (drill cores Y62 and Y78) plotted against a generalized lithology log of drill cores at KMR Mine. Note the negative correlation between $\delta^{13}C_{PDB}$ and Mn concentration, and the positive correlation between, $\delta^{18}O_{PDB}$ and Mn content, from zone D down succession

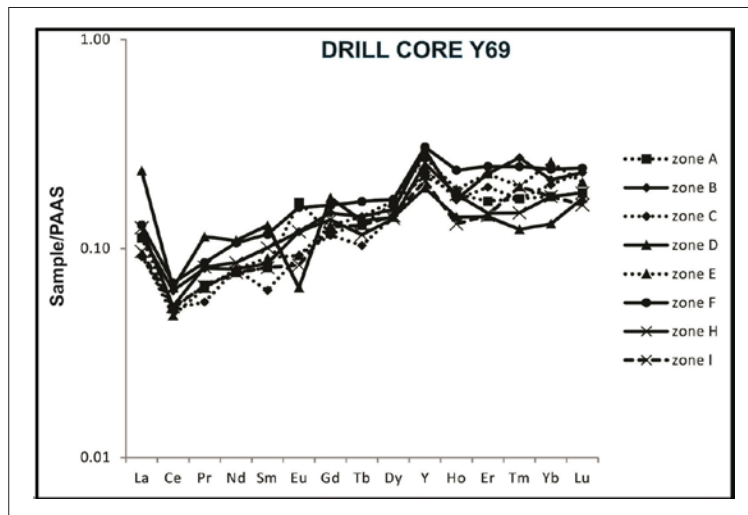


Figure 5. REY PAAS-normalized plot for a few samples taken from the upper Mn bed of drill core Y69.





GOLD MINERALIZATION WITHIN THE COLLETTE AND KJERSTI DEPOSITS OF THE JULIE BELT, NW GHANA.

Samuel Nunoo and Axel Hofmann

The discovery of gold in the Birimian of NW Ghana is much more recent compared with the Birimian terrains in the SW (especially the Ashanti and Sefwi belts), where commercial gold exploration and exploitation dates as far back as the early 1900's (Amponsah et al., 2015). The Birimian terrains of NW Ghana (Wa-Lawra and Julie belts) appear similar to those in the SW with respect to lithologies and metamorphism (Block et al., 2015), but differ in structural architecture and are less well exposed. The Julie belt (Fig. 1) is characterized by E-W trending Birimian metavolcanic rocks (mainly basalts) and metasedimentary rocks (shale and volcanoclastic rocks) intruded by granitoids. Rocks have experienced greenschist to, locally, amphibolite facies metamorphism. In order to investigate the nature of gold mineralization, the Collette and

Kjersti deposits (Fig. 1) of the Julie belt were considered in this study. Gold mineralization is considered mesothermal (Griffis et al., 2002) and mostly associated with sulphides (Fig. 2a) hosted in sheared shales, schists and metavolcanic rocks (basalt and diorite). The Collette mineralized zone is about 30 m wide and has a strike length of 600 m. The Kjersti mineralized zone is 30 – 50 m wide. Sulphides (arsenopyrite, pyrite and chalcopyrite) occur as intergrowth with or overgrowth on magnetite and/or chlorite (Fig. 2b and 2c, respectively). Gold is present as invisible, sub-microscopic grains within sulphides. Secondary minerals associated with gold mineralization are namely chlorite, sericite, K-feldspar, epidote, and silica (Fig. 2d). This mineral assemblage indicates greenschist condition of metamorphism (Block et al., 2015) during gold mineralization.

The origin of the mineralizing fluids (metamorphic or magmatic) is debatable with respect to Birimian gold. The association of gold with sulphides and graphite is documented in SW Ghana (e.g. Ashanti mines, Mücke and Dzigbodi-Adjimah, 1994) and relates to the widespread presence of black shale protoliths and potentially organic rich-hydrothermal fluids. The spatial and temporal association of sulphide-bearing metasedimentary and metavolcanic rocks may suggest either cogenetic or separate mineralizing fluid sources. There is also the likelihood of hydrothermal activity through devolatilization of Birimian volcano-sedimentary successions during the Eburnean metamorphic event (Berge et al., 2011).

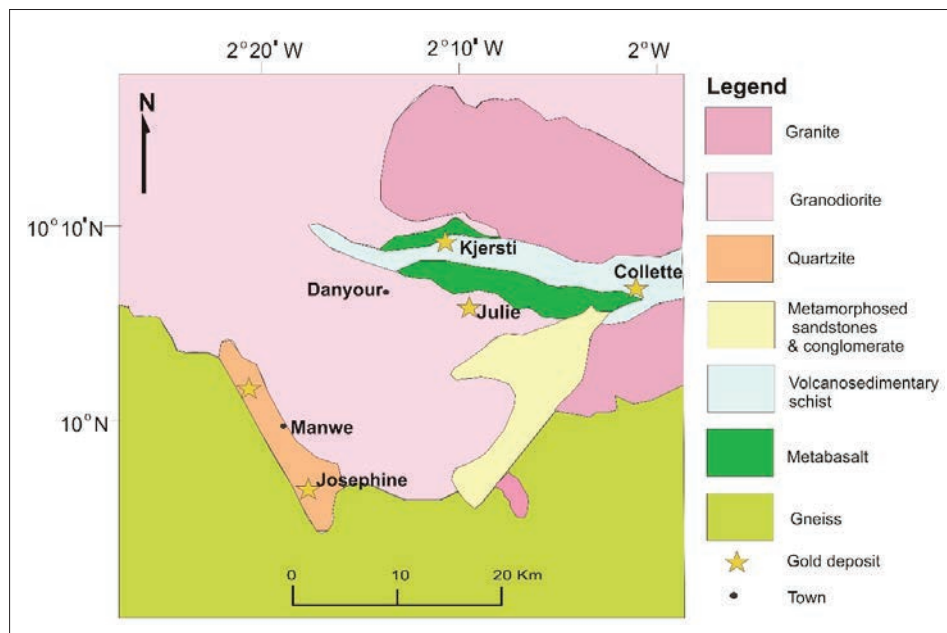


Figure 1. Simplified geological map showing the Julie belt with various gold deposits (Julie, Collette, Kjersti and Josephine) and other surrounding rocks (modified after Amponsah et al., 2015).

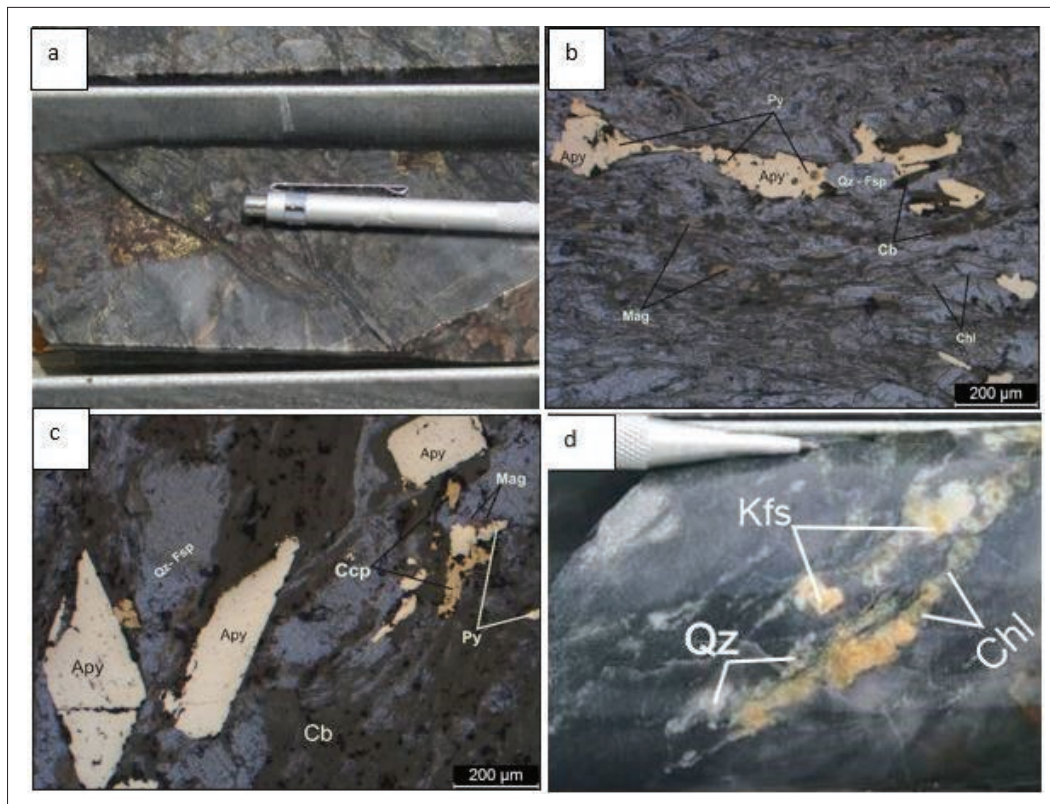


Figure 2. Features from diamond drill core and thin section photomicrographs (reflected light). (a) Apy (arrow) within sheared shale. (b) Intergrowth of Apy and Py along planes rich in carbonaceous matter, Chl and Mag. (c) Association of Apy, Py, Ccp and Mag; Ccp occurs as overgrowth along the fringes of Apy. (d) Sheared shale with Qz veins containing Kfs and Chl. (Qz-quartz, Chl-chlorite, Py-pyrite, Apy-arsenopyrite, Ccp-chalcocopyrite, Fsp-feldspar, Cb-carbonaceous matter, Mag-magnetite, Kfs-potassium feldspar).

References

- Amponsah, P.O., Salvi, S., Béziat, D., Jessell, M.W., Siebenaller, L., Baratoux, L., 2015. Geology and geochemistry of the shear-hosted Julie deposit, NW Ghana. *J. Afr. Earth Sci.* 112, 505 – 523.
- Berge, J., 2011. Paleoproterozoic, turbidite-hosted, gold deposits of the Ashanti gold belt (Ghana, West Africa): Comparative analysis of turbidite-hosted gold deposits and an updated genetic model. *Ore Geology Reviews* 39 (2011) 91–100.
- Block, S., Ganne, J., Baratoux, L., Zeh, L., Parra-Avila, A., Jessell, M., Ailleres, L., Siebenaller, L., 2015. Petrological and geochronological constraints on lower crust exhumation during Paleoproterozoic (Eburnean) orogeny, NW Ghana, West African Craton. *J. Metamorph. Geol.* 33, 463–494.
- Griffis, R.J., Barning, K., Agezo, F.L., Akosah, F.K., 2002. Gold Deposits of Ghana. *Minerals Commission, Accra, Ghana*, p. 438.
- Mücke, A., Dzigbodi-Adjimah, K., 1994. Ore textures and parageneses of the Prestea and Obuasi Gold deposits in the Ashanti Belt of Ghana: an ore microscopic study. *Geologisches Jahrbuch Reihe D100*, 167–199.





METALLOGENESIS OF THE PALEOPROTEROZOIC SISHEN IRON ORE DEPOSIT, NORTHERN CAPE PROVINCE, SOUTH AFRICA.

M.C. de Kock, A.J.B. Smith and N.J. Beukes

The iron ore deposit of the Sishen Mine, Griqualand West region, Northern Cape, South Africa has traditionally been considered to be of supergene origin. The age of iron mineralization is thought to be Post Transvaal Supergroup, but prior and during to Gamagara Formation deposition in the Griqualand West region at approximately 2200 Ma to 2000 Ma. BIF-hosted laminated, massive and breccia iron ores of the Manganore Formation occur below the basal Doornfontein Member hosting conglomeratic ore of the Gamagara Formation. Oxidized BIF and the Wolhaarkop breccia underlies the ore in karstic depression structures of the dolostone and limestone succession of the Campbellrand Subgroup. The ores thicken towards the middle of the depression structures. Outside of the karstic depressions the BIF-hosted iron ore and conglomeratic ore are not developed. A regional erosion surface known as pre-Gamagara unconformity occurs between the BIF-hosted iron ore and conglomeratic ores. The Doornfontein is suggested to have accumulated in sinkhole structures or either deposited in lower lying regions in the Paleoproterozoic. The metallogenesis of the iron mineralization in the BIF-host iron ore and the succeeding deposition of the conglomeratic Gamagara ores are put within in a regional geological context by this study. Randomly orientated microcrystalline to microplaty (supergene), patchy hematite crystals and larger cross-cutting microplaty to specular hematite (hypogene), which post-dates the initial supergene event were characterized with reflective light microscopy. Randomly

orientated microcrystalline to microplaty hematite crystals likely grew in the voids produced by the volume reduction of the dehydration of goethite to hematite during burial diagenesis or low grade metamorphism after the supergene event. This resulted in kink folding of soft saprolitic supergene ores. Which is shown by dissolution collapse textures of the non-porous lamellae into more porous lamellae and breccia fills. Later hypogene generation of microplaty to specular hematite of seems to enclose and mask pre-existing clasts of the conglomeratic ore.

The initial supergene event leached the ores of SiO₂, MnO, MgO, CaO, Na₂O, K₂O, P₂O₅, Cr₂O₃, Cu, Zn, Mo, Rb, Sr and Y; and residually enriched the ores in Fe₂O₃, TiO₂, Al₂O₃, V, Co, Ni, As, Zr, Nb and Pb. Phosphates occur in high quantities at the laminated ore – BIF contact, in breccia fills and veins. HREEs and Y are in all likelihood leached (became mobile) from protolith iron formation. Positive Ce anomalies are due to retention of Ce during leaching of REEs in supergene alteration. Oxygen isotopes of iron ore do not to display a large decrease in $\delta^{18}\text{O}$ compositions that would indicate a hydrothermal (high temperature) origin for the ores. Rather, the oxygen isotope signature of the protolith (Kuruman BIF) is mostly preserved, indicating low temperature epigenetic mineralizing fluids most likely of supergene origin. However, some degree of secondary alteration is indicated by $\delta^{18}\text{O}$ values of different ore types that indicate a slight negative shift from the protolith Kuruman iron formation. Distinct geochemical fingerprints with relatively higher Al₂O₃, K₂O,

TiO₂, Ba, LOI, V, LILEs, HFSEs and REYs values occur in brecciated and Gamagara Formation samples.

Radiometric (U-Th)/²¹Ne (mineral formation) and ⁴He/³He hematite (cooling) ages for seven samples from Sishen Mine were determined by this study. One iron-rich quartzite (Flagstone) sample from the Gamagara Formation gave a (U-Th)/²¹Ne age of 2110±94 Ma. This age is likely related to hematite crystallization associated with supergene enrichment in the Manganore Formation preceding or during formation of the pre-Gamagara unconformity, with later erosion depositing this component into the Flagstone. Several massive and laminated ore samples gave (U-Th)/²¹Ne ages between approximately 1900 Ma and 1600 Ma. The wide range of ages, that do not correspond to any known major tectonothermal event in the region, suggest that the dehydration reaction of goethite to microplaty hematite reset the (U-Th)/²¹Ne ages over an extended time period by burial diagenesis or low grade metamorphism below cover of sedimentary strata of the Kheis Supergroup. Three samples gave (U-Th)/²¹Ne ages that overlapped with the age of the 1st phase Namaqua-natal/Kheis metamorphic event occurring approximately between 1300 and 1170 Ma. These samples were from an iron-rich quartzite (Flagstone) (1200±54 Ma), a conglomeratic ore (1170±78 Ma) and a brecciated laminated ore (1270±68 Ma), and likely had higher permeability.

The study confirms numerous facets of existing ore-forming models for Sishen. It is thought that lateritic weathering took place to give rise to laminated,

massive and clastic textured ores of the Manganore Formation and reworked conglomeratic ores of the Gamagara Formation. Karstic collapse structures within the Campbellrand carbonates directly controlled the geometry of the deposits as the Manganore Formation slumped in

Paleoproterozoic sinkholes, thereafter the Doornfontein alluvial fan deposit further filled the structures and lower laying areas. The older hematite age populations encountered at Sishen reaffirm the ancient supergene genesis, but the younger age population appears to be indicative

of a regional-scale, but non-pervasive hypogene alteration event that affected the Manganore Formation in karst structures, overprinting the supergene signature in brecciated and Gamagara ores. This alteration was likely caused by the first phase Namaqua/Kheis metamorphic event.

THE TIMING AND NATURE OF IRON ORE FORMATION IN THE WOLHAARKOP DOME, NORTHERN CAPE PROVINCE, SOUTH AFRICA

M.P.N. Masangane, A.J.B. Smith and N.J. Beukes

The high-grade hematite iron ore deposits of the Griquatland West Basin in the Northern Cape, hosted in the Kuruman and Griquatown iron formations, are the largest known iron ore deposits in southern Africa. These deposits occur on or close to a regional anticline called the Maremane Dome; this includes the Wolhaarkop dome, a smaller anticlinal structure west of the Maremane Dome. The Wolhaarkop dome is the main structure in the Kolomela area and bordered by the Kheis Terrane to the west and Namaqua-Natal metamorphic province to the south (Figures 1, 2).

Iron mineralisation in the Wolhaarkop dome consists of laminated, massive and breccia ore making up iron ores from the Manganore Formation. These are overlain by detritally derived iron ores of the Gamagara Formation. The most prevalent ore type is the breccia ore and the rest of the ore types are not as developed. The rest of the stratigraphy is made up of conglomerates and iron-rich shales of the Doornfontein Conglomerate Member and quartzites and iron-rich shales of the Sishen Shale Member.

Several hematite textures, classified based on morphology and size, can be identified in the different iron ore types. This includes cryptocrystalline hematite, microplaty hematite, patchy hematite and martite as well as specularite. Mineralogically the iron ores are dominated by hematite. The gangue minerals present include quartz (chert), aluminium silicates, pyrite, barite, gypsum, apatite, calcite, monazite and xenotime.

The oxidised banded iron formation (BIF), iron ore and shales are characterised by the enrichment of Fe_2O_3 , Al_2O_3 , TiO_2 and K_2O and depletion of SiO_2 , MnO , MgO , CaO , Na_2O and P_2O_5 . The rare earth element (REE) PAAS (Post-Archean Australian shale) normalised diagrams reveal an influence of multiple events. This includes a prominent supergene event supported by light REE-enriched shale-normalised diagrams combined with positive Ce anomalies. A heavy REE-enriched signature is reflected in the iron ores and these typically have higher Al and Ti concentrations, Eu anomalies different to that in the protolith. Oxygen isotopes in samples from the present study are

comparable to those of the Sishen, Beeshoek and Rooinekke iron ore deposits.

The formation of iron ore deposit in the Wolhaarkop Dome formed from a multi-stage model combining an initial supergene event and subsequent reworking of the earlier formed ores. This was then followed by hydrothermal event reflected in specularite veins cross cutting the iron ore. Using (U-Th)/ ^4He and (U-Th)/ ^{21}Ne hematite dating, laminated and massive ores from the Wolhaarkop dome revealed ages of 1540 ± 103.31 Ma and 1400 ± 94 Ma, respectively. These ages correspond to a period of cratonic stability and therefore represent resetting ages during burial metamorphism, implying that the main ore-forming event precede these ages. Younger ages in specularite veins and BIF occurring at 1100 ± 230.71 Ma, 1100 ± 49.48 Ma and 966 ± 47.32 Ma, overlap with the Kheis and Namaqua-Natal orogeny. These ages are interpreted to represent non-pervasive hydrothermal fluid-flow on the Wolhaarkop dome that potentially could have caused further upgrading of the ore.



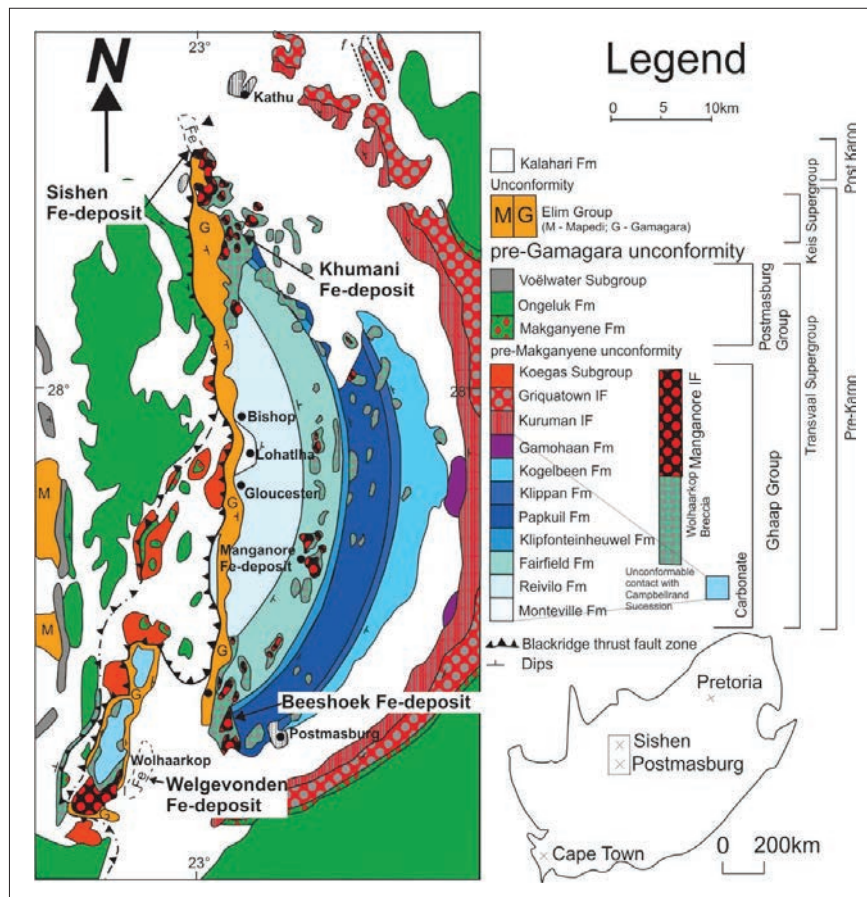


Figure 1: Regional geological map of the Maremane Dome region in the Northern Cape Province indicating the location of the Sishen, Khumani, Beeshoek and Sishen South iron ore deposits (taken from Smith and Beukes, 2016; modified after Van Schalkwyk and Beukes, 1986).

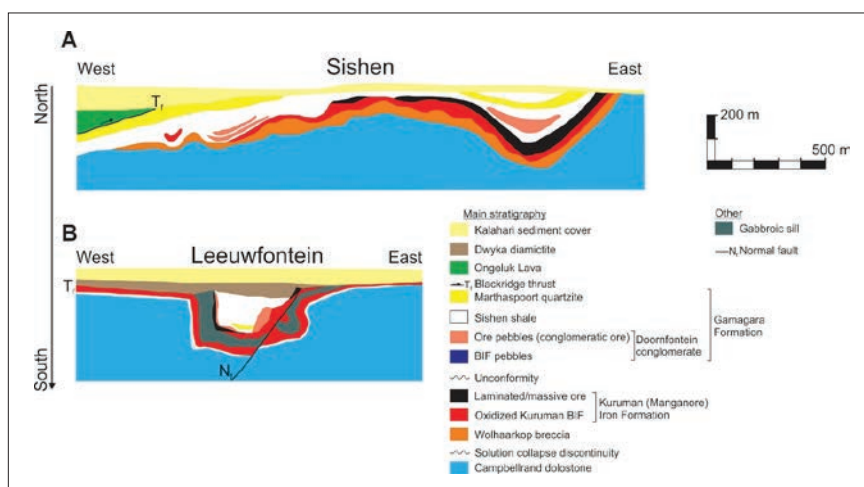


Figure 2: East-west cross sections (adapted from Smith and Beukes, 2016) illustrating the (A) Sishen iron ore deposit (adapted from Carney and Mienie, 2003; Van Deventer, 2009); and (B) Leeuwfontein ore body of the Kolomela iron ore deposit (adapted from Alchin and Botha, 2006).

THE TIMING AND NATURE OF IRON MINERALIZATION AT KOLOMELA MINE, NORTHERN CAPE, SOUTH AFRICA

B.L. Nthloro, A.J.B. Smith and N.J. Beukes

The Transvaal Supergroup in South Africa hosts some of the largest iron ore deposits in the world, with deposits hosted in two regions, namely the Griqualand West and Transvaal Basins. The high-grade iron ores hosted in the Kuruman and Griquatown Iron Formations (Asbesheuwels Subgroup) within the Maremane Dome in the Griqualand West region, Northern Cape Province, South Africa, are such examples. This study focuses on the iron ore bodies at Kumba Iron Ore's Kolomela Mine, which is situated on the southern margin of the Maremane Dome. These high-grade ores are typically preserved in karst structures, with the main ore body, comprising laminated and massive ores, lying above oxidized banded iron formations (which, together with the ores, are locally termed the Manganore Formation) and below the Pre-Gamagara Unconformity. Conglomeratic ore is hosted directly above the unconformity in the

Gamagara Formation (Figure 1). The banded iron formation (BIF), which is brecciated in some intervals, is more iron-rich at the top close to the contact with the ore, decreasing down the stratigraphy. The laminated ore, which occur at the bottom of the ore package, are made up of alternating high lustre and low lustre laminae and contain calcite, chlorite and biotite in the veins and the pores. The massive ores, which occur above the laminated ores, are made up of fine- to coarse grained rocks and textures varying between anhedral, microcrystalline, patchy and specular. The conglomeratic ore above the massive ores is made up of massive and laminated ore clasts; and the Doornfontein conglomerates contain BIF clasts with subordinate laminated and massive ore clasts, ferruginised quartz, shales and sandstone clasts. The Doornfontein conglomerates are not of ore-grade. Significant amounts of detrital pyrite were also found in

the shales and conglomerates. All the samples contain subordinate amounts of apatite, chlorite, biotite, ilmenite, allanite, ankerite, quartz and calcite as fillings in pores, veins and breccias.

The general stratigraphy shows an enrichment in Fe_2O_3 and a depletion in SiO_2 relative to unaltered Kuruman BIF, except in the Manganore BIF, where the Fe_2O_3 and SiO_2 are similar to unaltered BIF. There is also an enrichment in Al_2O_3 , TiO_2 and P_2O_5 and a depletion in MnO , MgO , and Na_2O compared to unaltered Kuruman BIF. Ba and Sr are enriched in most of the analysed samples.

The enrichment of shale-normalized light rare earth elements displayed by some the massive and laminated ores reveals a significant supergene enrichment event in the area, although some samples show an enrichment in HREY, which is thought to be the result of a later hydrothermal overprint. These samples show both positive and negative Ce

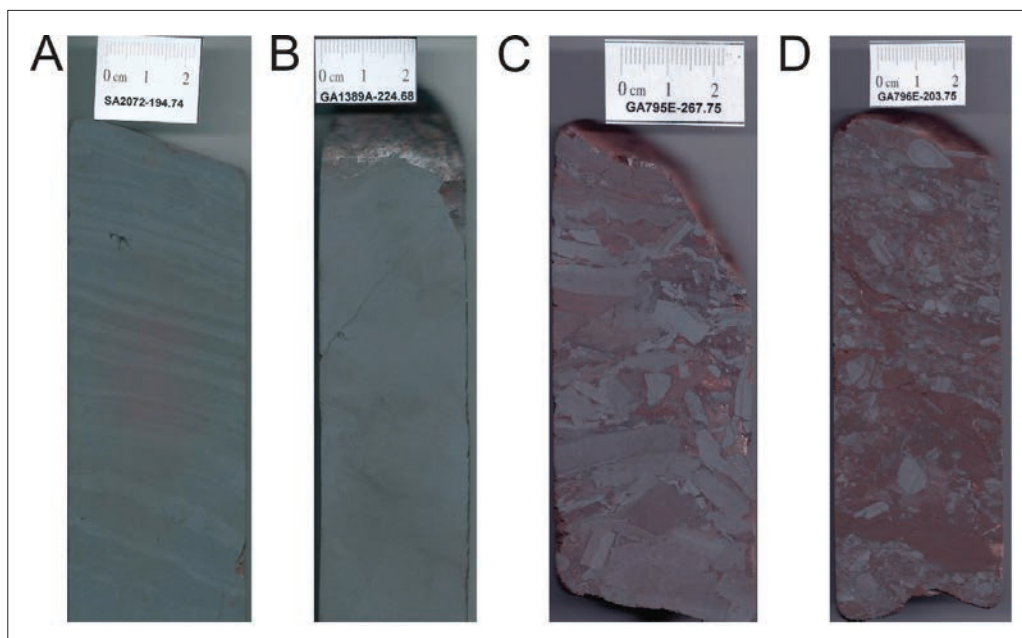
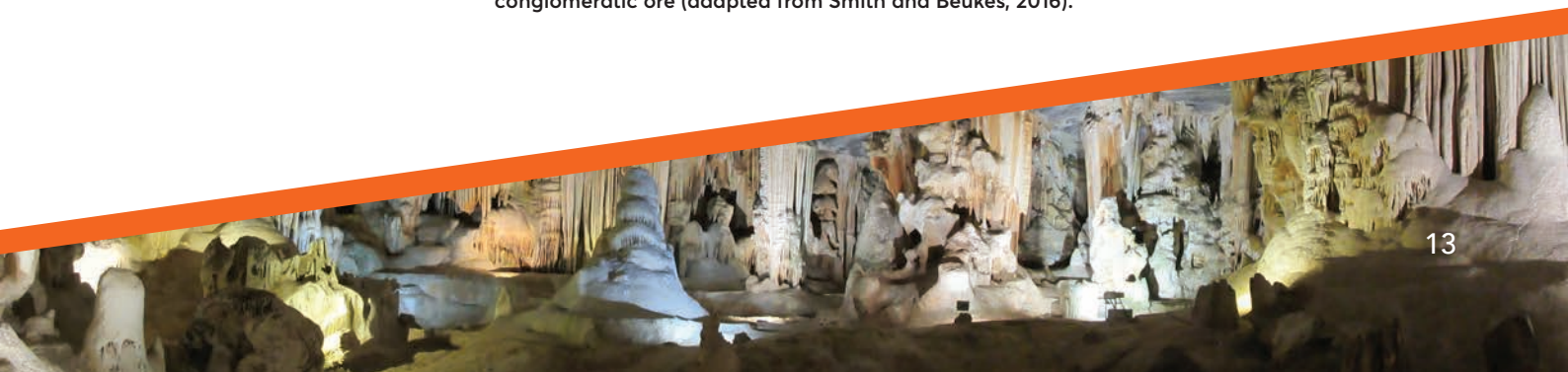


Figure 1: Core scans of the main ore types encountered in the Transvaal Supergroup-hosted high grade iron ores of South Africa. The main ore types are: A) laminated; B) massive; C) brecciated; and D) conglomeratic ore (adapted from Smith and Beukes, 2016).





anomalies, which are absent in pristine Asbesheuwels BIF, suggesting a post-depositional overprint by a high Eh fluid. The oxygen isotopes trends are comparable to those shown by iron ore from Sishen, Beeshoek and Rooineke Mines, which also occur below the Pre-Gamagara Unconformity and are considered to be typical supergene iron ores. The $^4\text{He}/^3\text{He}$ and $(\text{U}/\text{Th})/^{21}\text{Ne}$ ages acquired for hematite do not correspond to the approximate age of the Gamagara Unconformity (~2.2-1.9 Ga). A sample of massive ore had a hematite age of 1640 Ma \pm 123.1, which

does not correspond to any tectono-thermal activity in the region and is thought to be attributable to resetting from burial. Samples of brecciated ore, laminated ore and oxidized Manganore BIF gave hematite ages of 1340 \pm 72.2 Ma, 1050 \pm 70.40 Ma and 1070 \pm 57.6 Ma, respectively. The brecciated ore age potentially overlaps with the onset of the ~1.29-1.17 Ga Kheis orogeny or could be due to burial reset. However, laminated ore and oxidized Manganore BIF samples overlap with the Kheis and/or Namaqua-Natal (~1.2-1.0 Ga) orogenies.

Ages clearly predating these orogenies, in conjunction with stratigraphic and geochemical evidence, suggest that the main ore-forming event was a Pre-Gamagara Unconformity-related supergene event, with erosion of BIF-hosted ore from the flanks into the karst-related basins depositing the conglomeratic ore. The younger hematite ages that overlap with the Kheis and/or Namaqua-Natal orogenies suggest that a hydrothermal overprint also occurred, although it appears to be limited to more permeable lithologies.

References for above 3 contributions

- Alchin, D.J. and Botha, W.J. (2006). The structural/stratigraphic development of the Sishen South (Welgevonden) iron ore deposit, South Africa, as deduced from ground gravity data modelling. *Applied Earth Sciences (Trans. Inst. Min. Metall. B)*, 115, 174-186.
- Carney, M.D. and Mienie, P.J. (2003). A geological comparison of the Sishen and Sishen South (Welgevonden) iron ore deposits, Northern Cape Province, South Africa. *Applied Earth Sciences (Trans. Inst. Min. Metall. B)*, 112, B81-B88.
- Smith, A.J.B. and Beukes, N.J. (2016). Palaeoproterozoic banded iron formation-hosted high-grade hematite iron ore deposits of the Transvaal Supergroup, South Africa. *Episodes*, 39, 269-284.
- Van Deventer, W.F. (2009). Textural and geochemical evidence for a supergene origin of the Paleoproterozoic high-grade BIF-hosted iron ores of the Maremane Dome, Northern Cape Province, South Africa. MSc dissertation (unpubl.), University of Johannesburg, Johannesburg, 107pp.
- Van Schalkwyk, J.F. and Beukes, N.J. (1986). The Sishen iron ore deposit, Griqualand West. In: Anhaeusser, C.R. and Maske, S. (Eds), *Mineral Deposits of Southern Africa*, Geological Society of South Africa, Johannesburg, 931-956.

HREE ENRICHMENT WITHIN THE THRUSTED MANGANESE ORE ABOVE THE BLACKRIDGE THRUST FAULT, NORTHERN CAPE PROVINCE

Nicholas Vafeas

The Hotazel Formation of the Kalahari Manganese Field (KMF) is characterised by three laterally extensive manganese ore beds that are interbedded with finely laminated banded iron formation. Together, these three Paleoproterozoic (Beukes, 1983; Nel *et al.*, 1986) manganese ore beds host an estimated 77% of global land based manganese reserves (USGS, 2015). As a result of diagenesis and regional low-

temperature metamorphism, the low-grade Mamatwan-type ore, which is considered to be the most pristine ore-type in the area, has been modified through hydrothermal and/or supergene alteration, resulting in the high-grade Wessels-type and supergene ore. In addition, thrusting along the Blackridge thrust fault has duplicated the strata, resulting in near surface allochthonous deposits of Wessels-type ore along

the north-western portion of the KMF. The near surface position of the thrusting manganese ore has rendered it susceptible to supergene alteration below the overlying Kalahari unconformity, resulting in the development of a host of Mn⁴⁺ oxyhydroxides, including pyrolusite, which is seen in Figure 1, developing at the expense of pre-existing braunite II and Bixbyite.

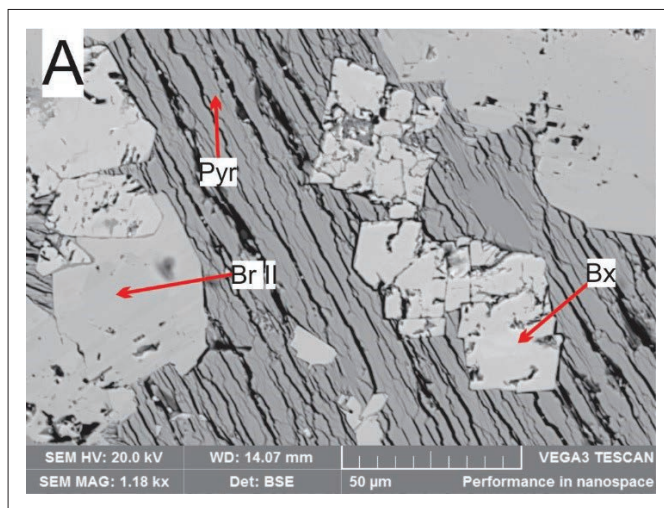


Figure 1. Supergene altered thrust manganese ore exhibiting the replacement of braunite II (Br II) and bixbyite (Bx) by pyrolusite (Pyr).

Whole-rock geochemical analyses into the rare earth element (REE) content within the lowermost and thickest manganese ore bed both, above and below the Blackridge thrust fault,

have revealed significant enrichments relative to Post Archean Average Shale (PAAS; Figure 2A), particularly within the heavy rare earth elements (HREE). Relative to PAAS, the Mamatwan-type

ore is depleted in both HREE and light rare earth elements (LREE), remaining relatively flat at around 0.1.

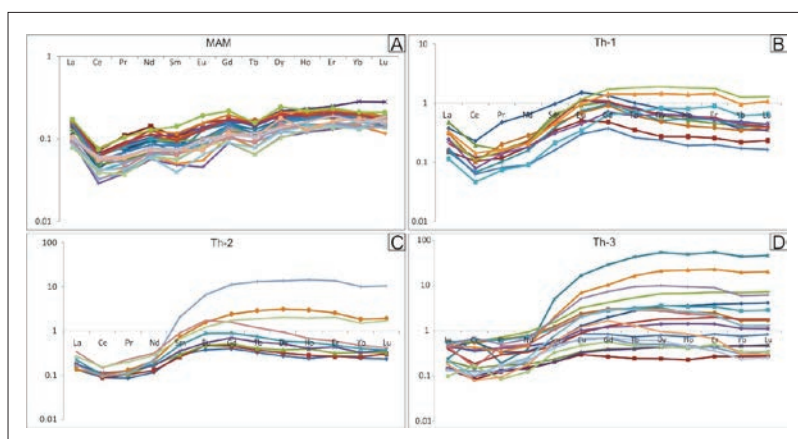


Figure 2. PAAS normalised REE diagrams illustrating the REE distribution within the lower manganese ore bed for the pristine Mamatwan-type manganese ore (A) and 3 examples of thrust manganese ore (B-D).

Within the thrust manganese ore, there is a significant enrichment in HREE from Nd to Lu relative to PAAS, resulting in a distinct "hump" in the REE pattern (Figure 2 B-D), attaining PAAS normalised values of close to

100 in some samples (Figure 2D). In comparison to the Mamatwan-type ore, the HREE enrichment is evidently unique to the thrust manganese ore. As of yet, mineralogical investigations into the source of the HREE

enrichment are currently underway which will potentially ascertain the origin of the HREE and to what extent this enrichment has affected the thrust manganese ore.

References:

Beukes, N.J. (1983). Palaeoenvironmental setting of iron formations in the depositional basin of the Transvaal Supergroup, South Africa. In: Trendall, A.F., and Morris, R.C.(eds). *Iron formations, facts and problems*, Elsevier, Amsterdam, 131-209.

Nel, C.J., Beukes, N.J. and De Villiers, J.P.R. (1986). The Mamatwan Manganese Mine of the Kalahari Manganese Field in: Annhaeusser C.R., and Maske, S. (eds.), *Mineral Deposits of Southern Africa. Geological Society of South Africa*. Johannesburg. 1. 965-971.

United States Geological Survey. (2015). Mineral Commodity Summaries: Manganese. Obtained from <http://minerals.usgs.gov/minerals/pubs/commodity/manganese/mcs-2015-manga.pdf>. Accessed 13/07/2015.



GEOCHEMISTRY OF A SOUTH AFRICAN COAL: INSIGHTS INTO THE FORMATION OF CERTAIN MACERALS

Ofentse M. Moroeng, James Roberts (UP) and Nicola Wagner

South African coals of the Main Karoo Basin, which are generally inertinite-rich, continue to be important to the country's economic prospects. The formation of inertinite macerals present in coal continues to be a subject of controversial discussion, and is generally attributed to multiple origin pathways. Although multiple origin pathways are generally recognized globally (ICCP, 2001; Hower et al., 2013; Richardson et al., 2012; O'Keefe et al., 2013), the various inertinite macerals in South African coals have historically been chiefly attributed to aerial oxidation of plant matter in a cold climate, with the degree of oxidation responsible for the maceral produced (Falcon, 1986; Hagelskamp and Snyman, 1988; Cadle et al., 1993; Snyman and Botha, 1993). However, the view that the processes responsible for the formation of inertinite present in South African coals were wholly exclusive of those recognized in other regions of the world is, at best, difficult to accept. If the cool, oxidizing conditions were solely responsible for the preservation of morphology, and subsequent formation of inertinite macerals in

the coals, it would be reasonable to think that similar macerals should be completely absent in coals formed in tropical climates such as the Pennsylvanian coals of the northern hemisphere.

It is important to mention that most work on the origin of inertinite macerals in South African coals was undertaken in the late 1980's (e.g., Falcon, 1986; Hagelskamp and Snyman, 1988; Cadle et al., 1993; Snyman and Botha, 1993). Following which, there was a general paucity until the work of Glasspool (2003a, 2003b). This latter work disagrees with the earlier studies regarding the origin of the inertinite macerals, with Glasspool (2003a, p. 966) stating "...the abundance of Gondwana semifusinite has been explained-to have formed as a direct result of sub-aerial exposure in a cold climate setting. This hypothesis is not accepted. No mechanism by which cold climate alone can form high reflecting inertinites has so far been satisfactorily demonstrated.

Conversely, wildfires can be demonstrated to produce a wide suite of inertinite morphologies and reflectances".

Glasspool (2003a, 2003b) was thus the first to show, through the description of what he termed "fossil charcoal", that inertinite macerals in South African coals are likely to have a pyrogenic origin. Macroscopic charcoal associated with the clastic sedimentary rocks of the Vryheid Formation (Vereeniging Coalfield) has also been documented (Jasper et al., 2013). Despite this, the now firmly entrenched view that the inertinite macerals are oxidation- and cold climate-derived continues to persist and is often cited as fact in the published literature on South African coals (e.g., Van Niekerk et al., 2008; O'Keefe et al., 2013). The controversy stems, in part, from the glacial/post-glacial climatic conditions prevailing in Gondwana in contrast to the more tropical conditions of Laurasia (Falcon, 1986; Snyman and Botha, 1993). The Gondwana conditions were previously assumed to have hindered the development of extensive wild and/or peat fires. However, as Jasper et al. (2013) argued in their paper, the concentration of free oxygen in the atmosphere peaked at around 30% in the Early Permian falling to



Figure 1: Mosaic photomicrograph showing fusinite (right; well-preserved structure, high reflectance) grading into semifusinite (structured still, lower reflectance), and finally into vitrinite (bottom left; unstructured, lowest reflectance) observed in the inertinite-rich sample. 500x magnification, reflected light under oil immersion. Scale is indicated.

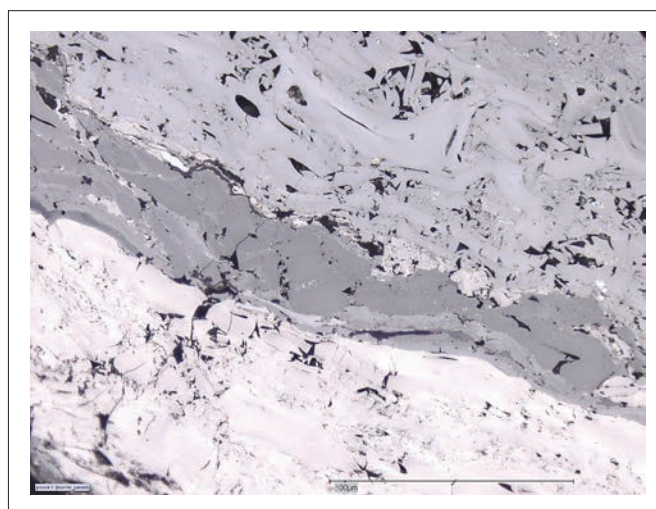


Figure 2: Inertinite macerals with varying reflectances observed in the inertinite-rich sample. 500x magnification, reflected light with oil immersion. Scale is indicated.

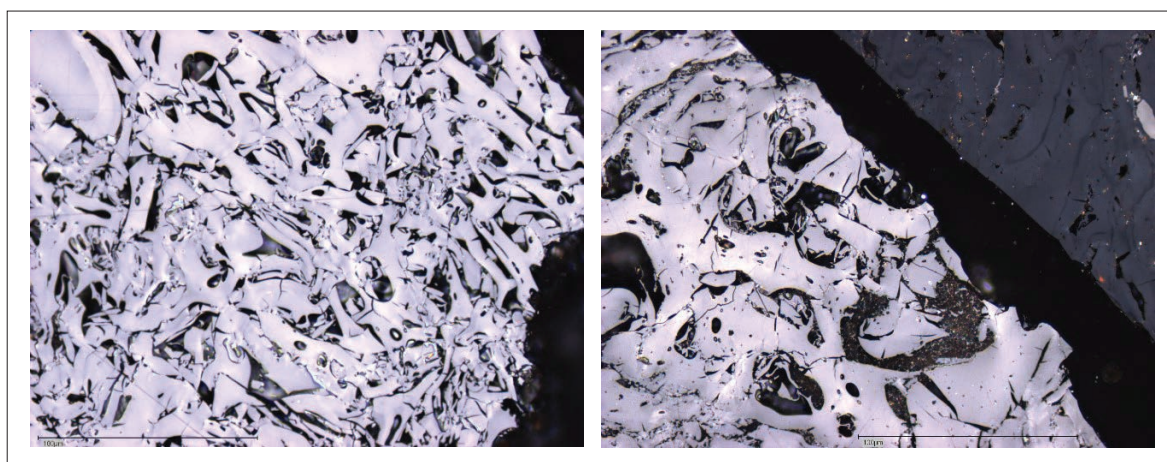


Figure 3: A and B – fusinites observed in the inertinite-rich sample. 500x magnification, reflected light with oil immersion. Scale is indicated.

around 20% in the Late Permian (see also, Berner, 1999; Diessel, 2010; Glasspool and Scott, 2010). Thus, with the atmospheric oxygen exceeding the minimum required to sustain a fire, plants would likely have been prone to fires even while wet (Jasper et al., 2013).

Our work is aimed at constraining the origin pathways for macerals present in a medium rank C bituminous South African coal using selected organic geochemical analytical techniques. A coal sample was obtained from the No. 4 Seam Upper of the Witbank Coalfield, South Africa. Following crushing, a portion of the original

sample was reserved to represent the “parent sample”, while the rest was density-fractionated to create iso-rank vitrinite-rich and inertinite-rich sub-samples. The analyses conducted on the samples include: (1) basic chemical characterization (proximate, elemental, and calorific value analysis); (2) detailed petrographic analysis (maceral, microlithotype, and mean random vitrinite reflectance); (3) electron spin resonance (ESR); (4) carbon-13 cross-polarization magic-angle-spinning solid-state nuclear magnetic resonance (^{13}C CP-MAS SS NMR), and (5) stable nitrogen and carbon isotopes ($\delta^{15}\text{N}$

and $\delta^{13}\text{C}$) values used in conjunction with the concentration of nitrogen functionalities (N-pyridinic, N-pyrrolic, N-quaternary, and N-oxide complexes) determined using X-ray photoelectron spectroscopy (XPS).

The parent sample comprises of 41.6 vol. % vitrinite and 48.5 vol. % inertinite (mineral-matter-included basis). The vitrinite-rich sample consists of 81 vol. % vitrinite (dominated by collotelinite and collodetrinite), whereas the inertinite-rich sample consists of 63 vol. % inertinite (dominated by fusinite, semifusinite, and inertodetrinite). Further, the samples comprise





of mostly vitrite and inertite microlithotypes. The ESR analysis revealed that the inertinite-rich sample has a higher radical concentration relative to the iso-rank vitrinite-rich sample, implying thermally driven pre-diagenesis metamorphism for the major components of the former sample (Austen et al., 1966). According to the NMR analysis, the inertinite-rich sample has an abundance of 6-aromatic carbon rings and the vitrinite-rich sample has multi-ring clusters. The 6-carbons ring in the inertinite-rich sample are interpreted to be guaiacol and syringol, the principal products of low-temperature (below 400 °C) lignin pyrolysis (Asmadi et al., 2011; Kawamoto, 2017). Based on the stable isotopes, the vitrinite-rich sample has the lower $\delta^{13}\text{C}$ and the lower ^{14}N value relative to inertinite-rich counterpart. Because of the higher N-quaternary and N-pyridinic, the loss of ^{14}N in the vitrinite-rich sample is attributed to bacterial degradation (Schulten and Schnitzer, 1998, and references therein; Kelemen et al., 2006; Rimmer et al., 2006). In contrast, the inertinite-rich sample has a higher

concentration of both N-pyrrolic and N-oxide complexes, with the latter interpreted to be indicative of exposure during charring of the dominant macerals of this sample. A fusinite-rich section of a coal particle was interpreted to represent the outermost layers of a plant organ. The inner, comparatively lower-reflectance portions of the same particle may then represent semifusinite. During charring, the outermost layers of a plant organ would have been directly exposed to the fire, whereas the inner portions would have been shielded and may thus, have remained relatively unaffected by the elevated temperature. This process accounts for a gradational boundary between fusinite and adjacent semifusinite, as shown in Figures 1 and 2. In the absence of a gradational contact between inertinite macerals as shown in Figure 3, the botanical organs can be interpreted to have been distinct and discrete. The degree of charring, controlled in part, by moisture and perhaps size of the affected plant organ, would then have determined

whether fusinite or semifusinite was formed. A fusinite particle of uniformly high reflectance (Figure 2.9) was interpreted to reflect charring when the botanical precursor had already died and was dried out, and was thus, more readily and evenly charred.

It was thus concluded that fusinite and semifusinite present in the No. 4 Seam Upper Witbank coal were formed through charring of plant matter, and that the moisture content of affected vegetation determined the degree of charring, and thus, the resultant inertinite maceral. Inertodetrinite was interpreted to have formed through the same process as the dominant, primary inertinite macerals. Inertodetrinite-forming particles were interpreted to reflect charred matter that was reworked by sedimentary processes. The dominance of monomacerals over bi- and trimacerals was interpreted to reflect an interchange between wet periods during which mostly vitrinite was formed, and relatively dry, inertinite-forming periods during which fires occurred.

References:

- Asmadi, M., Kawamoto, H., Saka, S., 2011. Thermal reactions of guaiacol and syringol as lignin model aromatic nuclei. *Journal of Analytical and Applied Pyrolysis* 92, 88-98.
- Austen, D.E.G., Ingram, D.J.E. Given, P.H., Binder, C.R., Hill, L.W., 1966. Electron Spin Resonance Study of Pure Macerals. In: Given, P.H., (Ed.). *Coal Science, Advances in Chemistry*, 55. American Chemical Society, Washington DC, pp. 344-362.
- Berner, R.A., 1999. Atmospheric oxygen over Phanerozoic time. *Proceedings of the National Academy of Sciences of the United States of America* 96 (20), 10955-10957.
- Cadle, A.B., Cairncross, B., Christie, A.D.M., Roberts, D.L., 1993. The Karoo Basin of South Africa: type basin for coal-bearing deposits of southern Africa. *International Journal of*
- Diessel, C.F.K., 2010. The stratigraphic distribution of inertinite. *International Journal of Coal Geology* 81 (4), 251-268.
- Falcon, R.M.S., 1986. A brief review of the origin, formation, and distribution of coal in southern Africa. In: Anhaeusser, C.R., Maske, S. (Eds.), *Mineral Deposits of Southern Africa*, Vols. I and II. Geological Society of South Africa, Johannesburg, pp. 1879-1898.
- Glasspool, I., 2003a. Palaeoecology of selected South African export coals from the Vryheid Formation, with emphasis on the role of heterosporous lycopods and wildfire derived inertinite. *Fuel* 82, 959-970.

Geometallurgy and Kimberlite Research

ORIGIN OF SHEARED CONTINENTAL PERIDOTITES: A COMBINED THERMOBAROMETRY, MANTLE REDOX AND SR-ND-CA ISOTOPE STUDY OF XENOLITHS FROM THE 1.15 GA PREMIER KIMBERLITE, KAAPVAAL CRATON

Sarah Milne, Sebastian Tappe, Malcolm Massuyeau, Katie A. Smart (Wits) and, Alan B. Woodland (Goethe-Universität, Frankfurt, Germany)

This study is centred around the world-famous Premier kimberlite pipe located on the central Kaapvaal craton. The kimberlite intruded into the rocks of the well-known and economically important Bushveld Igneous Complex. Previous studies have inferred that the ca. 2,056 Ma Bushveld magmatic event has had a large thermochemical impact on the Archean cratonic mantle lithosphere as sampled by the ca. 1,153 Ma Premier kimberlite. This inference is based on anomalous present-day seismic P-wave velocities and a notable Fe-Ti enrichment seen in some mantle-derived xenoliths from areas immediately surrounding the Bushveld Complex. The lithospheric mantle beneath the Premier kimberlite pipe also has a warmer paleogeotherm >40 mW/m², which according to previous studies may be linked to the Bushveld large igneous event.

The question remains as to whether

or not the Bushveld magmatic event at ca. 2,056 Ma had a large thermal and chemical impact on the central Kaapvaal mantle lithosphere, which was sampled at ca. 1,153 Ma by the Premier kimberlite magma. This question will be addressed by determining the origin of a newly collected suite of sheared peridotite xenoliths from the Premier kimberlite that hosts Cullinan Diamond Mine. Petrological and textural observations from these mantle-derived xenoliths and xenocrysts will provide important information about the thermal and chemical state of Earth's upper mantle at the time of kimberlite eruption. Major and minor element compositions of primary mineral assemblages (garnet, clinopyroxene, orthopyroxene and olivine) of the studied mantle xenoliths will be used in thermobarometry calculations to constrain the Premier kimberlite paleogeotherm. The newly defined Premier geotherm (>40 mW/m²) is

only slightly "hotter" compared to geotherms for other global kimberlite (~ 38 mW/m²) occurrences. This slightly warmer geotherm for Premier is not as anomalous as previously suggested, because the mantle potential temperature was slightly higher during the Mesoproterozoic compared to present-day. Older kimberlites $>1,000$ Ma are associated with warmer mantle potential temperatures and may therefore record hotter paleogeotherms compared to mantle lithosphere sections that were traversed and sampled by, for example, widespread Mesozoic kimberlite magmas. If correct, this inference suggests that the slightly elevated Premier paleogeotherm may not be a consequence of thermal input from the short-lived Bushveld magmatic event. The new peridotite xenolith-derived geotherm for Premier intersects the present-day mantle adiabat (1315°C) at ~ 186 km depth, which defines the petrological

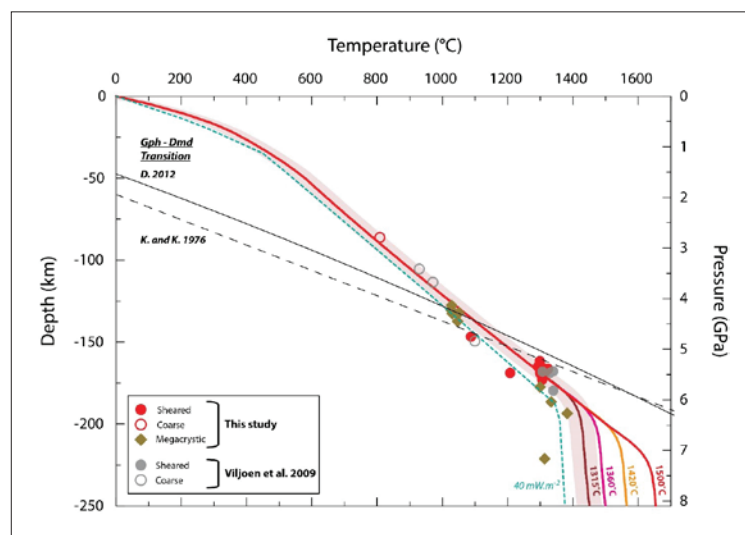
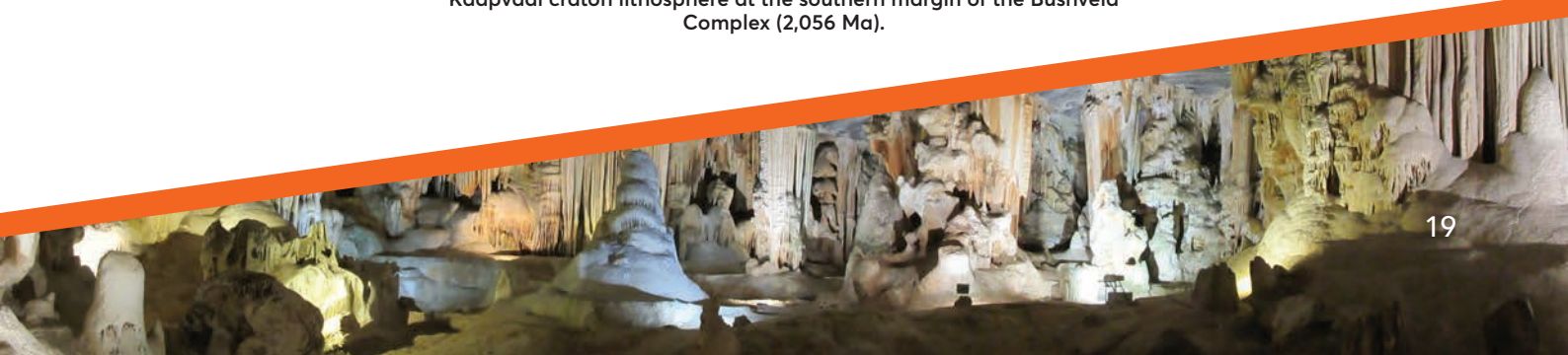


Figure 1: A newly defined paleogeotherm (1,150 Ma) for the central Kaapvaal craton lithosphere at the southern margin of the Bushveld Complex (2,056 Ma).





lithosphere-asthenosphere boundary (LAB). However, applying a more appropriate higher mantle adiabat temperature (i.e., 1360, 1420 and 1500°C) would define the petrological LAB at greater depths (194, 205 and 220 km, respectively). The sheared peridotite xenoliths studied here have an estimated equilibration depth of >170 km, which could suggest a possible origin from near the LAB at ca. 1,153 Ma. Trace element patterns of primary mineral phases from the sheared peridotites show little metasomatic input from a magmatic

event. Oxygen fugacity estimates for the sheared peridotite xenoliths indicate the absence of strong oxidative metasomatism beneath the central Kaapvaal craton.

To further test a potential impact of the Bushveld magmatic event on the central Kaapvaal mantle lithosphere, Sr-Nd isotope ratio determinations were done for clinopyroxene mineral separates from the sheared peridotite xenoliths and were then compared to Sr-Nd past studies completed on the Rooiberg (Bushveld). The Sr and Nd isotopic compositions

of the Premier peridotite xenoliths bear no resemblance to Bushveld magmatic signatures as inferred from the most primitive Rooiberg lavas, which negates a direct and simple petrogenetic link. However, the sheared peridotite Sr and Nd isotope signatures are similar to those of the 1,153 Ma Premier kimberlite, which suggests close relationships between mantle deformation, metasomatism, and kimberlite melt formation near the LAB of the central Kaapvaal craton during the Mesoproterozoic.

A URANIUM MINERALOGICAL CHARACTERISATION OF THE A1, UE1A, A5, AND E9EC REEFS AT COOKE SECTION (RANDFONTEIN ESTATES) IN THE WEST RAND GOLDFIELD.

Sindile Mkhathswa

The uranium (U)-enriched conglomeratic reefs of Cooke Section, located in the West Rand Goldfield, comprises the UE1A, A1, and A5 reefs (Cooke 3) as well as the E9EC reef (Cooke 4). The present study, which is towards a PhD thesis on the process mineralogy and geometallurgy of

these reefs (supervised by Fanus Viljoen, Bradley Guy and Bertus Smith), is aimed at reef characterisation involving quantitative (automated) mineralogy, as well as bench top uranium leach testing. This is done in order to gain an enhanced understanding of the influence of ore

mineralogy on leaching behaviour, and to optimise the metallurgical extraction of uranium in a cost-effective manner.

The reefs are dominated by quartz, with subordinate pyrite as well as a variety of accessory minerals present (Fig. 1 & 2).

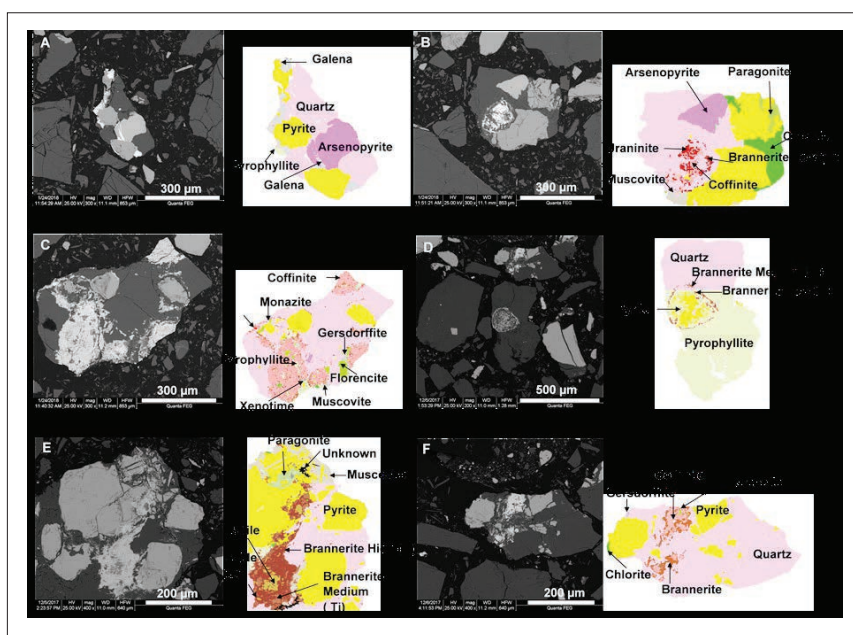


Figure 1. A-F are BSE (Backscatter Electron)-images of U-bearing minerals, identified within the samples under investigation, as well as their corresponding false colour images to the right of each BSE-image. Both image types were generated using the MLA (Mineral Liberation Analyser).

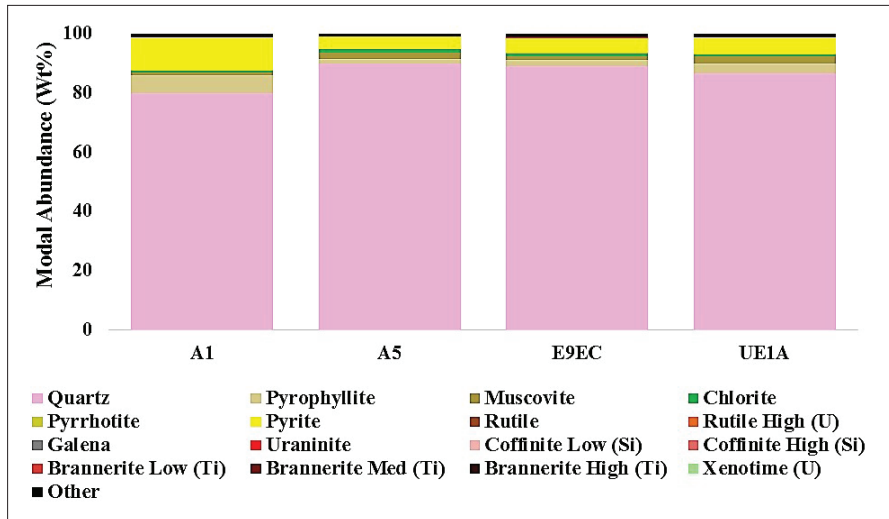


Figure 2. Modal abundances of minerals identified, indicating the most dominant minerals to be quartz, pyrite, pyrophyllite, muscovite, and chlorite.

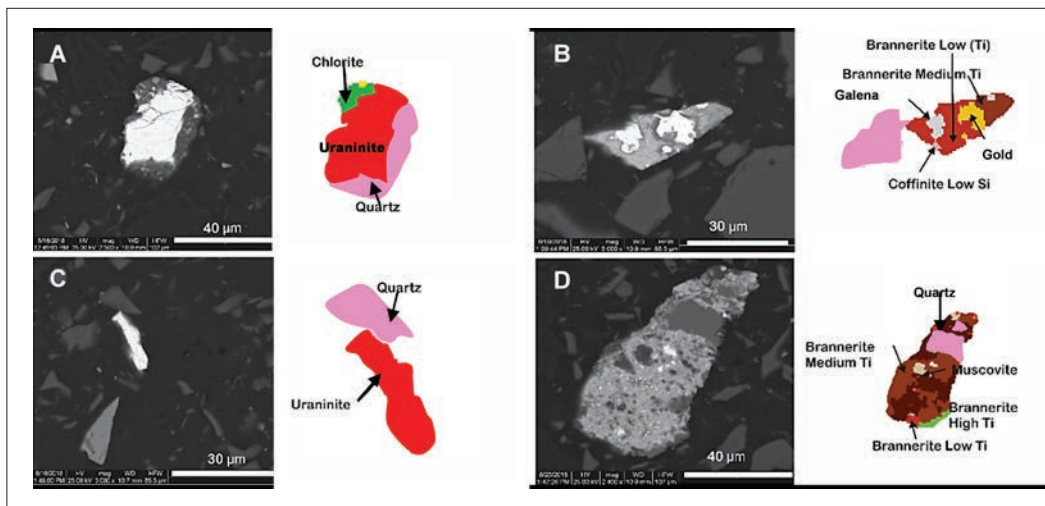


Figure 3. Backscatter electron images (left) and corresponding false colour image maps of various U-bearing phases within reef samples which have been milled to 80% passing 75 μm .

Gold is present as free gold and electrum, amenable to cyanide leaching. Relatively refractory brannerite, along with less refractory coffinite, is encountered in the various reefs, while easily leached uraninite (using sulphuric acid) is comparatively rare (Fig. 1, 2 & 3). Potential acid consumers and in some instances (those containing Iron)

Fe-contributors, such as pyrophyllite, muscovite, paragonite, chlorite and pyrrhotite are present in low abundance (Fig. 2). Significant potential acid consumers such as carbonate minerals, in acid leaching are present in negligible abundances.

Uraninite, galena, and xenotime have the least contribution towards U in the

samples especially within the A5 reef (< 5%) (Fig. 3). The E9EC has the most U distribution (~20%) within uraninite, in comparison with the other reefs (Fig. 3).

The average uranium head grade results within the A1, A5, E9EC, and UE1A reefs are ~800 ppm, ~350 ppm, 600 ppm, and ~590 ppm, respectively (Fig. 3 & Tab. 1).



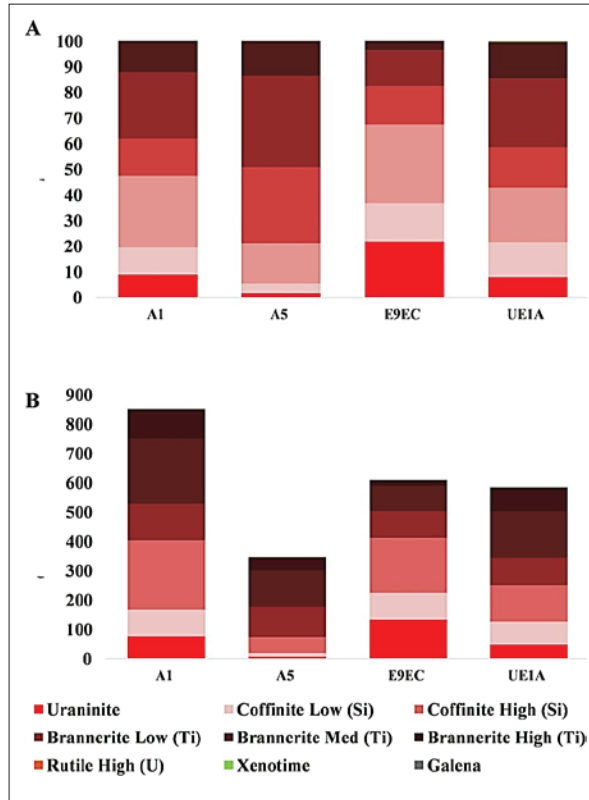


Figure 4. U department, within minerals of reef samples that were milled to 80% passing 75 μm , expressed in A) U percentage (%) and B) % normalised to assayed U grades.

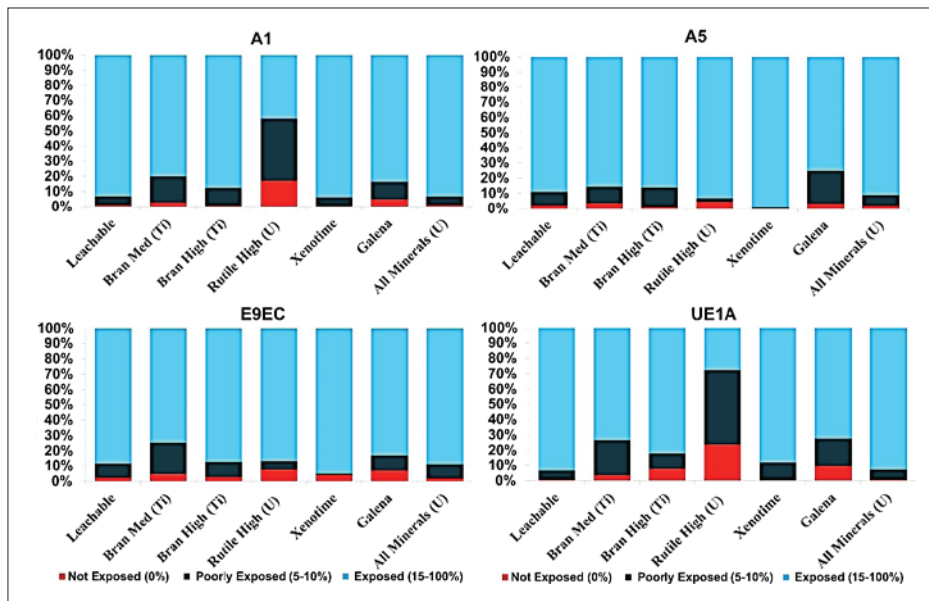


Figure 5. Distribution percent liberation by free surface, of the various U metallurgical phases, within milled (80% passing 75 μm) reef samples. Leachable = uraninite, coffinite and low Ti-brannerite.

Table 1. Percentage uranium recovered using Cooke bench top dissolution conditions. Int. = Interval.

Reef	Solids (%)	Solution (%)	Temp °C	Int.Sampling	Average mV	Residue U ₃ O ₈ (ppm)	Head U ₃ O ₈
A1	-	92	60	4	377	-	852
	-	86	60	8	377	-	
	94	94	60	24	377	59	
A5	-	73	60	4	434	-	346
	-	74	60	8	434	-	
	77	77	60	24	434	92	
E9EC	-	93	60	4	405	-	609
	-	95	60	8	405	-	
	96	96	60	24	405	29	
UE1A	-	82	60	4	376	-	586
	-	82	60	8	376	-	
	96	96	60	24	376	29	

U in the reef of lowest grade is distributed essentially within the refractory U-mineral phase brannerite and more so within brannerite of higher Ti-content. All acid soluble U-minerals are well exposed at 80% passing, 75µm. considering this, projected dissolutions within the various milled reef samples, in conjunction with department results, obtained within the present study, were expected to be in the regions of 61% for the A1, 52% for the A5, 80% for the E9EC and 57% for the UE1A-

reef (Fig. 6). However, better than expected dissolutions of 94%, 77%, 96% and 96% for the A1, A5, E9EC and UE1A-reefs were achieved, respectively, under Cooke bench top leaching conditions (Tab. 1), suggesting that the dissolved brannerite in the higher Ti-ranges may have radioactive damage and is therefore easier to dissolve than in typical scenarios (Fig. 7).

Leaching testwork revealed that U from adequately exposed brannerite, with low, medium and high Ti-content,

dissolves at Cooke conditions (30 kg/t H₂SO₄, 4 kg/t MnO₂, 60°C, 1:1 solid-solution ratio and 24 Hrs leaching residence time).

Characterisation of ore in this present study has confirmed through, mineralogy (Fig. 1, 2, 3, 4 & 5), laboratory-scale acid leaching experiments, and leached residue (Fig. 8) analyses, that the nature of ore and its mineralogy, have a significant role to play in influencing U-recovery factors.

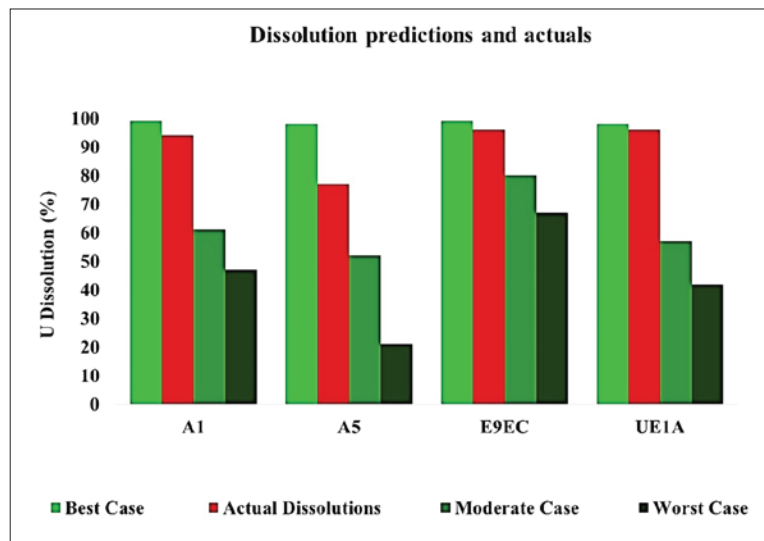


Figure 6. Bar graphs indicating predictions of bench top leaching dissolutions, as well as the actual dissolutions achieved. Calculations of predictions are based on department and exposure data. The best case scenario would be; if all exposed uranium minerals would leach, moderate case scenario = if uraninite, coffinite and low Ti-brannerite that is exposed, would leach. Worst case scenario = if only exposed uraninite and coffinite leach.



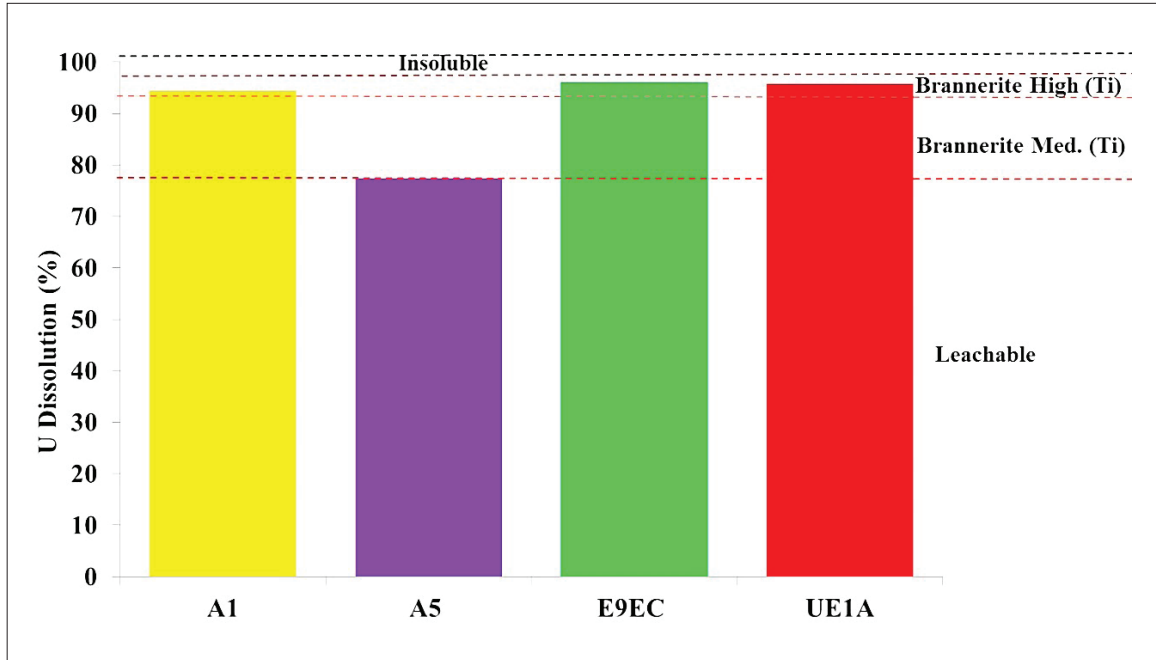


Figure 7. An interpretation of Cooke bench top leaching testwork results, based on the distribution of U within the various metallurgical phases, of the reefs under investigation.

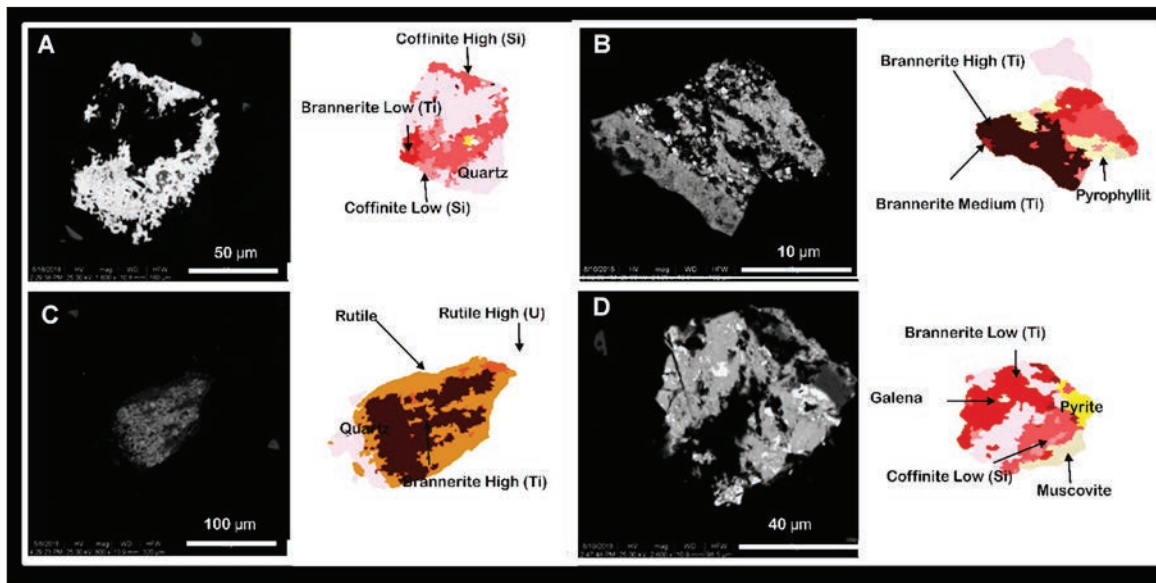


Figure 8. Backscatter electron images (left) and corresponding false colour image maps of various U-bearing phases within reef samples, which have been leached under the Cooke bench top conditions.

Precambrian environments, Geochronology and Tectonics

COMPLEXITY OF CHARACTERIZING GRANITOIDS IN HIGH-GRADE TERRANES: AN EXAMPLE FROM THE NEOARCHEAN VERBAARD GRANITOID, LIMPOPO COMPLEX, SOUTHERN AFRICA

G.A. Belyanin¹, H.M. Rajesh², O.G. Safonov^{1,3} and T.O. Basupi²

¹PPM, ²BIUST, Botswana, ³Korzhinskii Institute of Experimental Mineralogy RAS, Chernogolovka and Dept of Petrology, Moscow State University, Russia

Archean high-grade terranes are characterized by voluminous and diverse granitoid magmatism in relatively short time spans, and are good candidates to investigate the granitoid variants that characterize the Archean felsic crust (see reviews in Champion and Smithies, 2003; Condie et al., 2009; Laurent et al., 2014). However, a number of issues can complicate the characterization of these granitoids. Often it is difficult to map the extent of individual granitoid events in a given terrane. This is

because the different granitoids, which formed one after the other, occur interlayered with older supracrustal rocks, and are widely distributed rather than forming single continuous plutons. Thus in a given area within a high-grade terrane the granitoid variants can be tonalite-trondhjemites, tonalite-granodiorites or granodiorite-monzogranites, with the Na-rich ones having tonalite-trondhjemite-granodiorite (TTG)-like composition. But if considered together with occurrences of similar age from

other areas of the same terrane, TTG sensu stricto compositions can emerge. In such cases, whole-rock geochemistry can be a useful tool to characterize the different granitoid variants. Overprint event (s) are to be expected in high-grade terranes, and the granitoid can preserve effects of it. In such cases the compositional characterization need to be carefully carried out together with mineral chemical data and P-T modelling.

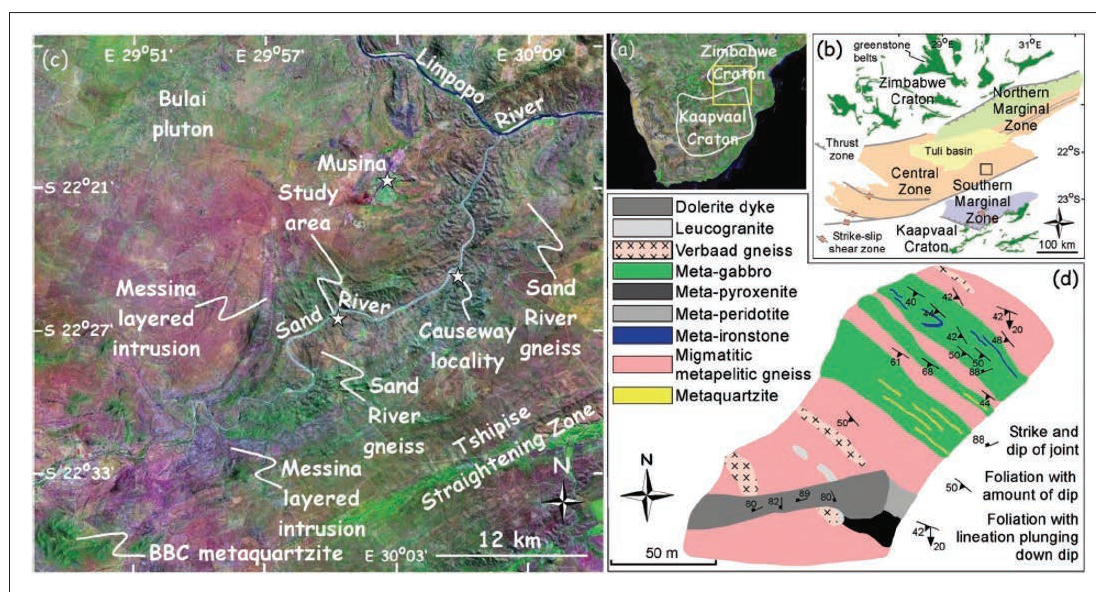


Figure 1. (a) TM742 compilation of southern Africa showing the approximate extent of the Archean Kaapvaal and Zimbabwe cratons. The box indicates the area covered in (b). (b) Generalized geologic map of the Limpopo Complex showing the approximate extents of the three zones, Southern Marginal Zone, Central Zone and Northern Marginal Zone. The box indicates the area covered in (c). (c) Geologic map of the area around Musina on a Landsat TM742 (as RGB) satellite image showing the Sand River section mapped in this study (indicated by star). (d) Geologic map of the Sand River section mapped as part of this study. BBC – Beit Bridge Complex.



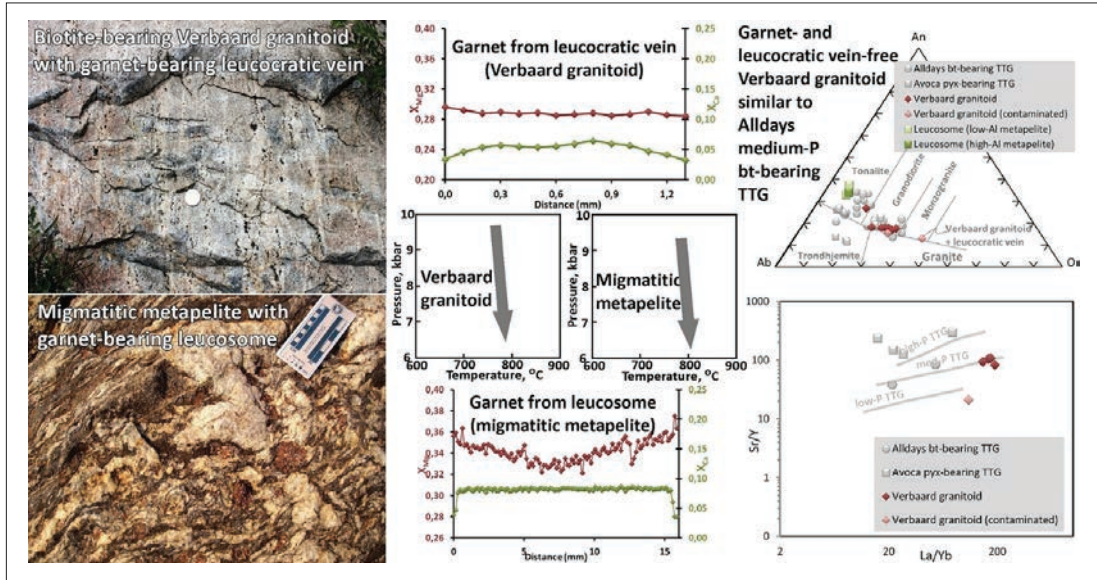


Figure 2. Generalization of the conclusions made in the study based on field, petrographic, mineral chemical, P-T modelling and whole-rock geochemical characteristics of the Neoproterozoic Verbaard granitoid and migmatitic metapelite. (left) leucocratic garnet-bearing veins associated with Verbaard granitoid and migmatitic metapelite hosting garnet-bearing leucosome, (middle) X(Mg) and X(Ca) profiles through garnets from the corresponding rock varieties as well as P-T modelling based on pseudosections applications (Rajesh et al, 2018), (right) geochemical diagrams showing pseudo-comparison of Verbaard granitoid with other granitoid types from the Central Zone of the Limpopo Complex.

Our study is focused on field, petrographic, mineral chemical and whole-rock geochemical characteristics of the Neoproterozoic Verbaard granitoid from the type locality in the central part of the Limpopo Complex in southern Africa (Fig. 1). Considering the occurrence of garnet, comparison with garnet-bearing migmatitic metapelite and associated garnet-bearing leucosome from the study area was carried out. Phase equilibria modeling of the migmatitic metapelite and Verbaard granitoid compositions was used to reconstruct P-T conditions of their evolution. After evaluating the provenance of garnet associated with the Verbaard granitoid, petrogenetic characterization of carefully selected granitoid samples was attempted. The results are compared with the data on other related Neoproterozoic granitoids from the region (Fig. 2).

The results of our study demonstrated that granitoids produced during the same magmatic cycle, but exposed

in different parts of a high-grade terrane, can exhibit effects of variable local overprint events and, hence, look different (for instance, Verbaard, Avoca, Alldays, Bulai etc granitoids from the Central Zone).

Whole-rock geochemical characteristics demonstrated that among other temporally and spatially associated Neoproterozoic granitoids of the Beit Bridge Complex (main component of the Central Zone), the closest correlatives for the Verbaard granitoids are the Alldays granitoids. Thus, the Verbaard granitoid represents just a local manifestation of the voluminous Alldays TTG granitoid magmatism in the Verbaard area.

The Verbaard granitoids were subjected to both metamorphic and partial melting events recorded in formation of garnet in the rocks and garnet-bearing leucocratic veins. Phase equilibria modelling indicates that rare low X(Ca) garnets in the granitoids are re-equilibrated relics related to a low-pressure stage

(7.5–6.5 kbar) of the ~2.61 Ga high-grade event that affected the rocks. In comparison, higher-Ca cores of large garnets in leucocratic veins associated with the granitoids are interpreted to represent an earlier high-pressure stage of the Neoproterozoic event (9.0–9.5 kbar). Thus, the veins served as potential sites for preservation of different stages of garnet formation in the granitoids. Compositional variations of garnets in the Verbaard granitoids reflect a decompression at temperatures 740 to 800 °C during the Neoproterozoic high-grade event.

Similar metamorphic evolution is recorded in garnets in country metapelites intruded by the Verbaard granitoids. Compositional evolution of garnet from the leucosomes associated with migmatitic metapelites is comparable to that of garnet in the leucocratic veins in the Verbaard granitoids, arguing for a common decompression-related evolution during the same Neoproterozoic high-grade event.

During decompression, segregated melts differently affected the Verbaard granitoids and migmatitic metapelites. The tonalitic composition of the

leucosomes in metapelites shows that melt loss was prominent in them. The granitic leucocratic vein in the Verbaard granitoid represents the

closest starting composition of the anatexic melt, which underwent complete crystallization without (or with negligible) melt loss.

References

Champion, D.C., Smithies, R.H., 2003. Archean granites. In: Blevin, P.L., Chappell, B.W., Jones, M. (Eds.), *Magmas to Mineralisation: The Ishihara Symposium*. AGSO Geoscience Australia, pp. 19–24 (Record 2003/14).

Condie, K.C., Belousova, E., Griffin, W.L., Sircombe, K.N., 2009. Granitoid events in space and time: constraints from igneous and detrital zircon age spectra. *Gondwana Research* 15, 228–242.

Laurent, O., Martin, H., Moyen, J.F., Doucelance, R., 2014. The diversity and evolution of late-Archean granitoids: evidence for the onset of "modern-style" plate tectonics between 3.0 and 2.5 Ga. *Lithos* 205, 208–235.

Rajesh HM, Safonov OG, Basupi TO, Belyanin GA, Tsunogae T (2018) Complexity of characterizing granitoids in high-grade terranes: An example from the Neoproterozoic Verbaard granitoid, Limpopo Complex, Southern Africa. *Lithos*, 318-319, 399-418.

AGE AND ORIGIN OF THE ULTRAMAFIC-MAFIC STOLZBURG COMPLEX IN THE BARBERTON GREENSTONE BELT, SOUTH AFRICA

Gabrielle Ficq, Sebastian Tappe (PPM), Robert Bolhar, Allan Wilson (Wits) and Chris Harris (UCT)

Much debate surrounds the origin of Earth's first continents. In this debate the evolution of granite-greenstone terranes plays a central role. The Barberton Greenstone Belt (BGB) has one of the best-preserved Early Archean rock records worldwide. A striking feature of the BGB is the occurrence of some 27 ultramafic

complexes that are interleaved with the volcano-sedimentary successions of the Onverwacht Group. These complexes have been variably interpreted as remnants of Early Archean oceanic lithosphere and deep plumbing systems to the BGB komatiite volcanic systems on stabilizing continental lithosphere.

However, the petrology and age relationships of the ultramafic complexes remain poorly constrained, which hampers our understanding of the tectonic evolution of the BGB, and Archean continent formation in general.

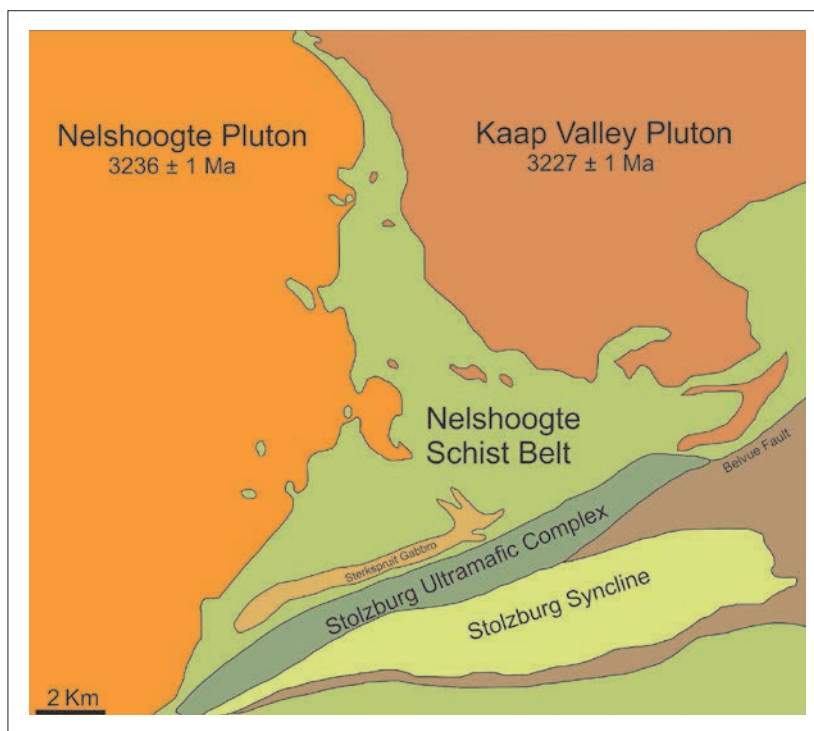
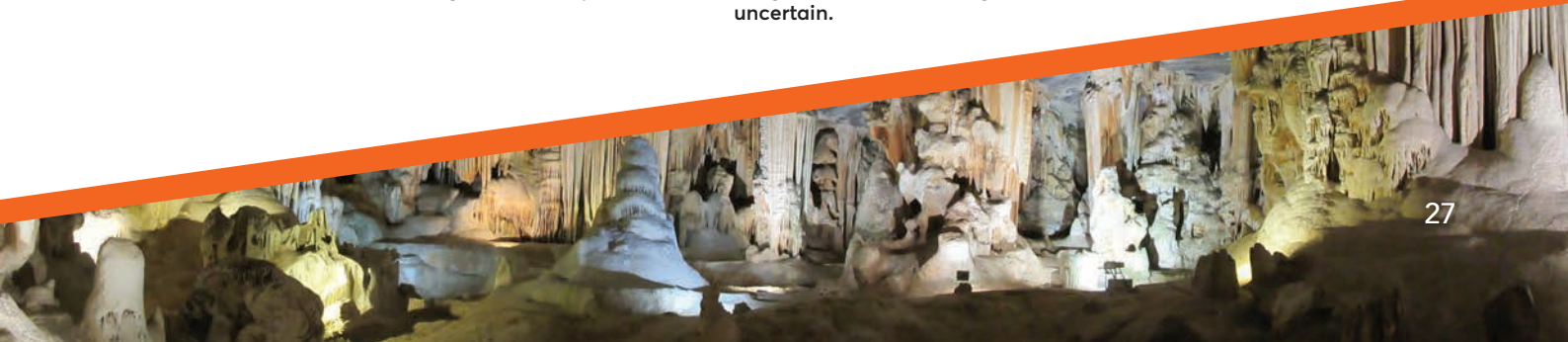


Figure 1: Location map of the ultramafic-mafic Stolzburg Complex within the northern Barberton Greenstone Belt (adapted from Anhaeusser, 2001). The Complex is part of the Nelshoogte Schist Belt of the Onverwacht Group, but its age relationship to the surrounding TTG intrusions and greenstone units is uncertain.





We currently investigate the petrology, geochemistry and geochronology of ultramafic and mafic rocks from the Stolzberg Complex (northern BGB; Figure 1), which represents one of the largest and best-preserved ultramafic complexes. LA-MC-ICPMS U/Pb titanite age determinations for gabbroic rocks yield ages between 3,236 and 3,270 Ma. Although these radiometric dates are interpreted as minimum ages probably representing the timing of seafloor alteration, they are considered to be close approximations of the formation age of the Stolzberg Complex as part of the ca. 3.3 Ga Weltevreden Formation (uppermost Onverwacht Group). An important role for seafloor alteration

processes in the early evolution of the Stolzberg Complex is indicated by metasomatic growth of albite and titanite in the gabbros. Furthermore, the oxygen isotopic compositions of the gabbroic rocks range from +5‰ (i.e., mantle-like) to +10‰ $\delta^{18}\text{O}$, with the upper end of the spectrum being typical for low-temperature hydrothermal alteration. Massive pyroxenite bodies record surprisingly low crystallization temperatures between 900 and 1100°C. These relatively low temperatures preclude a direct association with hot komatiite magmas; rather they support an origin as cumulates from basaltic magmas within cooler oceanic crust. This idea is supported by orthopyroxene trace

element modelling, which suggests that the liquid in equilibrium with the cumulate crystals was basaltic in composition. Olivine from peridotitic cumulates has a relatively low forsterite content between 88 and 89 mol.%, which provides an additional line of evidence against a komatiite connection at Stolzberg.

The currently available data for the Stolzberg Complex point toward an origin as tectonically dismembered pieces of ca. 3.3 Ga oceanic lithosphere (including an oceanic plateau option), with an important role for cumulate processes and seawater interaction, similar to modern ophiolites.

References:

Anhaeusser, C.R., 2001. The anatomy of an extrusive-intrusive Archaean mafic-ultramafic sequence: The Nelshoogte Schist Belt and Stolzberg Layered Ultramafic Complex, Barberton Greenstone Belt, South Africa. *South African Journal of Geology* 104, 167-204.

UNRAVELLING THE ARCHAEOAN RECORD OF THE SINGHBHUM CRATON: GEOBIOLOGICAL INSIGHTS FROM THE 3.51 GA OLD DAITARI GREENSTONE BELT, INDIA

J. Jodder¹, J. A. Hofmann¹, E.E. Stüeken², H. Xie³, A. Wilson⁴ and C. Reinke¹

¹PPM and SPECTRUM analytical facility, UJ; ²University of St. Andrews, Scotland, UK; ³Beijing SHRIMP Centre, Chinese Academy of Geological Sciences, China; ⁴Wits University

The Singhbhum craton of India has an Archaean geological history quite similar to the Kaapvaal craton. The most ancient rocks currently known in the Singhbhum craton include 3.5 Ga old TTG gneisses and greenstone belts known as the southern and eastern Iron Ore Group (IOG). Felsic volcanoclastic rocks dated at 3.51 Ga (Mukhopadhyay et al., 2008) allow direct comparisons with the lower portions of the Onverwacht and Nondweni groups of the Kaapvaal craton. Palaeoarchaean successions wrap around or are intruded by the Singhbhum granite complex, an assemblage of TTG and granite, the youngest suite of which is 3.1 Ga old (Saha, 1994). Emplacement of the granite complex was associated with

stabilization of the central part of the Singhbhum craton, in much the same way as the widespread intrusion of 3.1 Ga granites of the Kaapvaal craton. Layered mafic-ultramafic complexes are widespread in both cratons. In the Singhbhum craton, these contain important PGE and chromite deposits and have been dated at c. 3.12 Ga (Augé et al., 2003). Such complexes in the Kaapvaal craton are as yet undated, and no metal deposits have been found so far.

Although the spatial distribution of these supracrustal blocks was established from mapping conducted by various workers and the Geological Survey of India (GSI), a definite stratigraphic understanding is lacking. The IOG stratigraphic

term lumps together a number of different volcano-sedimentary units, such as (1) typical greenstone belt assemblages of the North-Eastern IOG, Daitari (Southern) IOG, and correlative greenstone belts and (2) intracontinental successions of the North-Western IOG that include metabasalt, quartzite, shale, BIF and, locally, dolomite. The IOG hosts important iron ore deposit associated with banded iron formation and other well-preserved Archaean rock units that have the potential to provide important new information on geological processes operating in the Archaean. The Daitari greenstone belt of the southern Singhbhum has experienced only low-grade metamorphism and includes a well-

perpetuated submarine volcano-sedimentary succession of mafic-ultramafic rocks, felsic volcanics dated at 3.51 Ga, and intercalated banded cherts, shales and iron formation. The Daitari greenstone belt thus provides a new window into the early Earth. The extensively studied Palaeoarchaean rocks of the Barberton greenstone belt, Kaapvaal craton, and the Pilbara craton, Western Australia, provide direct geologic evidence of the nature and evolution of early Earth processes, and the habitat of early life. Even older, but higher-grade metasedimentary succession are reported from the >3.7Ga Isua supracrustal belt of Greenland and the Nuvvuagittuq Belt in Quebec. Vestiges of early life have been postulated in both these regions based on inconclusive isotopic constraints. However, these rocks have undergone

amphibolite facies metamorphism, obscuring geologic constraints on early Earth surface environment. Bonafide microfossils and microfossil assemblages, such as reworked microbial mats (Tice and Lowe, 2004), organic-walled microfossil assemblages (Javaux et al., 2010; Sugitani et al., 2015) and filamentous microfossils (Walsh, 1992) have been documented from different Paleo-Mesoarchaean volcano-sedimentary successions of both cratons, allowing a valuable insight into early life on Earth. In this study, we have examined hints of akin biosignatures from the low-grade carbonaceous cherts of the 3.51 Ga old Daitari belt of the Singhbhum craton. Detailed field, petrographic and geochemical studies of chemical sedimentary rocks of the Sindurimundi Parbat Formation, consisting of

carbonaceous chert and BIF, reveal their strong similarity with the Buck Reef Chert of the Barberton belt and suggest primary biogenic processes for the origin of carbonaceous matter. Carbonaceous matter preserved in these cherts is preserved as (1) composite carbonaceous grains, (2) reworked carbonaceous clasts, (3) finely laminated carbonaceous layers and (4) ripped off microbial mats (Fig 1b&d). Carbon isotopic compositions of the carbonaceous sediments are highly depleted in $\delta^{13}\text{C}$ ranging from -33‰ to -21‰, which advocates for the organic matter to have been derived in a shallow water environment. Further, evidence of spindle-shaped microfossils (Fig 1a&b) from these cherts are highly indicative of an active biological niche in the Palaeoarchaean Earth.

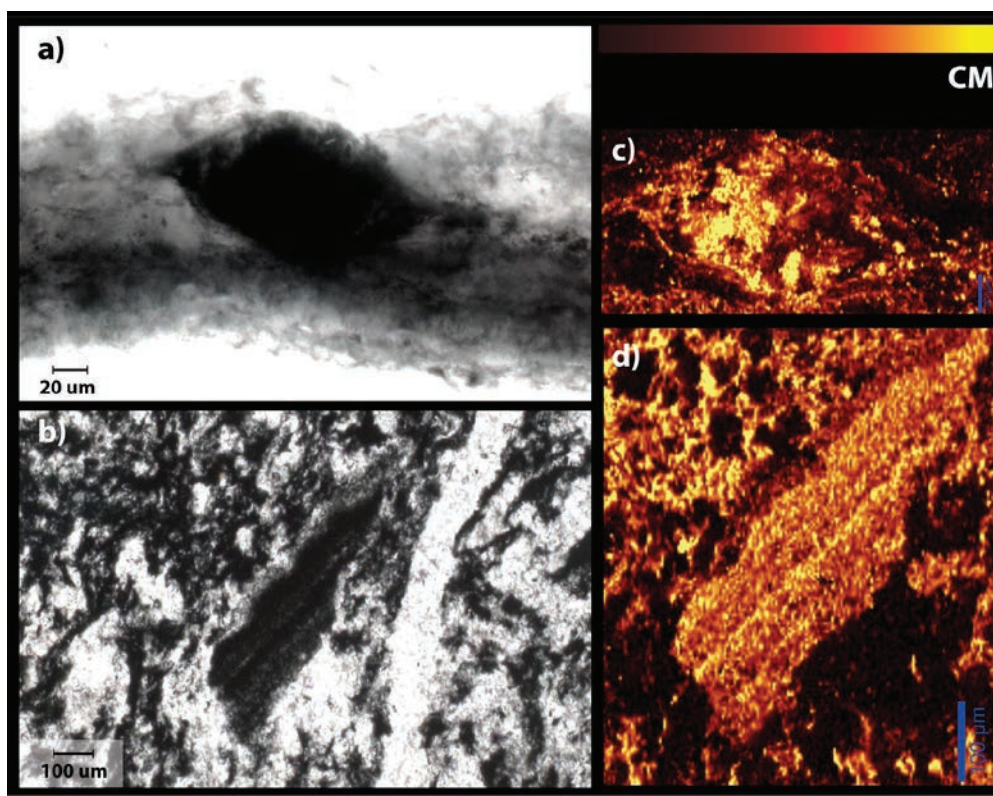


Figure 1: a) Spindle shape microfossil b) Ripped up segment of a crinkle layered mat-like lamination entrained within a matrix of microcrystalline chert and carbonaceous matter c) & d) Raman maps of carbonaceous matter (CM) G band at $\sim 1,589\text{ cm}^{-1}$, of spindle shape microfossil and microbial mat-like lamination. Brighter areas within Raman maps reflect higher intensities of carbon spectra.





References

Augé, T., Cocherie, A., Genna, A., Armstrong, R., Guerrot, C., Mukherjee, M.M., Patra, R.N., 2003. Age of the Baula PGE mineralization (Orissa, India) and its implications concerning the Singhbhum Archaean nucleus. *Precambrian Res.* 121, 85–101. [https://doi.org/10.1016/S0301-9268\(02\)00202-4](https://doi.org/10.1016/S0301-9268(02)00202-4)

Javaux, E.J., Marshall, C.P., Bekker, A., 2010. Organic-walled microfossils in 3.2-billion-year-old shallow-marine siliciclastic deposits. *Nature* 463, 934–938. <https://doi.org/10.1038/nature08793>

Mukhopadhyay, J., Beukes, N.J., Armstrong, R.A., Zimmermann, U., Ghosh, G., Medda, R.A., 2008. Dating the Oldest Greenstone in India: A 3.51-Ga Precise U-Pb SHRIMP Zircon Age for Dacitic Lava of the Southern Iron Ore Group, Singhbhum Craton. *J. Geol.* 116, 449–461. <https://doi.org/10.1086/590133>

Saha, A.K., 1994. Crustal evolution of Singhbhum-North Orissa, Eastern India. Geological Society of India, Memoir 27, Bangalore, 341, 1994

Sugitani, K., Mimura, K., Takeuchi, M., Yamaguchi, T., Suzuki, K., Senda, R., Asahara, Y., Wallis, S., Van Kranendonk, M.J., 2015. A Paleoproterozoic coastal hydrothermal field inhabited by diverse microbial communities: The Strelley Pool Formation, Pilbara Craton, Western Australia. *Geobiology* 13, 522–545. <https://doi.org/10.1111/gbi.12150>

Tice, M.M., Lowe, D.R., 2004. Photosynthetic microbial mats in the 3,416-Myr-old ocean. *Nature* 431, 549–552. <https://doi.org/10.1038/nature02888>

Walsh, M.W., 1992. Microfossils and possible microfossils from the early archaean onverwacht group, Barberton mountain land, South Africa. *Precambrian Res.* 54, 271–293. [https://doi.org/10.1016/0301-9268\(92\)90074-X](https://doi.org/10.1016/0301-9268(92)90074-X)

THE BUEM OPHIOLITE AND ITS IMPLICATION TO THE EVOLUTION OF THE PAN-AFRICAN DAHOMEYIDE OROGEN, WEST AFRICA

Daniel Kwayisi, Jeremie Lehmann and Marlina Elburg

The geodynamic setting and tectonic evolution of the Buem Structural Unit (BSU) remain contentious, as the BSU's origin within the Pan-African Dahomeyide Orogen is not

well constrained. The major question is whether the BSU represents an ophiolite sequence and thereby, how it relates to the suture zone of the Pan-African Dahomeyide Orogen. Burke

and Dewey (1972) considered the BSU as an ophiolite sequence, which marks a suture between two collided continents (West African Craton and Saharan Metacraton). However,



Figure 1: Pillow lava with tilted face to the East.

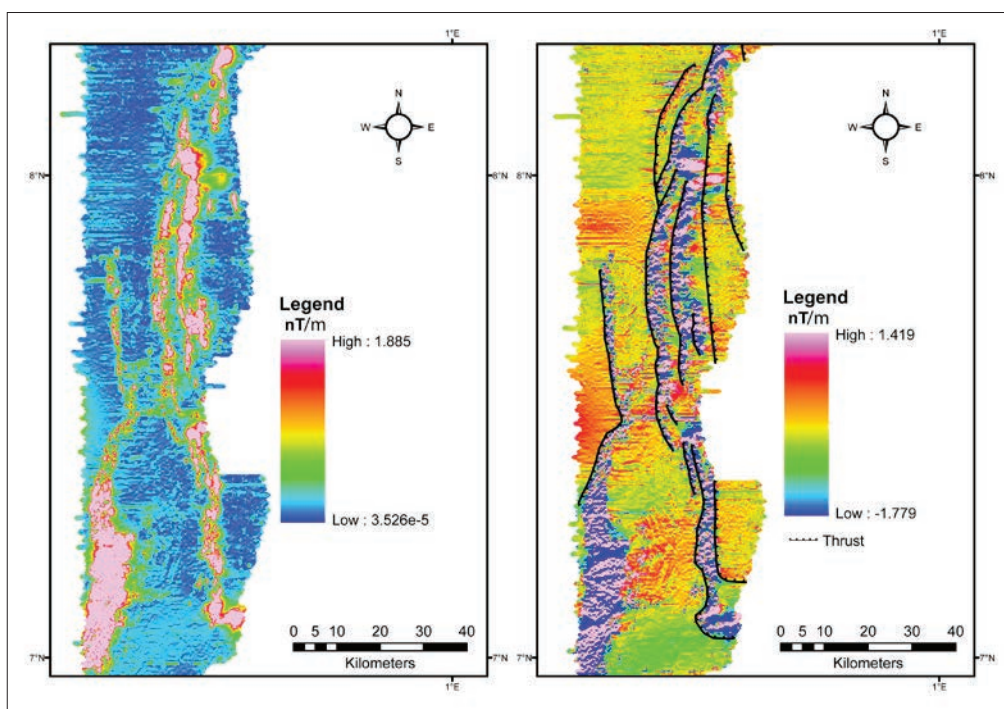


Figure 2: (a) Analytical signal (AS) and (b) First vertical derivative (VD1). Major thrust faults have been interpreted based on cyclic map repetition of same magnetic signal and asymmetric sharp changes on the western side of the magnetic highs. These thrust faults were identified in the field in areas where strongly schistose serpentinites are in contact with or at places overlies the sedimentary rocks.

according to Affaton et al. (1997) the BSU cannot represent a Pan-African major or cryptic suture zone owing to its occurrence within rocks of the western passive margin of the Pan-African paleo-ocean. This study presents preliminary field, structural, airborne geophysical and geochemical data on the BSU to better constrain its origin within the Pan-African Dahomeyide Orogen and propose a model for its geodynamic setting. Rocks of the BSU are sandstones and shales of both marine and continental origin, pillow lavas, gabbros and serpentinitized peridotites. Geochemical data for the mafic-ultramafic igneous

rocks show their affinity to MORB with both alkaline and subalkaline characteristics. This assemblage of rocks, coupled with their geochemical signature may suggest the existence of an oceanic basin, and because all these rocks were deformed by the Pan-African orogenic events, it is inferred that the BSU could represent an ophiolite suite. Field observations and aeromagnetic data indicate that the mafic-ultramafic igneous rocks generally trend NNW and occur as tectonic slices, marking the boundaries between thrust sheets within the BSU. One important observation made from the geophysical data is

the conspicuous ENE-trending long wavelength magnetic anomalies in the BSU that are continuous and along-strike with the regional structures of the West African Craton (WAC) to the West. This supports thrusting and nappe stacking of the BSU on the WAC during the Pan-African orogeny. Thus the ophiolites of the BSU could be part of the lower plate stripped off and accreted onto the WAC during subduction. These, coupled with the association of rocks (continental and marine sediments), and the structures suggest that the BSU may be part of the accretionary wedge of the Pan-African Dahomeyide arc.

References

- Affaton, P., Aguirre, L. and Ménot, R.-P. (1997). Thermal and geodynamic setting of the Buem volcanic rocks near Tiélé, Northwest Benin, West Africa. *Precamb. Res.* Vol. 82, pp. 191–209.
- Burke, K.C., Dewey, J.F. (1972). Orogeny in Africa. In: Dessauvagie, T.F.J., Whiteman, A.J. (Eds.), *African Geology*. Dept. Geol., Univ. Ibadan, Nigeria, pp. 583–608.





THE TIMING, ORIGIN AND SIGNIFICANCE OF WITWATERSRAND BASIN CARBONACEOUS MATTER

Tshepang Lechekoane

The Archaean Witwatersrand Basin in South Africa is a classic example of a palaeoplacer gold deposit hosted in quartz pebble conglomerates, also known as reefs. These reefs have

produced an estimated 52 000 tons of gold from the onset of mining in the late 1800s to date. Consequently, this makes the Witwatersrand Basin the richest and the single most important

gold province in the world. The reefs also host a large array of detrital heavy minerals - mainly pyrite, but also zircon, rutile, uraninite and many others - indicating prolonged periods

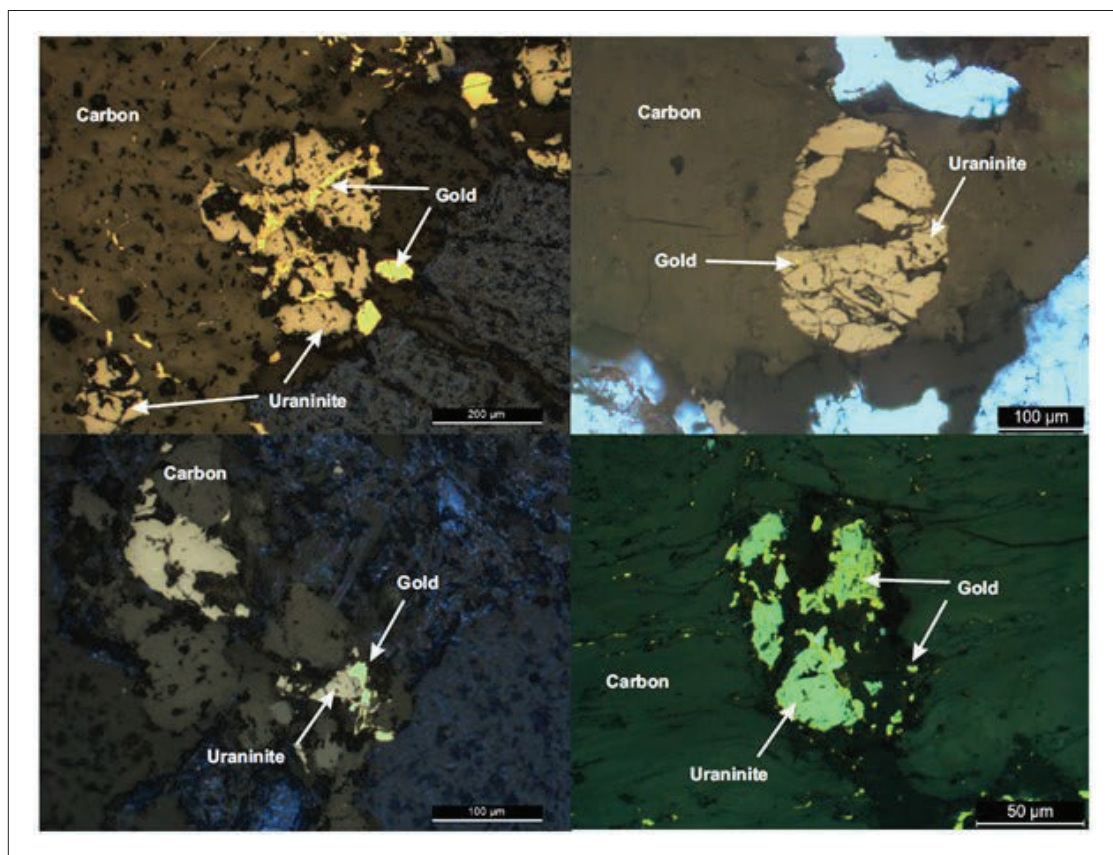


Figure 1: Microphotographs from various reefs showing the intimate association between carbon, gold and uraninite. Note that uraninite is present as detrital and secondary grains.

of sedimentary reworking and placer mineral concentrations. Following deposition, diagenetic, hydrothermal and metamorphic fluids (aqueous and hydrocarbon-bearing) modified the primary mineralogy of the reefs, giving rise to remobilization of some of the primary ore constituents, including gold and uranium-bearing minerals.

An important aspect of the gold ore involves the presence of ubiquitous carbonaceous matter in many reefs, as seams of columnar-textured bitumen and sand-sized nodules as well as cross-cutting veinlets. There is a clear spatial association between gold and carbonaceous matter (fig 1), and carbon-bearing reefs have been some of the most economically productive (Spangenberg and Frimmel, 1999). The origin of this carbonaceous matter is highly debated in both older and more recent literature. Interpretations of the origin of the carbonaceous matter have been polarized between two main models, in line with the debate on the origin of gold. One model argues for the origin of the carbon seams as fossil microbial mats that trapped detrital gold, uraninite and other heavy minerals (Snyman, 1965; Feather and Koen, 1975; Hallbauer, 1975, 1981, 1986; Minter, 1978, 1993; Zumberge et al., 1978, 1981; Smits, 1984; Ebert et al., 1990). While this model has been largely discounted in studies done 15-20 years ago, it continues to be regarded viable by several researchers (Horscroft et al., 2011; Frimmel and Hennigh, 2015; Heinrich, 2015). For example, Heinrich (2015) argued that dissolved gold

transported in aqueous solutions became fixed by microbial mats resulting in the rich gold endowment of the carbon seams. There is however little petrographic evidence in support of this interpretation. In fact, there is a wealth of evidence that does not support a microbial mat origin for the carbon seams (e.g. Parnell, 1999; England et al., 2001).

The more widely accepted model for the origin of the carbonaceous matter argues for its introduction after deposition, in the form of oil that was generated at different times in the evolution of the Witwatersrand Basin (Liebenberg, 1955; Schidlowski, 1981; Robb et al., 1994, 1997a, b, c; Robb and Meyer, 1995; Parnell, 1996, 1999; Barnicoat et al., 1997; Buick et al., 1998; Gray et al., 1998; Drennan et al., 1999; Spangenberg and Frimmel, 1999; Fuchs et al., 2016). There are two variations to this model, with one variant arguing for the distribution of bitumen to be entirely fracture-controlled (e.g. Parnell, 1999), while the other model argues for a primary mineralogical-stratigraphic control for the bitumen distribution (England et al., 2001). The two model variants also differ in the interpretation of the origin of uraninite that is widely distributed in the gold reefs. It is generally acknowledged that the emission of alpha- and beta-particles during the radioactive decay of U and Th abundant in some minerals (uraninite, but also monazite) can lead to radiolytic polymerization and solidification of mobile hydrocarbons around such grains (e.g. Schidlowski,

1981). The origin of the carbonaceous matter as residues of migrating hydrocarbons is convincing, as nearly all carbonaceous matter in the Witwatersrand Basin is associated with U-bearing minerals, principally uraninite and its alteration products (Schidlowski, 1981). While the one model variant argues for the uraninite to be largely hydrothermal in origin (Phillips and Myers, 1989; Parnell, 1996, 1999; Barnicoat et al., 1997; Gray et al.; 1998; Mc-Cready and Parnell, 1998), there is overwhelming evidence for much of the rounded uraninite to represent detrital grains (Ramdohr, 1958; Grandstaff, 1974; Minter, 1978; Schidlowski, 1981; Feather, 1981; Feather and Glatthaar, 1987; Robb and Meyer, 1995; Burron et al., 2018).

Although the evidence of bitumen and uraninite association is overwhelming, not all bitumen is associated with uraninite. Nonuraniferous bitumen is observed as overgrowths on pre-existing (possibly much older) uraniferous bitumen nodules, and lobate shaped nodules interstitial between grains (fig 2). Other forms of nonuraniferous bitumen are observed as infill in veinlets and fractures within quartz grains and associated framework mineralogy. Here we present clear evidence of at least two generations of carbon in the Vaal Reef. The nonuraniferous carbon could represent an entirely different event of hydrocarbon circulation which is unrelated to that which is associated with uraninite.



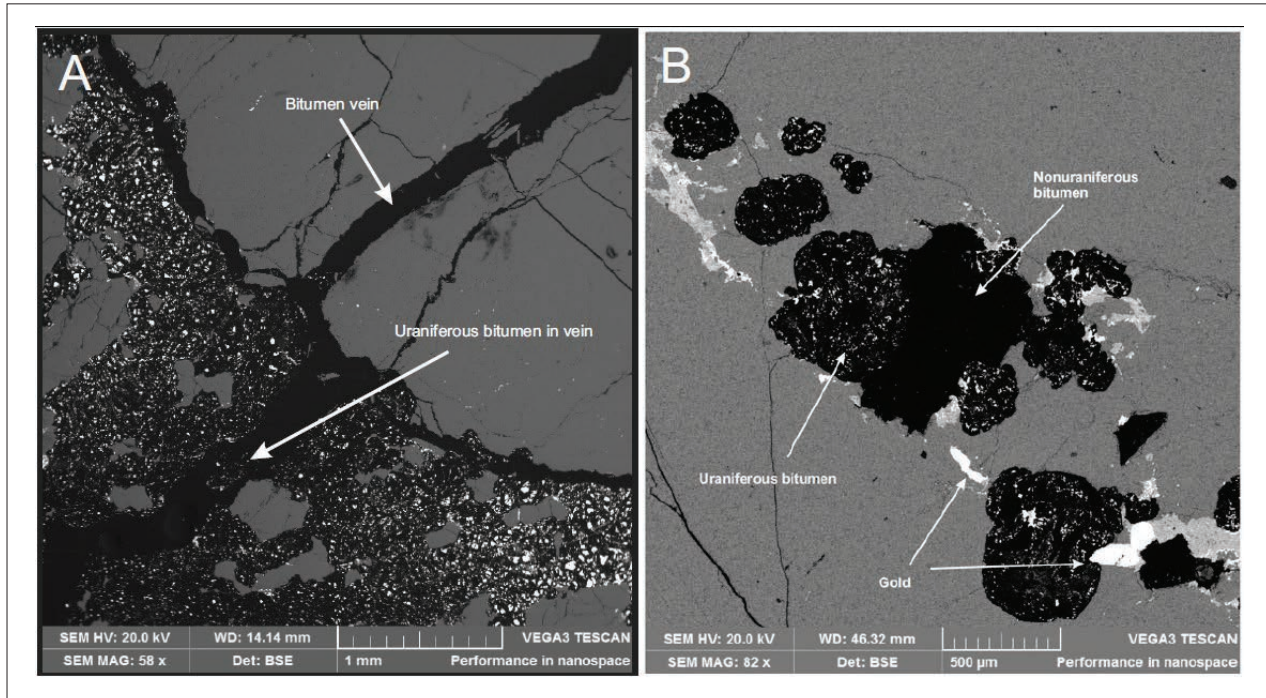


Figure 2: Scanning Electron Microscope (back scattered election) image of the Vaal Reef showing an inclusion of uraniferous bitumen in a nonuraniferous bitumen vein (A) and (B) - nonuraniferous bitumen overgrowth on uraniferous bitumen. White specs are uranium-bearing minerals.

References:

- Barnicoat, A.C., Henderson, I.H.K., Knipe, R.J., Yardley, B.W.D. et al., 1997, *Nature*, 386, 820–824.
- Buick, R., Rasmussen, B., and Krapez, B., 1998, *AAPG Bulletin*, 82, 50–69.
- Burron, I., da Costa, G., Sharpe, R., Fayek, M., Gauert, C. and Hofmann, A., 2018, *Geology*, 46, 295–298.
- Drennan, G.R., Boiron, M.-C., Cathelineau, M., and Robb, L.J., 1999, *Mineralogy and Petrology*, 66, 83–109.
- Dutkiewicz, A., Rasmussen, B., and Buick, R., 1998, *Nature*, 395, 885–888.
- Ebert, L.B., Robbins, E.I., Rose, K.D., Kastrup, et al., 1990, *Ore Geology Reviews*, v. 5, p. 423–444.
- England, G. L., Rasmussen, B., Krapež, B., & Groves, D. I. 2001. *Economic Geology*, 96, 1907–1920.
- England, G.L., Rasmussen, B., Krapez, B. & Groves, D.I. 2002. *J. of the Geol. Soc.* 159, 189–201.
- Feather, C.E., and Glatthaar, C.W., 1987, IAEA Technical Document 427, p. 355–386.
- Feather, C.E., 1981, U.S. Geological Survey Professional Paper, v. 1161-Q, p. 1–23.
- Feather, C.E., and Koen, G.M., 1975, *Mineral Sciences and Engineering*, v. 7, p. 189–224.
- Frimmel, H. E., Groves, D. I., Kirk, J., Ruiz, J., Chesley, J. & Minter, W. E. L. 2005, *Economic Geology 100th Anniversary Volume*, 769–797.
- Frimmel, H. E., & Hennigh, Q. 2015. *Mineralium Deposita*, 50(1), 5–23.
- Grandstaff, D.E., 1974, *Geological Society of South Africa Transactions*, v. 77, p. 291–294.
- Gray, G.J., Lawrence, S.R., Kenyon, K., and Cornford, C., 1998, *Journal of the Geological Society of London*, v. 155, p. 39–59.
- Hallbauer, D.K., 1975, *The plant origin of Witwatersrand carbon: Mineral Sciences and Engineering*, v. 7, p. 111–131.
- Hallbauer, D.K., 1981, U.S. Geological Survey Professional Paper, v. 1161-M, p. 1–22.
- Hallbauer, D.K., 1986, in Anhaeusser, C.R., and Maske, S., eds., *Mineral deposits of southern Africa: Johannesburg*, Geological Society of South Africa, p. 731–752.
- Heinrich, C. A. 2015. *Nature Geoscience*, 8(3), 206–209.
- Hoefs, J., & Schidlowski, M. (1967). *Science*, 155, 1096–1097.
- Horscroft et al., 2011. *SEPM Special Publication No. 101*, pp. 75–95.
- Landais, P., Michels, R., Poty, B. and Monthieux, M., 1989. *Journal of analytical and applied pyrolysis*, 16(2), pp.103–115.
- Liebenberg, W.R., 1955, *Geological Society of South Africa Transactions*, v. 58, p. 101–227.
- Meady, A.J., and Parnell, J., 1998, *Transactions of the Institute of Mining and Metallurgy*, v. 107, p. B89–B97.
- Minter, W.E.L., 1978, *Memoir of the Canadian Society of Petroleum Geologists*, v. 5, p. 801–829.

- Minter, W.E.L., 1993, in Foster, R.P., ed., *Gold metallogeny and exploration*: London, Chapman and Hall, p. 283–308.
- Parnell, J., 1996, *ECONOMIC GEOLOGY*, v. 91, p. 55–62.
- Parnell, J., 1999, *Journal of Sedimentary Research*, v. 69, p. 164–170.
- Phillips, G.N., and Myers, R.E., 1989, *ECONOMIC GEOLOGY MONOGRAPH 6*, p. 598–608.
- Ramdohr, P., 1958, *Geological Society of South Africa Transactions, Annexure 61*, p. 1–50.
- Robb, L.J., Landais, P., Drennan, G., and Dubessy, J., 1997a, [ext. abs.]: *Geofluids II 97*, Belfast, The Queen's University, Extended Abstract Volume, p. 452–455.
- Robb, L.J., Charlesworth, E.G., Drennan, G.R., Gibson, R.L., and Tongu, E.L., 1997b, *Australian Journal of Earth Sciences*, v. 44, p. 353–371.
- Robb, L.J., Landais, P., Drennan, G.R., and Dubessy, J., 1997c, *University of the Witwatersrand, Economic Geology Research Unit Information Circular*, v. 312, 34 p.
- Robb, L.J., and Meyer, F.M., 1995, *Ore Geology Reviews*, v. 10, p. 67–94.
- Schidlowski, M., 1981, *U.S. Geological Survey Professional Paper*, v. 1161- N, p. 1–23.
- Smits, G., 1984, *Precambrian Research*, v. 25, p. 37–59.
- Spangenberg, J., and Frimmel, H., 1999, in Stanley, P.W., et al., eds., *Mineral deposits: Processes to processing*: Rotterdam, Balkema p. 271–274.
- Spangenberg, J. E., & Frimmel, H. E. 2001, *Chemical Geology*, 173, 339–355.
- Snyman, C.P., 1965, *Geological Society of South Africa Transactions*, v. 68, p. 225–235.
- Xiong Y, Wood S.A. 2000, *Mineral Petrol* 68:1–28
- Zumberge, J.E., Sigleo, A.C., and Nagy, B., 1978, *Mineral Sciences and Engineering*, v. 10, p. 223–246.
- Zumberge, J.E., Nagy, B., and Nagy, L., 1981, *U.S. Geological Survey Professional Paper*, v. 1161-O, p. 1–7.

STRUCTURAL AND GEOCHRONOLOGICAL CONSTRAINTS ON POLYPHASE DEFORMATION OF THE ZWARTKOPS HILLS, CENTRAL KAAPVAAL CRATON

Robyn Ormond, J  r  mie Lehmann and Georgy Belyanin

We use structural, geochronological and microstructural data for evaluating the tectonic record of a small portion of the Kaapvaal Craton at Zwartkops Hills. These hills, located close to the northwest margin of the Johannesburg Dome, represent an outlier of Witwatersrand Supergroup rocks situated on Archean basement. The supracrustal sequences include Witwatersrand, Ventersdorp and Transvaal Supergroup rocks.

The post-Mesoarchean structural evolution of the Zwartkops outlier can be separated into three deformation events. The oldest structures D_1 include steep N-S striking bedding planes and contacts between Witwatersrand and Ventersdorp Supergroup lithologies. The S_0 was later transposed to shallow SW-dipping S_2 , expressed as biotite-grade greenschist facies schistosity in greenschists of the Archean basement, Witwatersrand Supergroup pelitic schists and felsic volcanic schists of the Ventersdorp Supergroup. S_2 is axial planar to 100 m-scale, recumbent

folding F_2 exposed in quartzites of the Witwatersrand Supergroup (Fig. 1). D_2 top-to-the-south or -south-west kinematics is interpreted from the orientation and geometry of the recumbent fold. Lower greenschist facies schistosity S_3 in shales of the Transvaal Supergroup dips shallowly to the SW and is axial planar to open, decameter-scale folds in basal Transvaal Supergroup sandstones. While D_2 and D_3 schistosities are similarly oriented, the discrepancy in metamorphic grade and intensity of deformation suggest they were formed during separate events.

$^{40}\text{Ar}/^{39}\text{Ar}$ stepwise heating plateau ages obtained from synkinematic white micas, separated by suspension-settling and hand-picking methods, yielded two age populations. Ages of ca. 2026–2016 Ma (2σ) were obtained from leucogranite, Archean basement (white mica ± 2 mm) and a schistose S_2 cataclastite, derived from basement leucogranite located at the contact basement-supracrustal sequence

(white mica $< 100 \mu\text{m}$). White micas in quartzite and metapsammite (micas $\pm 500 \mu\text{m}$) of the Witwatersrand Supergroup yielded older ages of ca. 2072–2044 Ma (2σ). 2026–2016 Ma and 2072–2044 Ma age populations suggest that the Vredefort Impact Structure (VIS), located ± 120 km to the SW of Zwartkops, and the Bushveld Igneous Complex (BIC), located ± 30 km to the north, may have respectively affected the argon retention in micas.

The structural record points to an early E-W shortening D_1 that was strongly overprinted by top-to-the-south D_2 shearing. A post-Transvaal D_3 N-S shortening affected all rocks in the area. 2072–2044 Ma and 2026–2016 Ma ages from D_2 structures, therefore, do not record the D_2 deformation age. The deformation record at Zwartkops shows that intense and repeated tectonic activity was not only localized at the margins of the Kaapvaal Craton but also affected its core during the Neoproterozoic and Proterozoic.



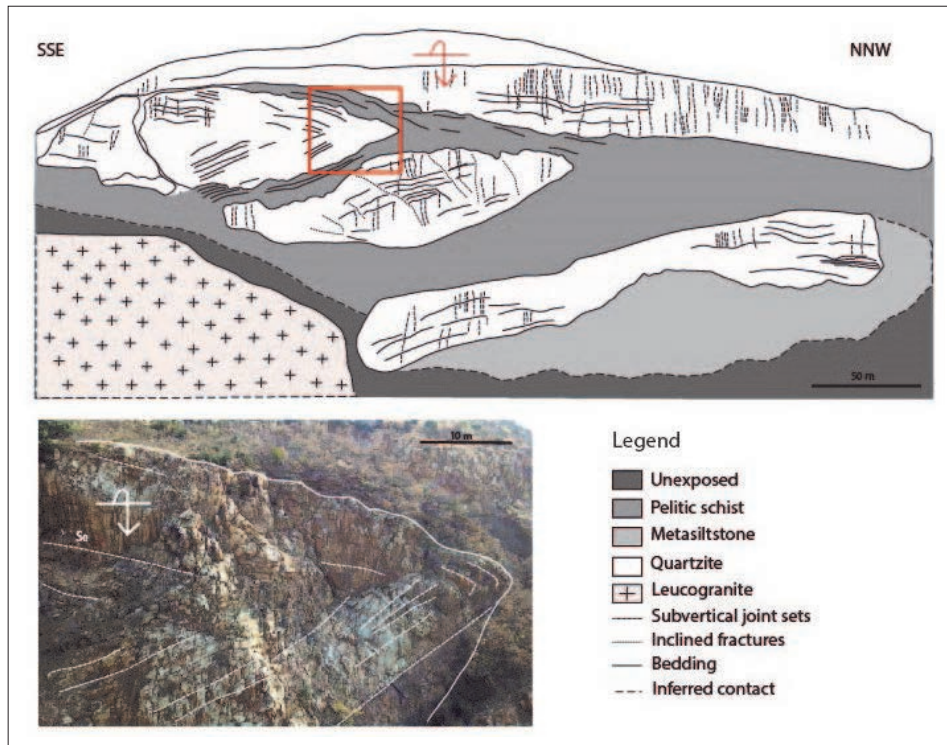


Figure 1: Panoramic sketch of the east-facing cliff, south Zwartkops, showing the 100 m-scale overturned recumbent F_2 fold in Witwatersrand quartzites. An annotated photograph highlights the fold hinge indicated on the panorama.

MINERALISED MAFIC-ULTRAMAFIC INTRUSIONS ADJACENT TO THE KUNENE ANORTHOSITE COMPLEX IN SOUTHERN ANGOLA

Welhemina Sito, Mbali Masilela, Trishya Owen-Smith, Grant Bybee (Wits) and Sebastian Tappe

The Kunene Anorthosite Complex (KAC) of southern Angola and northern Namibia is one of the largest Proterozoic massif-type anorthosite complexes in the world, with an area

of ~18 000 km² [1]. The complex is a composite plutonic body consisting mainly of anorthosite sensu stricto, leucogabbro, leuconorite and leucotroctolite; i.e. dominated by

plagioclase.

There are no ultramafic rocks in the complex itself, but numerous (more than 20) small mafic-ultramafic intrusions occur along the western

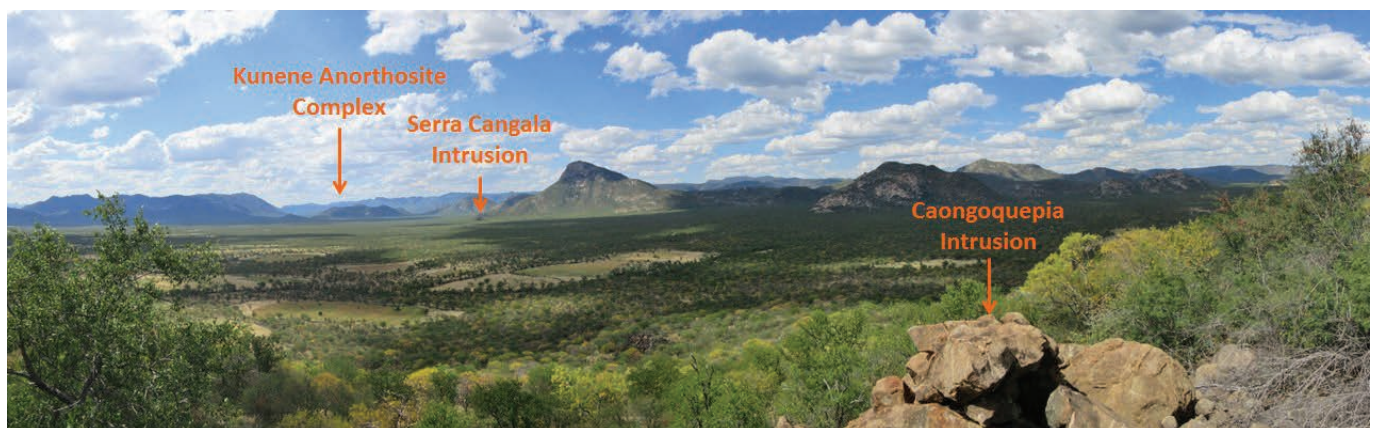


Figure 1: View north-eastwards from the Caongoquepia mafic intrusion towards the Serra Cangala mafic intrusion and the Kunene Anorthosite Complex in the far distance. The other prominent hills are Palaeoproterozoic granitoids that form the country rocks to the KAC.

and southern margins of the KAC (Fig. 1). This apparent spatial association has led to the suggestion that the intrusions are cogenetic with the Kunene magmatism [2, 3]. The 'satellite' intrusions to anorthosite complexes have been identified as key exploration targets, following the discovery of the world-class Voisey's Bay Ni–Cu sulphide deposit, a troctolitic satellite intrusion to the Nain Plutonic Suite in Canada [4].

Previous research on KAC 'satellite' intrusions in Namibia has shown that some of these rocks contain significant chromite- and Ni–Cu–PGE-mineralisation [3]. However, in Angola the potential KAC satellite

intrusions are largely unstudied, due to past difficulties in accessibility and decades of political unrest. Only one of the intrusions (in Namibia) has been dated—at ~140 Myr younger than the latest KAC magmas [3]—and thus the genetic links between the KAC and mafic–ultramafic bodies remain uncertain.

Our research team is currently examining a selection of mafic–ultramafic intrusions on the periphery of the KAC in southern Angola, to better constrain their petrogenesis and assess their economic potential. The rock types represented in the Angolan intrusions range from dunites and harzburgites, through gabbros,

to diorites and leucodiorites. Some of the ultramafic and dioritic rocks host disseminated sulphide mineralisation. Our preliminary findings suggest that the Angolan suite of intrusions has distinct petrographic and geochemical properties to the Namibian suite and the KAC, and is predominantly PGE-poor. New $^{40}\text{Ar}/^{39}\text{Ar}$ and U–Pb zircon ages (Fig. 2) for 5 of the intrusions indicate emplacement between 1950 and 1760 Ma. We propose that these intrusions represent a previously unrecognised mafic component of Palaeoproterozoic arc magmatism on the south-western margin of the Congo Craton.

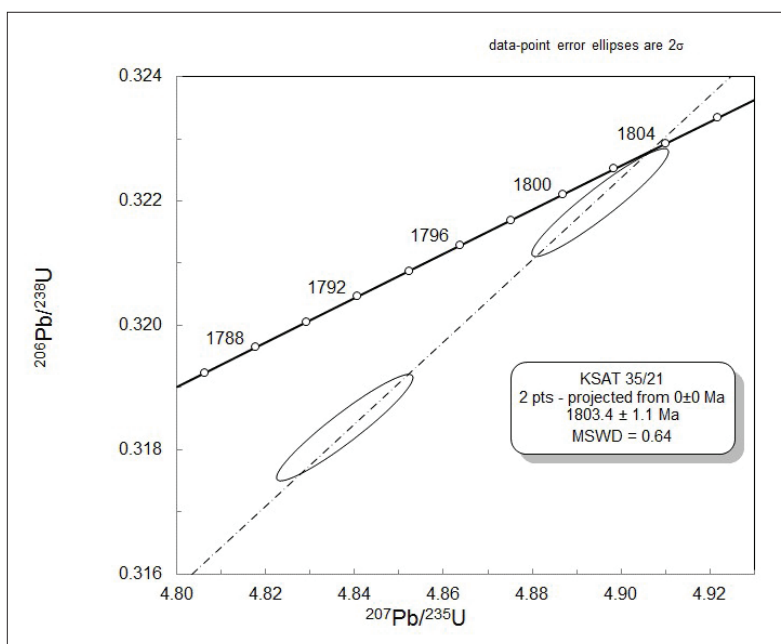
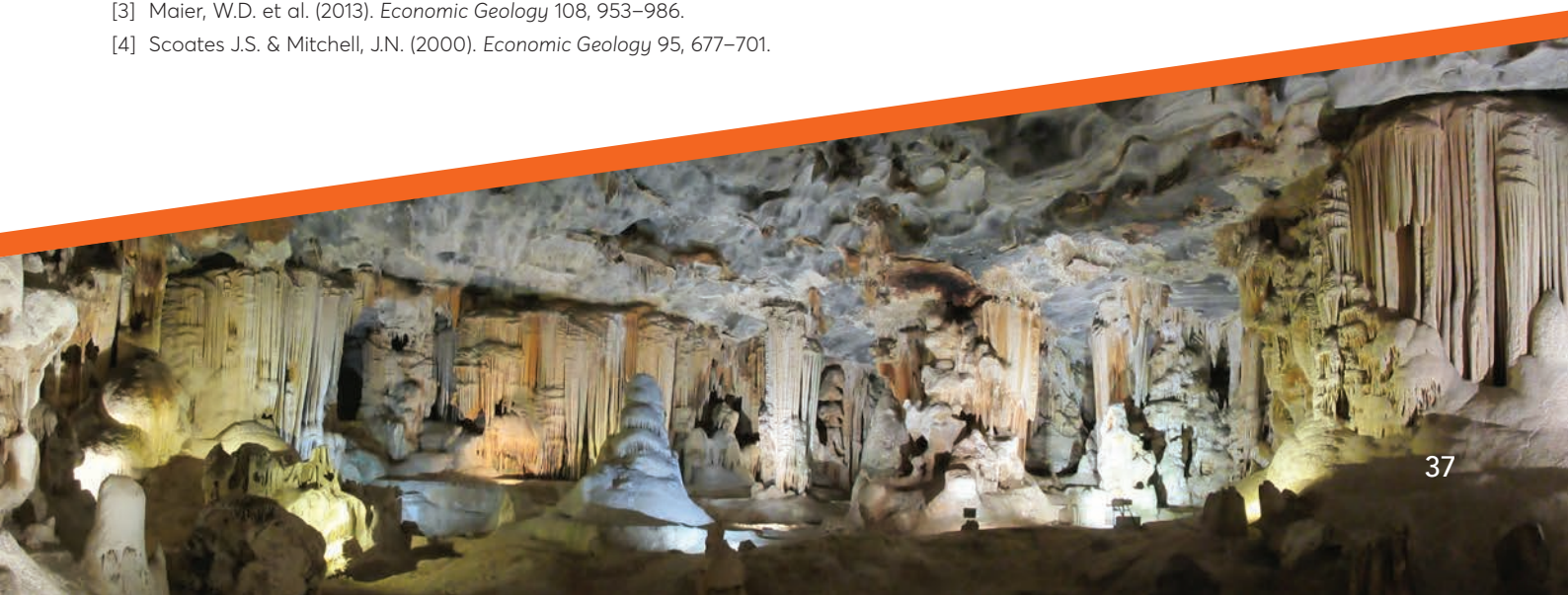


Figure 2: Concordia diagram showing the U–Pb zircon TIMS age determined for a leucodiorite from the Caongoquepia intrusion.

References:

- [1] Ashwal L.D. & Twist D. (1994). *Geology Magazine* 131 (5), 579–591.
- [2] Simpson, E.S.W. (1970). In Clifford et al., *African magmatism and tectonics*. Oliver and Boyd, Edinburgh.
- [3] Maier, W.D. et al. (2013). *Economic Geology* 108, 953–986.
- [4] Scoates J.S. & Mitchell, J.N. (2000). *Economic Geology* 95, 677–701.





Palaeomagnetism and Sediment Provenance

RESEARCH ACTIVITIES AT THE UJ PALEOMAGNETISM LABORATORY: AN OVERVIEW

Hervé Wabo

During 2018, the Palaeomagnetism Lab saw important analytical developments, including the acquisition of a second specialized furnace for sample demagnetization, an upgrade of our SQUID magnetometer with replacement of pickup coils, and the acquisition of an updated version of the paleomagnetic code and computer that operate the system. A new software program for visualizing and diagramming paleomagnetic data, Multiplot, was developed by PhD candidate Casey Luskin. With these improvements, ongoing research projects of students and staff, and outside collaborations, progressed well.

In January 2017, Prof Nic Beukes and Dr Hervé Wabo travelled to India for paleomagnetic sampling of sedimentary successions in the Purana basins. This trip forms part of an ongoing research project which aims to produce precise ages and reliable paleopoles for Cratonic India in the Mesoproterozoic. Indian collaborators on the project include Prof J. Mukhopadhyay of Presidency University and Prof S. Petranabis-Deb of the Indian Statistical Institute. Later in 2017 our Lab received a visit from Prof J Kirshvink of CalTech (USA)—a world expert in Paleomagnetism—and two of his students from the Tokyo Institute of Technology (Japan). Based on a long-standing collaboration, Kirshvink's group spent time in the Vredefort Dome area with Prof Michiel de Kock, sampling altered Vredefort granites for analyses of lightning episodes on single crystals using a SQUID microscope.

Prof NJ Beukes, Prof MO de Kock, and Dr H Wabo attended the ICDP Workshop "Scientific drilling in the Moodies Group" held in Barberton, 6-8 October 2017. The event included a field excursion observing unique formations of the Moodies Group in order to select the best sites for a deep drill core into this Paleoarchean-aged Formation. Dr R. Fu, head of Paleomagnetism Laboratory of Harvard University (USA), spent two days at UJ on his way back from the Moodies workshop to establish a new collaboration with Dr. H Wabo on the study of BIFs of the Fig Tree Group for which the UJ Paleomagnetism Lab has been active over the last 3-4 years.

A significant outcome of an ongoing cooperative project between the UJ Paleomagnetism Lab and geoscientists at Lund University (Sweden) was an article in the high impact journal *PNAS*, lead authored by UJ Paleomag alumnus Ashley Gumsley, on the timing of the Great Oxidation Event. Other 2017 publications from Lab affiliates included two papers by Sciscio et al. and one by Humbert et al. The year 2018 saw the appointment of a new Postdoc fellow, Dr Lara Sciscio (previously PhD visitor in the Lab), who will be working with Prof MO de Kock to study the magnetostratigraphy of the Elliott Formation in the Karoo Supergroup. Dr Sciscio's postdoctoral research will be funded by the Claude Leon Foundation.

Two PhD candidates, Cedric Djeutchou and Casey Luskin, who respectively are investigating the paleomagnetism of ~1.9 Ga dykes swarms in South Africa

and the paleomagnetism of volcanics of the ~2.9 Ga Pongola Supergroup, are expected to submit their theses in mid-2019. Much of their results were presented at the GeoCongress (18-20 July 2018) held at UJ. Articles related to other Lab projects were also published in international journals (e.g., Wabo et al., 2018; Adeniyi et al., 2018; Humbert et al., 2018 a,b; De Kock et al., 2018; Gumsley et al., 2018). Most recently, Lab members contributed several chapters in two Springer volumes, *Dyke Swarms of the World: A Modern Perspective* and *The Archaean Geology of the Kaapvaal Craton, Southern Africa*, both scheduled for publication in 2019. As a follow-up to an article lead-authored by H Wabo in the Springer *Dyke Swarms* book, Dr A Gumsley (now a research associate in Poland), Prof D Evans (who has a long-standing research collaboration with our Lab) from Yale University, and Prof MO de Kock spent three days in the Mashishing area of the Mpumalanga Province investigating further sampling prospects for paleomagnetic and precise dating analyses.

The collaboration between the UJ Lab and other facilities around the world (e.g., Yale, Caltech, Harvard, Liverpool, São Paulo, Berkeley, MIT, etc.) is done under the umbrella of "RAPID," a consortium of all paleomagnetic laboratories using the automated sample-changing systems designed by Prof J Kirshvink. Abosede Abubakre, a UJ PhD candidate who is studying the paleomagnetism of Karoo sediments in South Africa, made use of this collaboration while spending three months (June-Sept 2018) working

at the Caltech Paleomagnetism Laboratory. In December 2018, Dr. H Wabo was invited by Harvard University to present his recent research results from the Fig Tree BIFs and to perform additional analyses on the Quantum Diamond Microscope at the Harvard Paleomagnetism Lab. Subsequently, Herve spent a week at Yale University collaborating with Prof D Evans. During his trip to the USA, Herve also attended the AGU 2018 Fall meeting in Washington DC along with C Djeutchou and C Luskin who

presented results of their PhD research projects. During this conference, the UJ group, together with other paleomagnetists from over twenty labs worldwide, attended the annual lunch for RAPID-affiliated researchers where they shared experiences with the RAPID system and made suggestions for improvements. Subsequently, Cedric and Casey were invited by Joe Kirschvink to visit the Caltech Lab for further networking. Also at this meeting, a collaboration with the Paleomagnetism Lab at

the University of São Paulo was established, and Casey was invited to visit their lab in 2019.

In the coming years, we hope to build on these successes to continue exploring new research areas, in particular those related to expanding the paleomagnetic record and reconstruction of the continental core of Southern Africa—the Kaapvaal Craton. If you are interested in collaborating, please contact Dr H Wabo (hwabo@uj.ac.za).



Figure 1: UJ PhD candidate Cedric Djeutchou at the AGU Fall Meeting 2018 in Washington DC, presenting his poster to Prof Lisa Tauxe, a member of the U.S. National Academy of Sciences and head of the Paleomagnetism Lab at Scripps Institution for Oceanography.



PALEOMAGNETIC RESULTS OF THE PONGOLA SUPERGROUP AND A POSSIBLE POST-PONGOLA POLE ON THE KAAPVAAL CRATON

C.R. Luskin, M.O. de Kock¹ and H. Wabo

Paleomagnetism is a useful tool for studying the paleogeography of the Kaapvaal Craton (Figure 1). However, the Mesoproterozoic Kaapvaal Craton lacks reliable and spatiotemporally dense paleomagnetic data, obscuring its relationship to contemporary cratons, such as the Pilbara Craton (Western Australia). Extending for 270 km along what was once the SE shallow-water marine margin of the Kaapvaal Craton, the ~2.99–2.87

Ga Pongola Supergroup is a largely undeformed and unaltered succession of volcanic and sedimentary rocks that provides a potential target for Archean paleomagnetic study. At the base of the Pongola Supergroup is the primarily volcanic Nsuze Group, overlain by the predominantly sedimentary Mozaan Group which has been proposed to correlate with portions of the Witwatersrand Supergroup. As part of this study's

investigation, 21 Nsuze Group lava sites at the White Mfolozi Inlier (Figure 1) and 2 sites from a quartz porphyry sill intruding the Mozaan Group in Swaziland were sampled and then demagnetized at the University of Johannesburg Paleomagnetism Laboratory. 10 of these sites yielded well-constrained high-temperature components (HTCs).

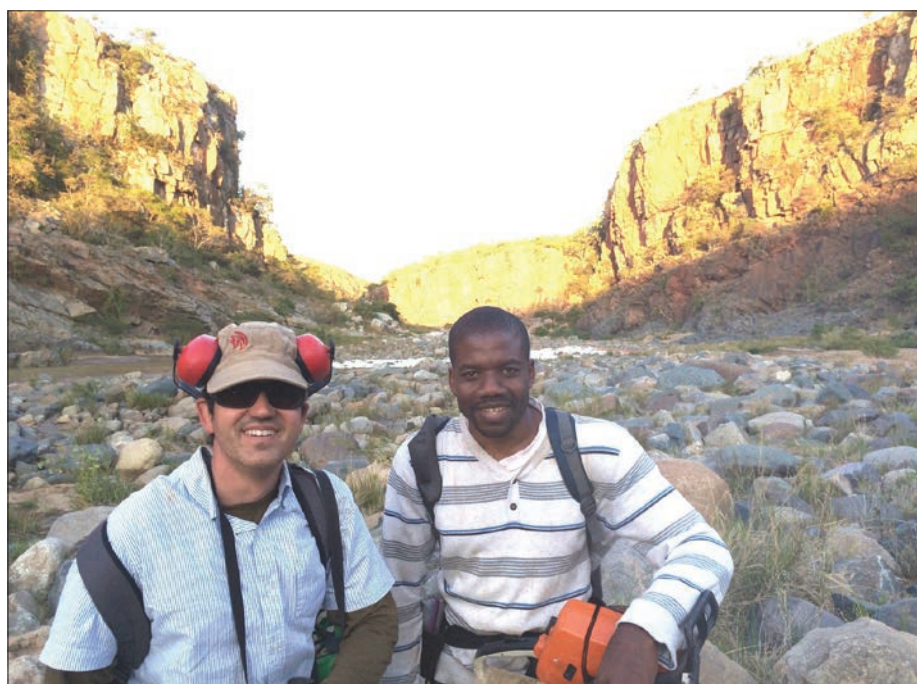


Figure 1. Casey Luskin and Dr Herve Wabo sampling Nsuze Group volcanics at the White Mfolozi River Gorge.

Nhlebelala / Pypklipberg Formation lava sites of the lower Nsuze Group did not generally yield stable HTCs. Agatha Formation volcanics of the upper Nsuze Group reveal two distinct HTCs: (1) A westerly HTC with positive inclination corresponding to a virtual geomagnetic pole (VGP) at 27.3°S, 335.2°E (N=6, $\alpha_{95} = 6.8^\circ$), similar to the Agatha Formation VGP obtained by

Strik et al. (2007), and also similar to later 2.7–2.8 Ga poles on the Kaapvaal Craton (Wingate 1998; Gumsley et al. 2013). (2) A southerly HTC with positive inclination corresponding to a VGP at 66.8°S, 126.7°E (N=2, $\alpha_{95} = 2.5^\circ$), similar to a VGP obtained by Lubnina et al. (2010) for Agatha Formation basalts and a nearby presumed 2.95 Ga dyke. Both HTCs could represent

overprinting by 2.7–2.8 Ga post-Pongola granites intruding the SE Kaapvaal Craton. Dating of nearby dykes (labelled NL-12 and NL-13a by Lubnina et al. 2010) showing these two HTCs (Figure 2) was attempted, however both dykes proved too altered to extract usable baddeleyite crystals.

Most of the Mozaan Group crops

out in a SSE-plunging syncline in the Kubutu-Mooihoek area of Swaziland (Nhleko 2003) where it is intruded by a 2837 ± 5 Ma quartz porphyry that is deformed along with other Mozaan Group strata (Gutzmer et al. 1999). The nearby 2824 ± 6 Ma Mooihoek Pluton is post-tectonic (Maphalala and Kröner 1993), constraining the age of deformation to ~ 2842 – 2818 Ma. The quartz porphyry sill was sampled on opposing limbs of the syncline for a fold test. Since the deformation timing is known, a positive fold test would constrain the magnetization to ~ 2842 – 2818 Ma. However, the East Limb shows scattered directions, likely

due to lightning, making the fold test inconclusive. Further sampling of the syncline could yield a more definitive fold test.

Nonetheless, the West Limb yields a well-constrained southerly HTC with positive inclination, very similar to the Agatha southerly HTC. Its geographic (non-tilt-corrected) direction is much closer to the Agatha southerly HTC in geographic coordinates than after tilt-correction (7.7° difference vs. 17.4° difference; Figure 2), suggesting a negative regional consistency test which indicates these directions are probably post-tilt overprints.

The corresponding West Limb VGP (located at 79.2°S , 243.6°E) is similar to other Mozaan Group poles obtained by Nhleko (2003), Strik et al. (2007), Lechekeane (2016), as well as to later Kaapvaal Craton poles derived from the 2.7 Ga Allanridge Formation (de Kock et al. 2009), the 1.11 Ga Umkondo LIP (Swanson-Hysell 2015), and 180 Ma Karoo dolerites (Hargraves et al. 1997). The West Limb direction, Agatha southerly HTC, and other Mozaan Group directions may also be overprints related to 2.7–2.8 Ga post-Pongola granitoid intrusions on the eastern Kaapvaal Craton.

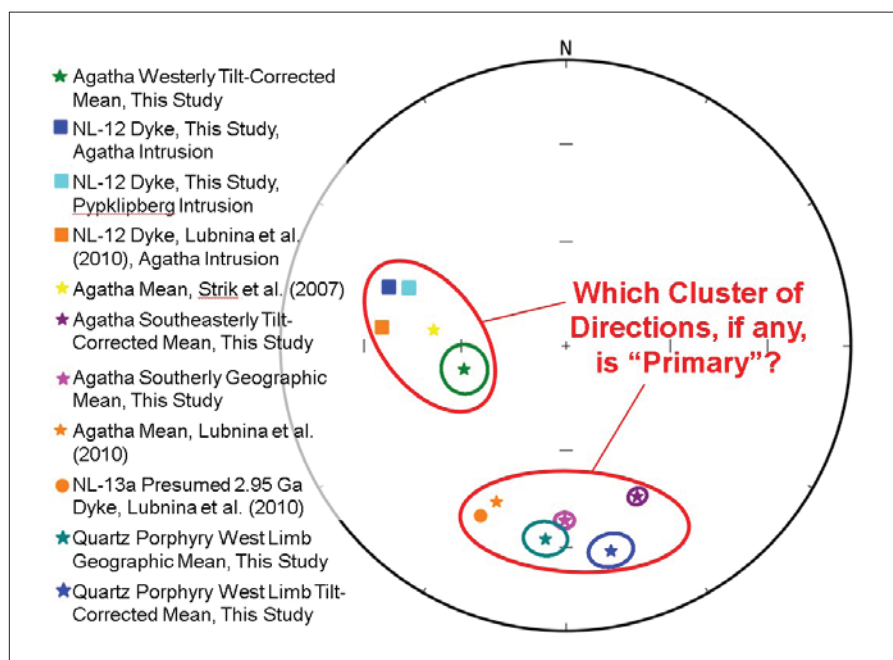


Figure 2: Equal area projection of various paleomagnetic directions obtained by This Study and previous studies of the Nsuze Group volcanics and other rocks of the Pongola Supergroup. Two clusters of positively inclined directions emerge, a westerly direction and a southerly direction, leading to the question: Which cluster, if any, is primary?

A lack of positive or conclusive field tests makes it difficult to definitively determine which paleomagnetic directions obtained in This Study are older, and if any are primary. However, if we assume that the various HTCs obtained in This Study are primary, the Kaapvaal Craton underwent drift from ~ 2.99 – 2.84 Ga during Pongola Supergroup deposition (Figure 3):

- If the quartz porphyry HTC is primary, this implies a relatively low paleolatitude for the Kaapvaal Craton at ~ 2.84 Ga of $\pm 17.9^\circ$ – 11.4° (mean $\pm 14.5^\circ$), seemingly inconsistent with reports of the Mozaan Group bearing the world's oldest glacial sequence (Young et al. 1998).
- If the Agatha westerly HTC is primary, then ~ 2.99 Ga Kaapvaal Craton paleolatitude was between $\pm 49.4^\circ$ – 33.8° (mean $\pm 40.9^\circ$). Maximum latitudinal Kaapvaal Craton drift was from $\pm 49.4^\circ$ to $\pm 17.9^\circ$ between ~ 2.99 – 2.84 Ga, drifting ~ 7400 km over 150 Ma, or ~ 4.9 cm/year, which is within modern drift rates. Minimal





latitudinal drift would be 1750 km over this time period, a rate of 1.2 cm/year.

- If the Agatha southerly HTC is primary, ~2.99 Ga Agatha paleolatitude was between $\pm 25.5^\circ$ – 21.8° (mean $\pm 23.6^\circ$), and maximum latitudinal Kaapvaal Craton drift was from $\pm 25.5^\circ$ to $\pm 17.9^\circ$ during this time, implying a latitudinal drift of

~4050 km over 150 Ma, or ~3.2 cm/year. This is also similar to modern drift rates. Minimal Kaapvaal Craton latitudinal drift would have been 0.3 cm/year.

These results highlight challenges of studying Archaean paleomagnetism. Even if primary directions can be obtained, they only reveal maximum *latitudinal* drift; if longitudinal drift

could be inferred, total drift would likely be greater. These results also provide a cautionary tale of how ancient rocks are potentially exposed to many overprinting events and effects such as lightning, complicating efforts to determine which paleomagnetic directions are primary (Figure 2).

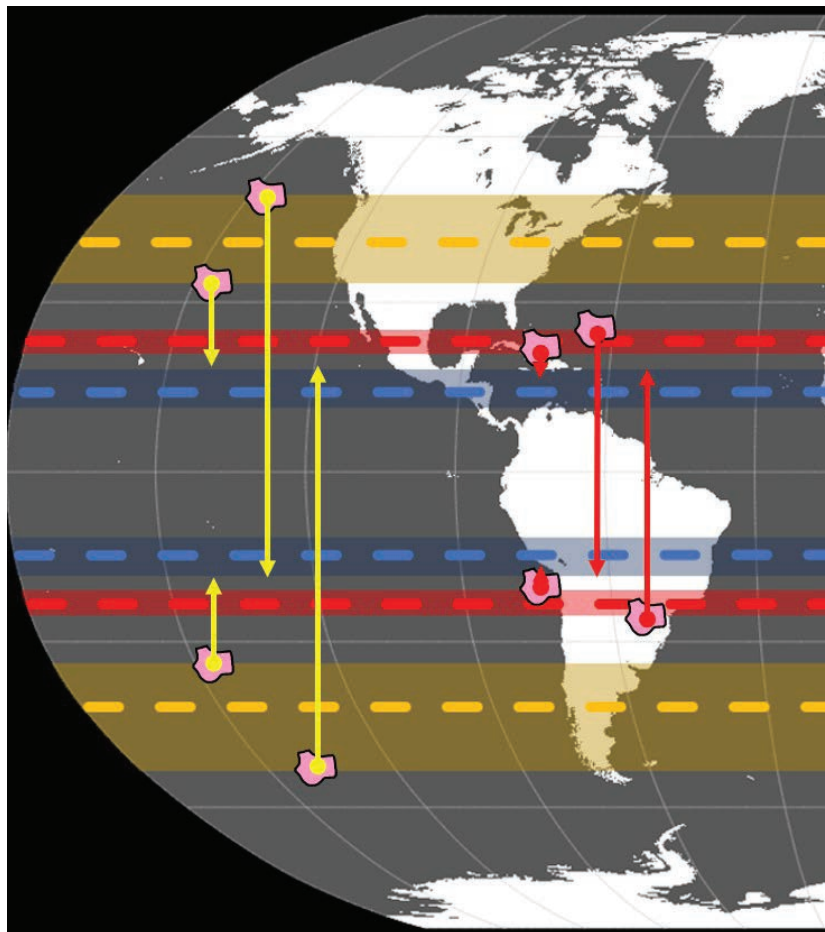


Figure 3: Minimum and maximum Kaapvaal Craton paleolatitudes and latitudinal drift during Pongola Supergroup deposition, assuming various HTCs obtained in This Study are primary. Yellow shading indicates possible Agatha westerly HTC paleolatitudes. Red shading indicates possible Agatha southerly HTC paleolatitudes. Blue shading indicates possible Quartz Porphyry paleolatitudes. Note: Diagram shows latitude only; longitude is for illustration purposes.

MINERAL TRANSFORMATIONS DURING THERMAL DEMAGNETIZATION OF SIDERITIC JASPER MESOBANDS IN JASPILITES OF THE ~3.25 GA FIG TREE GROUP IN THE BARBERTON GREENSTONE BELT, KAAPVAAL CRATON (SOUTH AFRICA)

H. Wabo^{1,2}, L.P. Maré³, N.J. Beukes^{1,2}, F.H. Kruger^{1,2} and M.O. de Kock^{1,2}

¹PPM Research Group and ²Cimera; ³Council for Geoscience, Pretoria

The study describes the mineral changes associated with the thermal demagnetization of sideritic jasper mesobands in the ~3.25 Ga Manzimnyame Iron Formation Bed of the Fig Tree Group in the Barberton Greenstone Belt (Fig.1). This research was initiated to determine the timing of hematite formation using paleomagnetic fold and conglomerate tests. If the hematite could be proven

to be of early diagenetic sedimentary rather than late post-depositional origin, it could hold important clues as to redox conditions in Early Archean depositional basins. However, the stepwise demagnetization of samples was characterized by an increase of magnetic intensity moment from heating steps above 400°C, with erratic directions related to cooling down of samples in a magnetically-

shielded room. Follow-up thermal rock-magnetic studies combined with X-ray diffraction identification of mineral phases in unheated samples and samples that were cooled down after heating to 700°C, indicated that the siderites reacted to form new magnetic iron-rich spinels during heating (Fig.2). Some of the siderites are Mg-poor and gave rise to the formation of magnetite with a Curie

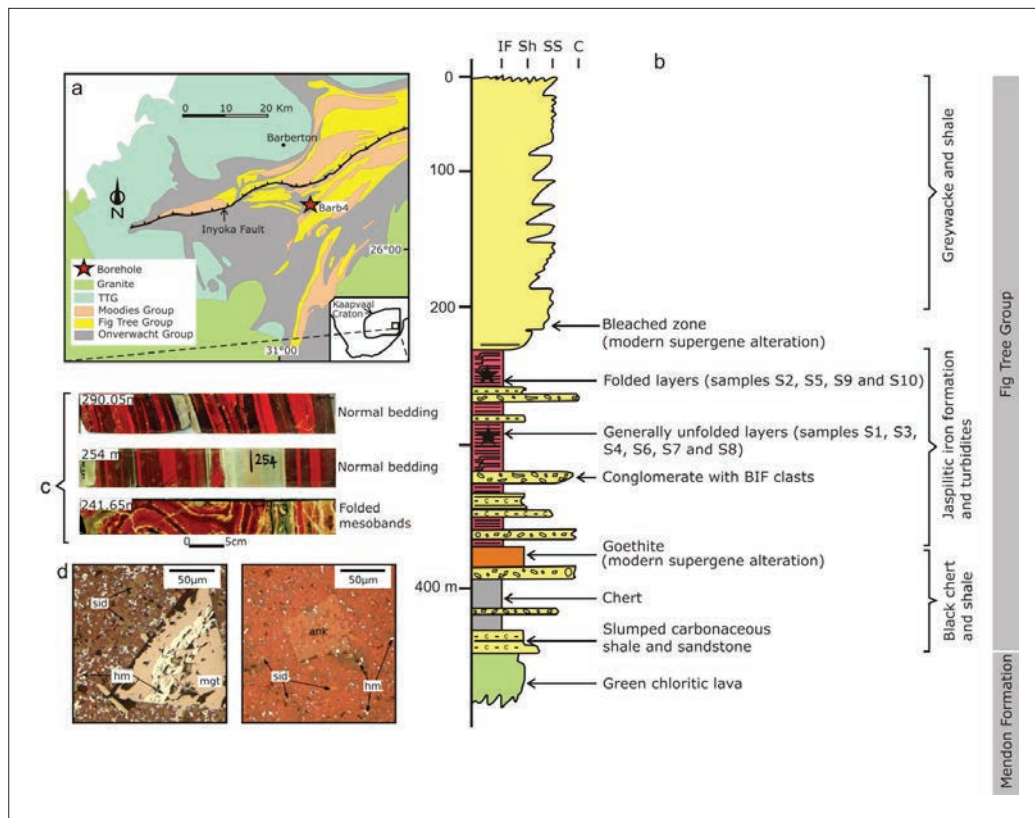


Figure 1. (a) Generalized geology of the central part of the Barberton Greenstone Belt (e.g. Byerly and Palmer, 1991). The Barb4 borehole (drill site shown by a red star at S25°54'23.8"; E31° 05' 48.1") plunges at 70° in direction 305° (b) Generalized stratigraphic log of the Barb4 core. Black stars represent approximate stratigraphic locations where samples S1 to S10 were collected. (c) Photographs of Fig Tree jaspilites defining normal (unfolded) sedimentary bedding, folded jasper mesobands and a jasper flat-pebble conglomerate (d) Microphotograph showing hematite (hm) finely intergrown with quartz and siderite (sid) in a jasper mesoband. mgt = magnetite. The core is stored in the Department of Geology at the Auckland Park Kingsway Campus of the University of Johannesburg.





temperature (T_C) of $\sim 575^\circ\text{C}$ (Fig 2). In contrast, Mg-bearing siderites apparently formed magnesioferrite with a T_C of $\sim 550^\circ\text{C}$ (Fig. 2). Hematite, with a T_C of $\sim 680^\circ\text{C}$, persisted as a stable mineral during the entire heating cycle (Fig.2). Maghemite is another spinel that formed apparently

at the expense of magnetite during cooling of samples from below 575°C (Fig 2). These newly-formed iron spinels acquired strong erratic magnetizations that concealed the preexisting remanence of hematite. The timing of formation of the hematite nor its *in situ* magnetic remanence could

thus not be determined. Our results can, however, be used to develop alternative techniques to establish the remanence of hematite not only in the Manzimnyame jaspilite but also in other Precambrian iron formations in general.

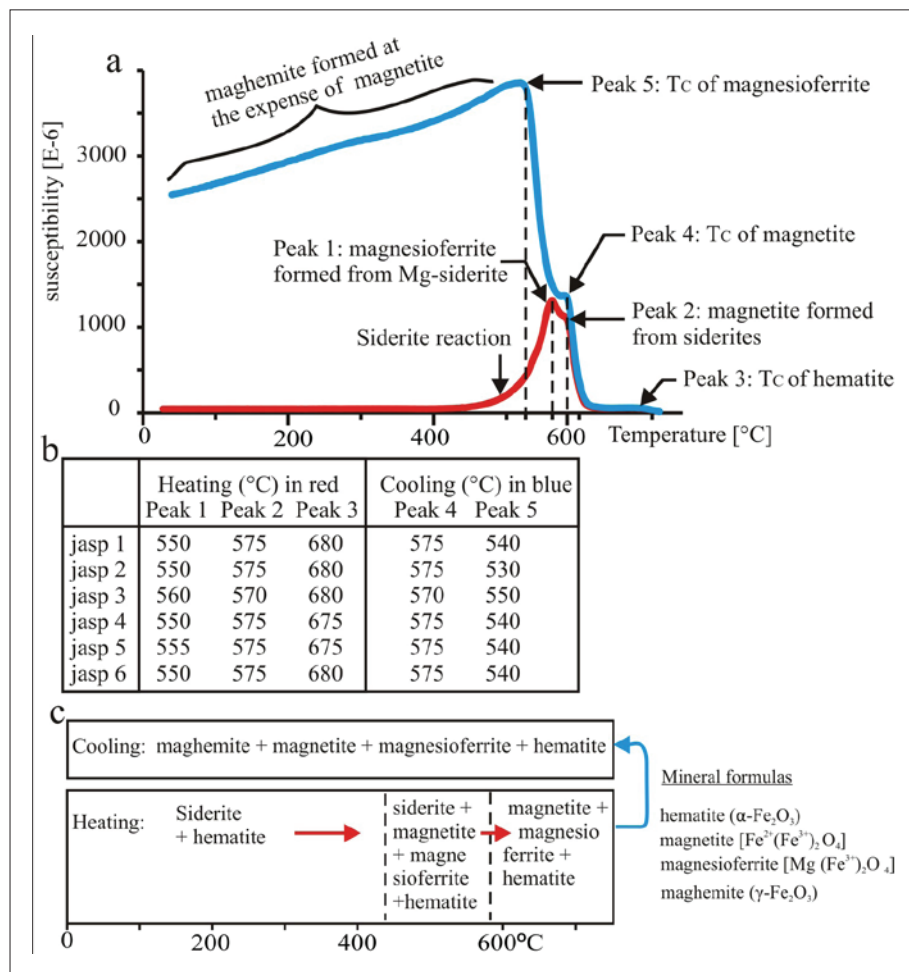


Figure 2. (a) Typical heating (red) and cooling (blue) cycle showing the successive mineral transformations identified by total loss of susceptibility at the Curie temperatures (peak) of the main magnetic carriers. (b) Curie temperatures of the main magnetic carriers (peaks) identified in individual sample curves (see Figure 3). (c) Mineral sequences during heating and cooling cycles. T_C = Curie temperature.

Subrecent, Environmental and Medical Geology

ADVANCES IN THE METHOD DEVELOPMENT FOR (U,Th)-HE DATING OF CALCIUM CARBONATE SPELEOTHEMS

Tebogo V. Makhubela and Jan D. Kramers

We report an update on our efforts to set-up a method for dating calcium carbonate (CaCO_3) speleothems (mainly horizontally-deposited flowstones that bracket sediments) using the (U,Th)-He dating technique. The (U,Th)-He dating method is based on the radioactive decay of ^{235}U , ^{238}U and ^{232}Th to lead isotopes ^{207}Pb , ^{206}Pb and ^{208}Pb , respectively, with each decay scheme producing 7, 8 and 6 atoms of ^4He , respectively. The He/(U + Th) ratio yields the last time or event when the sample cooled down to below the closure temperature at which He is retained in a particular mineral (Copeland et al., 2007). When assuming that at the start (i.e. time = 0) of mineral formation no ^4He was incorporated into the speleothem (which is often a valid assumption because ^4He constitutes ca. 5 ppm of Earth's atmosphere and is not an adsorbing gas), then the amount of time it takes to accumulate ^4He in the speleothem is proportional to the age of the speleothem. Following our initial attempts reported in the 2015 PPM Annual Report, we have explored the combination of U-series disequilibria with the (U,Th)-He system to date speleothems older than 500 ka. In the U-series disequilibrium dating method, commonly denoted U/Th, ^{238}U decays to ^{230}Th via a series of 'intermediate daughter' nuclides

that are radioactive. First it decays by alpha (α)-decay to ^{234}Th , followed by a beta (β)-decay to ^{234}mPa (proactinium (^{234}Pa)) leading to ^{234}U after another β -decay and ultimately to ^{230}Th after α -decay (Bourdon et al., 2003). When the U/Th system is not in secular equilibrium, then the rate of decay of each intermediate daughter nuclide is not equal to that of the parent. As a result, the activity (number of decay events per unit time) ratios of $^{234}\text{U}/^{238}\text{U}$ and $^{230}\text{Th}/^{238}\text{U}$ are both not equal to 1 (Hellstrom and Pickering, 2015). The system's gradual return to equilibrium is the fundamental basis of the U/Th disequilibrium dating method (Bourdon et al., 2003).

All the analytical aspects for the development of the (U,Th)-He dating method were carried out at the SPECTRUM Analytical Facility of the University of Johannesburg. Analyses of He and U/Th were done from the same sample aliquots, and He extraction always preceded measurements of U and Th. The extraction of ^4He from calcite and aragonite flowstones was a major component of the method development. Initial work involved using a laser for the heating and degassing of samples, but after the challenges experienced and unsatisfactory results, we now use an in-house built miniature furnace. It has

enabled us to improve the efficiency of heating the samples (heating for 1-1.5 hours at about 900 °C) and to also analyse larger samples (up to 100 mg per sample). Helium was extracted and purified in an ultra-high vacuum (UHV) extraction line and measurements were done using the MAP 215-50 Noble-Gas mass spectrometer, using a calibrated ^3He spike. U/Th measurements were carried out using the Nu Plasma II® multicollector ICP-MS (MC-ICP-MS). Concentrations and disequilibria were measured after column chemistry using a $^{229}\text{Th} + ^{236}\text{U}$ double spike. A two-cycle dynamic multi-collector protocol was employed in which ^{238}U and ^{232}Th were measured on Faraday collectors, while ^{236}U , ^{235}U , ^{234}U , ^{230}Th and ^{229}Th were measured in ion counting electron multipliers. To calculate the ages, a data reduction program written in Visual Basic® 6, SP4 (developed by Jan Kramers) was used. This program calculates the age using three methods: (1) method for samples with equilibrium for ($^{230}\text{Th}/^{238}\text{U}$) and ($^{234}\text{U}/^{238}\text{U}$) disequilibrium, (2) method for old samples with secular equilibrium for both ($^{230}\text{Th}/^{238}\text{U}$) and ($^{234}\text{U}/^{238}\text{U}$), and (3) method for young samples with ($^{230}\text{Th}/^{238}\text{U}$) as well as ($^{234}\text{U}/^{238}\text{U}$) disequilibrium.





Figure 1: Photographs of flowstones used to test and validate the (U,Th)-He dating method. Samples from Rising Star Caves are (A) JR03 and (B) ER2G. (C) SWK5 is from Swartkrans Caves whereas (D) M2 is from Sterkfontein Caves.

To test the new method, we used samples that had previously been dated using the uranium-lead (U-Pb) and U/Th dating methods. Here we report the results of five samples (Figure 1, Table 1) from the fossil-bearing cave deposits of the Swartkrans (SWK5), Sterkfontein (M2 and BH1-8) and Rising Star (JR03 and ER2G) caves in the Cradle of Humankind UNESCO World Heritage Site. The ^4He concentrations, the isotopic compositions of U and Th, and the (U,Th)-He ages are given in Table 2. All the old (> 1800 ka) samples from Swartkrans (SWK5) and Sterkfontein

caves (BH1-15, BH1-8 and BH4-9) are in secular equilibrium for ($^{234}\text{U}/^{238}\text{U}$) and close to it for ($^{230}\text{Th}/^{238}\text{U}$). These samples also yield the highest concentrations of He, which range from $12.7 \times 10^{-8} \mu\text{mol}$ to $47.9 \times 10^{-8} \mu\text{mol}$ (Table 2). In contrast, the young M2 and the Dinaledi Chamber samples yield ($^{230}\text{Th}/^{238}\text{U}$) and ($^{234}\text{U}/^{238}\text{U}$) disequilibrium. The U concentrations range from 0.224 ppm to 2.04 ppm, whereas the Th concentrations are lower than 0.075 ppm for all samples. The comparison of our exploratory results with the published ages of the analysed samples (Table 2)

shows that the method holds great potential for dating speleothems. It shows considerable promise throughout the tested age range and will in future complement other geochronology techniques currently used to date cave deposits. The results of JR03 and ER2G are important for confirming that the dated flowstone is significantly older than the published U/Th dates. The (U,Th)-He ages are between the Brunhes chron and the Jaramillo subchron, in agreement with palaeomagnetic results which indicate that the flowstone is older than 780 ka as suspected by Dirks et al. (2017).

Table 1: Flowstone samples used to test and validate the (U,Th)-He dating method.

Sample ID	Sample description and location	Published age
JR03	Both samples from the same flowstone 1a layer overlying unit 2. Samples were collected from the wall on the entry shaft into the Dinaledi Chamber. Palaeomagnetic results of JR03 show that it has a normal chron and a reverse chron dating to ~ 780 ka.	RS23 dated to 502 +181/-53 ka by Dirks et al. (2017)
ER2G		RS22 dated to 478 +107/-41 ka by Dirks et al. (2017)
SWK5	Sampled by Pickering et al. (2011) from the uppermost layer of flowstone that overlies sediment on the Hanging Remnant (a deposit exposed at surface).	Dated to 1800 ± 5 ka by Pickering et al. (2011) using U-Pb
M2	Sampled by Pickering et al. (2010) from a well calcified sediment cone in the Milner Hall of Sterkfontein Caves.	Dated to 142-148 ka by Pickering et al. (2010) using U/Th
BH1-8	Taken from flowstone horizons in drill cores of the Sterkfontein Cave described in Pickering and Kramers (2010).	Dated to 2830 ± 344 ka by Pickering and Kramers (2010) using U-Pb

Table 2: (U,Th)-He ages, He, U and Th concentrations and isotopic compositions for flowstones of the Swartkrans, Sterkfontein and Rising Star caves.

Sample ID, Mass (mg)	⁴ He (μmol ± 1μ) (×10 ⁻⁸)	U ppm	Th ppm	(²³⁴ U/ ²³⁸ U) ± 1σ	(²³⁰ Th/ ²³⁸ U) ± 1σ	Meth. 1 age ka ± 95% *)	Meth. 2 age ka ± 95%	Meth. 3 age ka ± 95% *)	Meth. 3 initial (²³⁰ Th/ ²³⁸ U) ± 95% **)
Swk5, 43.07	20.8 ± 0.07	0.46	0.002	1.006 ± 0.004	0.981 ± 0.009	1774 ± 197 (1.85 ± 0.67)	1364 ± 475	885 ± 158 (0.98 ± 0.04)	14.75 ± 2.10 (5/500)
M2-(2), 33.56	1.67 ± 0.30	0.87	0.005	1.378 ± 0.004	1.096 ± 0.014	134 ± 32 (1.55 ± 0.05)	89 ± 60	107 ± 42 (1.51 ± 0.06)	0.52 ± 0.39 (446/500)
M2-(1), 40.23	0.83 ± 0.14	0.26	0.002	1.354 ± 0.005	1.012 ± 0.01	174 ± 39 (1.59 ± 0.07)	118 ± 78	125 ± 21 (1.50 ± 0.03)	0.17 ± 0.25 (20/500)
BH1-8, 58.5	173 ± 0.24	1.45	0.075	1.0045 ± 0.0035	0.964 ± 0.007	3101 ± 286 (3.40 ± 0.98)	3094 ± 822	no solution	
JR03-bottom, 32.27	8.58 ± 0.17	0.44	0.005	1.138 ± 0.005	1.169 ± 0.011	827 ± 24 (2.43 ± 0.10)	681 ± 485	722 ± 143 (1.99 ± 0.39)	3.03 ± 3.32 (3/500)
JR03-mid, 38.78	5.29 ± 0.10	0.22	0.004	1.154 ± 0.005	1.182 ± 0.011	813 ± 22 (2.53 ± 0.10)	701 ± 492	708 ± 31 (2.07 ± 0.06)	2.97 ± 0.08 (2/500)
ER2G-top, 11.26	6.28 ± 0.02	0.69	0.033	1.079 ± 0.005	1.144 ± 0.013	1087 ± 26 (2.69 ± 0.10)	941 ± 626	640 ± 115 (1.49 ± 0.23)	10.41 ± 2.35 (493/500)
ER2G-bottom, 31.29	7.50 ± 0.01	0.31	0.007	1.234 ± 0.010	1.294 ± 0.016	852 ± 20 (3.61 ± 0.10)	900 ± 598	712 ± 149 (2.63 ± 0.73)	5.45 ± 4.74 (19/500)

*) Included in brackets: initial (²³⁴U/²³⁸U) ± 95% confidence uncertainty limits for methods (1) and (3) (the value for method (2) is always 3.5 ± 2.9).

**) For methods (1) and (2), the initial (²³⁰Th/²³⁸U) activity ratios are always set at 0.01 ± 0.003 by default, and therefore are not listed in the Table. Included in this column in brackets: number of solutions out of 500 Monte Carlo attempts in calculation method (3).

***) The preferred solutions are given in bold





References

Bourdon, B., Henderson, G. M., Lundstrom, C. C., Turner, S., 2003. Introduction of U-series geochemistry. In: Rosso, J.J., Ribbe, P.H. (Eds.), *Reviews in Mineralogy and Geochemistry*. Mineralogical Society of America, Washington.

Copeland, P., Watson, E. B., Urizar, S. C., Patterson, D., and Lapen, T. J., 2007. Alpha thermochronology of carbonates. *Geochimica et Cosmochimica Acta*, 71(18), 4488–4511.

Dirks, P. H. G. M., Roberts, E. M., Hilbert-Wolf, H., Kramers, J. D., Hawks, J., Dosseto, A., Duval, M., Elliott, M., Evans, M., Grün, R., Hellstrom, J., Herries, A. I. R., Joannes-Boyau, R., Makhubela, T. V., Placzek, C. J., Robbins, J., Spandler, C., Wiersma, J., Woodhead, J., Berger, L. R., 2017. The age of Homo naledi and associated sediments in the Rising Star Cave, South Africa. *eLife* 6: e24231. doi: 10.7554/eLife.24231

Hellstrom, J., Pickering, R., 2015. Recent advances and future prospects of the U–Th and U–Pb chronometers applicable to archaeology. *Journal of Archaeological Science*, 56, 32-40.

Pickering, R., Kramers, J. D., 2010. Re-appraisal of the stratigraphy and determination of new U-Pb dates for the Sterkfontein hominin site, South Africa. *Journal of Human Evolution*, 59, 70- 86.

Pickering, R., Kramers, J. D., Hancox, P. J., De Ruiter, D. J., Woodhead, J. D., 2011. Contemporary flowstone development links early hominin bearing cave deposits in South Africa. *Earth and Planetary Science Letters*, 306, 23–32.

QUANTIFYING THE DISAPPEARANCE OF THE VREDEFORT DOME

Riconingo Khosa

Introduction

The Vredefort Dome, situated approximately 120km SW of Johannesburg, is the largest and oldest confirmed meteorite impact crater in the world (UNESCO.org). The impact crater is deeply eroded but there are effectively no published or known long-term bedrock erosion rates for the area. Even with most of the crater having been eroded, the

original size of the Vredefort impact structure is estimated to be 250-300 km in diameter, based on regional distribution of shock-metamorphosed and brecciated material, shatter cones, and geophysical modelling. The dome is host to some fluvial systems (e.g. Wilge and Klip rivers) that contribute to shaping its landscape by form of water erosion. These are mainly dominated by the Vaal River,

which flows through from the east to the west, also creating the boundary between the North West and Free State provinces. The anabranching character, in the Parys area, of the typically meandering Vaal River is distinctive and is an important determinant of erosion along the river and island formation. This fluid erosion influences and contributes to the changes and the wider landscape.

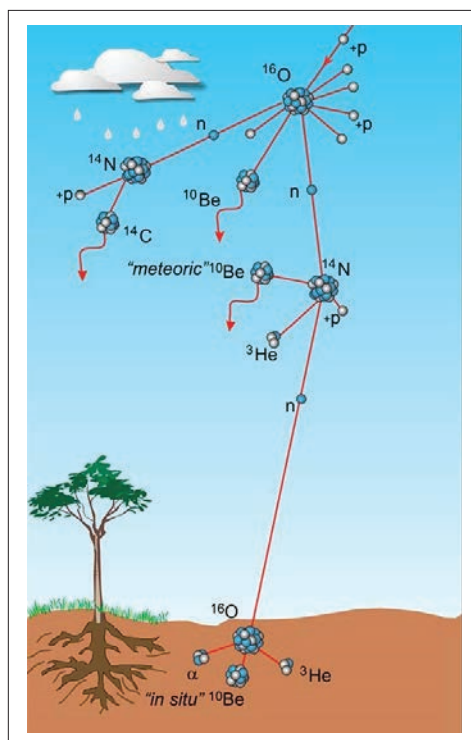


Figure 1: Sketch of how cosmogenic nuclides form in the atmosphere and the surface of the earth (von Blanckenburg and Willenbring, 2014).

To develop an understanding of the evolution of the Vaal River and the Vredefort Dome landscape, measurement of bedrock erosion rates and exposure ages along the river using cosmogenic nuclides is essential. The use of cosmogenic nuclides plays a significant role in determining erosion rates and/or exposure ages and reconstructing landscape evolution. Cosmogenic nuclides are isotopes produced by high-energy secondary cosmic-ray interactions with atomic nuclei in the upper atmosphere, forming meteoric cosmogenic nuclides, and in minerals of terrestrial rocks, forming in-situ cosmogenic nuclides (Figure 1). Cosmic rays that are able to reach the surface and even penetrate a few metres of the earth interact with atomic nuclei in the minerals, and largely through a process of spallation, produce a range of distinctive cosmogenic nuclides. One of the most abundant minerals in the Earth's lithosphere, quartz, is made up of both Si and O, making it a suitable mineral for studies towards erosion processes. Quartz is also a highly resistant and robust mineral, which makes it possible and relatively easy to separate it from the other mineral constituents in rocks.

The two most commonly used cosmogenic nuclides in landscape evolution are beryllium-10 (^{10}Be) and aluminium-26 (^{26}Al), which form during the interaction of cosmic rays with oxygen (O) and silicon (Si) atoms in the quartz, respectively.

Accelerator mass spectrometry allows for the analysis of these nuclides by use of Accelerator Mass Spectrometer (AMS). The first AMS in Africa was launched in July 2014 at the iThemba Laboratory for Accelerator Based Sciences (LABS) in Johannesburg, South Africa. It has allowed for the analysis to be done in the country as previously this would have been done in the United States or Europe.

Aims and Objectives

The aim of this study was to determine the erosion rates and accompanying exposure ages along the valley of the Vaal River in the Vredefort Dome, particularly in the Parys area, using the *in-situ* produced cosmogenic nuclides ^{10}Be and ^{26}Al . One of the main questions we aimed to address was how quickly the bedrock in the area is eroding. In this area, the river flows largely on the Archaean basement granitoids and also traverses the more resistant quartzites of the Dominion and West Rand Groups downstream. The study also aimed to determine the relative erosion rates and exposure ages of the different lithologies. Our knowledge of these relative erosion rates and exposure ages will help us understand the long-term development of the river and how the river has changed the broader landscape of the Vredefort Dome. It is expected that the erosion rates of the granitoids will be faster than those of the typically more resistant quartzites, and that the sampled quartzites on the ridge will have relatively older exposure ages compared to the samples at lower elevation.

Methods of Investigation

Fourteen bedrock samples of granitic and quartzitic composition were collected along the Vaal River in the dome for analysis by AMS. The crushed samples were treated to a series of chemical leaches and etches, density separation and/or froth floatation to separate the quartz minerals from the other minerals in the rocks. The clean quartz was then checked for its purity by elemental composition by Inductively Coupled Plasma Optical Emission Spectrometry (ICP-OES) at the University of Johannesburg's Spectrum facility. The pure quartz samples were shipped to the University of Vermont (UVM) to extract the isotopes by chromatography. The extracted

hydroxide isotopes were "dried" and packed into steel cathodes for analysis at iThemba LABS. The samples were analysed and the AMS gave raw ratios and their accompanying uncertainties. From these results, Balco's (2008) reduction method was used to determine the concentrations of the isotopes and their accompanying uncertainties (Table 1). Erosion rates are a function of latitude, longitude, elevation, production rate, sample thickness, the density of the sample and shielding (This also applies for exposure ages, with the condition that erosion is negligible).

Results

For this publication, we will be taking consideration of the concentrations that were deduced from the AMS results (Balco, 2006) and also looking at the relationship between the sample with regards to where their concentrations plot on a $^{26}\text{Al}/^{10}\text{Be}$ vs ^{10}Be curve (Banana Plot) to see whether the samples experience steady erosion and/or constant exposure. This will be able to indicate to us whether the samples are experiencing relatively high or low erosion and which samples should be considered and discussed for steady erosion or constant exposure.

Of the sampled quartzites with a general range of concentrations of 2.15×10^6 atoms/g, Vaal 1 has the highest concentration, with Vaal 5 and Vaal 8 having the same low concentrations at 1.68×10^6 atoms/g. (This was considered by using the ^{10}Be concentrations)

The granitoids have a lower range with 1.53×10^6 atoms/g between the sample with the highest concentration (Vaal 10) and the one with the lowest concentration (Vaal 14). (This was considered by using the ^{10}Be concentrations)

Figure 2 shows the relationship of the samples as labelled. From this we can already see that the seven





evident samples that are experiencing constant exposure are samples Vaal 1, Vaal 4, Vaal 6, Vaal 7, Vaal 9, Vaal 10 and Vaal 11. However, Vaal 4, Vaal 6 and Vaal 9 are also lying in between the curves and their bottom boundaries are overlapping the

steady erosion curve slightly. The rest of samples not discussed above (i.e. Vaal 2, Vaal 3, Vaal 5, Vaal 8, Vaal 12, Vaal 13 and Vaal 14) are overlapping both the steady erosion and exposure curves.

The average concentration of the sampled quartzites is 2.15×10^6 atoms/g $\pm 6.96 \times 10^4$ and that of the granitoids is 2.27×10^6 atoms/g $\pm 1.12 \times 10^5$.

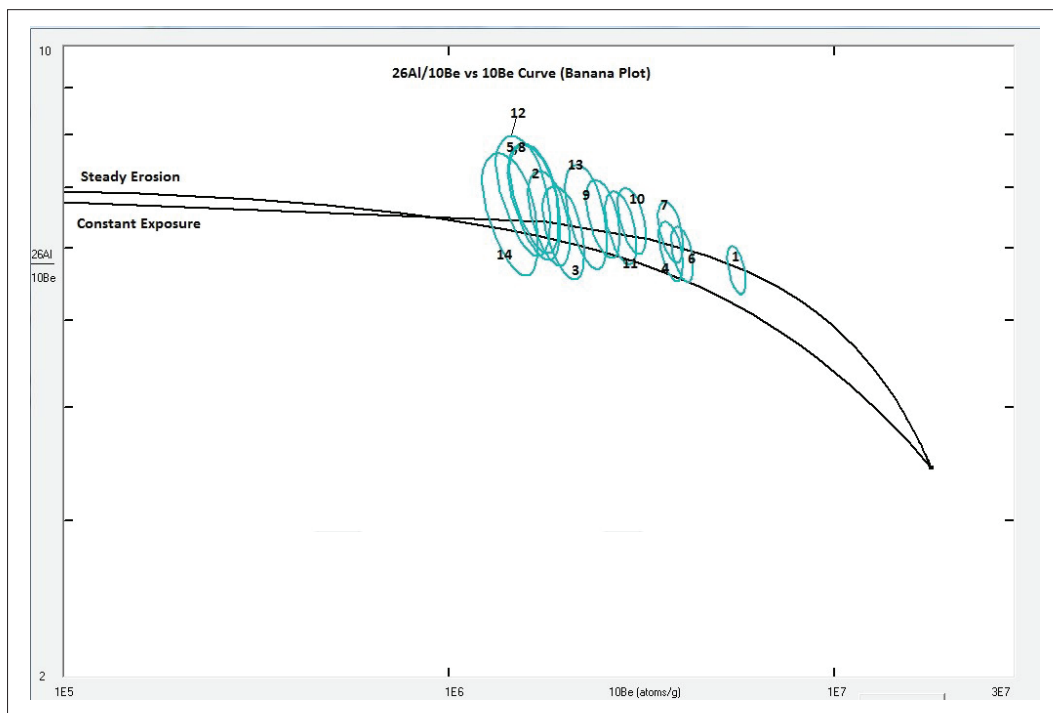


Figure 2: $^{26}\text{Al}/^{10}\text{Be}$ vs ^{10}Be curve (Banana Plot)

Discussion and Conclusion

The results show that samples Vaal 1, Vaal 4, Vaal 6 and Vaal 7 of the quartzites do not actively experience any erosion, but exposure instead. From https://hess.ess.washington.edu/math/al_be_v23/al_be_erosion_multiple_v23.php, we can calculate the exposure ages (assuming zero erosion) and therefore be able to determine how long Vaal 1, Vaal 4, Vaal 6 and Vaal 7 have been exposed to cosmogenic nuclide input and that can indicate how long the channel has been lowering over the years. Samples Vaal 2, Vaal 3, Vaal 5 and Vaal 8 show similar isotopic

concentrations and therefore are treated as those experiencing erosion. Because Vaal 2 and Vaal 3 were sampled outside the bounds of the current river channel, considerations need to be made to explain what kind of erosion (or denudation rather) could be driving their similar concentrations to Vaal 5 and Vaal 8. From https://hess.ess.washington.edu/math/al_be_v23/al_be_erosion_multiple_v23.php we can also calculate the exact erosion rates using the data in Table 1. Taking consideration of the banana plot, it is clear that the samples discussed as experiencing exposure are evident. However, since the other

samples are experiencing what seems to be both exposure and erosion, more geologic and geomorphologic considerations need to be made. However looking at the average of the different lithologies, it is clear that, although not significantly large a difference, it appears that the quartzites are experiencing faster erosion as compared to the granitoids. This means that what we initially thought does not apply and considerations based on more than just the lithology type need to be made for this study.

Table 1: Data used for CRONUS Online Calculator with the last column also used for the Banana Plot

Sample ID	Lithology	Lat.	Long.	Elev. (m)	Sample Thickness (cm)	Sample Density (g.cm ³)	Shielding Correction	¹⁰ Be (atoms/g)	σ ¹⁰ Be (atoms/g)	²⁶ Al (atoms/g)	σ ²⁶ Al (atoms/g)	²⁶ Al/ ¹⁰ Be
Vaal 1	Quartzite	-26.88547	27.35634	1376	5.2	2.65	0.9994	3.83E+06	4.69E+04	3.17E+07	6.13E+05	5.681
Vaal 2	Quartzite	-26.88507	27.35669	1361	9.2	2.65	0.9927	1.83E+06	9.99E+04	1.19E+07	2.82E+05	6.503
Vaal 3	Quartzite	-26.88476	27.35693	1351	6.8	2.65	0.9999	1.99E+06	1.07E+05	1.25E+07	2.98E+05	6.281
Vaal 4	Quartzite	-26.88458	27.35704	1349	8.9	2.65	0.9987	2.01E+06	2.70E+04	2.25E+07	4.68E+05	5.968
Vaal 5	Quartzite	-26.88390	27.35769	1334	7.1	2.65	0.9983	1.68E+06	1.07E+05	1.15E+07	2.74E+05	6.845
Vaal 6	Quartzite	-26.88392	27.35777	1339	5.5	2.65	0.9994	2.23E+06	2.62E+04	2.39E+07	4.98E+05	5.916
Vaal 7	Quartzite	-26.88392	27.35777	1338	8.3	2.65	0.9994	1.99E+06	2.84E+04	2.36E+07	4.91E+05	6.260
Vaal 8	Quartzite	-26.88396	27.35772	1336	6.7	2.65	0.9980	1.68E+06	1.14E+05	1.15E+07	3.11E+05	6.845
Vaal 9	Granitoid	-26.90150	27.28810	1347	3.6	2.65	0.9998	2.52E+06	1.12E+05	1.63E+07	3.48E+05	6.468
Vaal 10	Granitoid	-26.90187	27.38825	1350	10	2.65	0.9999	2.99E+06	1.09E+05	1.93E+07	3.97E+05	6.455
Vaal 11	Granitoid	-26.90149	27.38791	1350	6.0	2.65	0.9995	2.80E+06	1.14E+05	1.78E+07	3.80E+05	6.357
Vaal 12	Granitoid	-26.90230	27.38837	1344	3.0	2.65	0.9998	1.57E+06	1.10E+05	1.09E+07	3.11E+05	6.943
Vaal 13	Granitoid	-26.90207	27.38820	1343	5.9	2.65	0.9997	2.28E+06	1.24E+05	1.49E+07	5.58E+05	6.535
Vaal 14	Granitoid	-26.90195	27.38804	1346	5.1	2.65	0.9994	1.46E+06	1.05E+05	9.65E+06	2.59E+05	6.60959

References

Balco, G., 2006. *Converting Al and Be isotope ration measurements to nuclide concentrations in quartz*. Cosmogenic Nuclide Lab, University of Washington. https://hess.ess.washington.edu/math/al_be_v23/al_be_erosion_multiple_v23.php.

Tooth, S. and McCarthy, T.S., 2004. Anabranching in mixed bedrock-alluvial rivers: the example of the Orange River above Augrabies Falls, Northern Cape Province, South Africa. *Geomorphology* 57, 235-262.

United Nations Educational, Scientific and Cultural Organization (UNESCO) <https://whc.unesco.org/en/list/1162>

Von Blanckenburg, F. and Willenbring, J.K., 2014. Cosmogenic Nuclides: Dates and Rates of Earth-Surface Change. *Elements*, 10, 341-346.

Presentations made as posters at The European Geoscience Union Meeting, Vienna, 8-13 April 2018, and as talks at The "Medical Geology In Africa" Meeting at UJ, 1 December 2017, by The Medical Geology Group.



Figure 1: The Medical Geology Team on the occasion of the 1st Postgraduate Student Seminar held at UJ, 1st December 2017.





Geophagic clay and impact on human health: a case study from Anfoega in Volta Region and Mfensi-Adankwame in Ashanti Region of Ghana

Ahlijah E.Y.¹, Mouri H.¹, Arhin E.², Candeias C.³

¹Department of Geology, University of Johannesburg, Auckland Park Campus, South Africa, ²University for Development Studies, Faculty of Applied Sciences, Department of Earth and Environmental Sciences, P. O. Box 24, Navrongo, Ghana, ³EpiUnit, Public Health Institute, University of Porto, Portugal / GeoBioTec, Geosciences Department, University of SantiagoAveiro, AveiroSantiago Campus, Portugal

Geophagy is the act of ingesting earthly or soil-like materials due to different motives. Though geophagy is known and reported to be a common practice among the rural communities in Ghana, there is no documented evidence on its prevalence or its health effects. The present study aims, therefore to investigate the mineralogy and concentrations of major and trace elements composition of geophagic clays from Anfoega in Volta Region and Mfensi-Adankwame in Ashanti Region of Ghana in order to understand their possible health impact on the consumers in the study area.

The mineralogical results revealed that quartz, muscovite, kaolinite, and illite as the main mineral phases of the studied geophagic materials. The geochemistry results revealed concentrations of Al, Fe, Mg, K, and Si; and trace elements such as As, Co, Cr, Hg, Ni and V, which are higher than the Recommended Daily Intake/Allowance for adults. The prevalence of geophagy in the study area was 66.7% and the health data collected from the Ghana Health Directorate revealed prevalence of some geophagia related health issues such as anaemia, diarrhoea and anaemia in pregnancy.

High fluoride and dental fluorosis prevalence: A case study from Nakuru area, the Kenyan Rift

Gevera P¹, Mouri H¹, and Maronga G²

¹Department of Geology, University of Johannesburg, South Africa, ²Resident Dentist, St. Mary's Rift Valley Mission Hospital, P.O. Box 168-20116 Gilgil, Kenya

High fluoride concentration is a major groundwater issue in most regions in Africa such as Nakuru County in the Kenyan Rift Valley. Cases of dental and skeletal fluorosis are common in the area due to the consumption of such highly contaminated groundwater. In this study, fluoride concentrations and distributions in the Nakuru aquifers and the status of dental fluorosis affecting the local population was investigated using groundwater quality data and clinical studies from two local health facilities. The water assessment results showed a Na-HCO₃ and slightly Na-HCO₃-Cl groundwater type dominated mainly by sodium, fluoride, and bicarbonate. Fluoride levels ranged from 0.5 to 72 mg/l with a mean of 11.08 mg/l, where, 87.50% of the boreholes had higher concentrations than the World Health Organization (WHO) recommended value of 1.5 mg/l for safe drinking water. Spatial analysis showed the highest fluoride concentrations in aquifers in the rift floor and lowest in the escarpments. High rainfall and little residence time led to low fluoride in the escarpments while, high concentrations in the rift floor was due to accumulation along groundwater flow path and evaporative enrichment. The clinical studies from the two health facilities showed high dental fluorosis prevalence (79.49 and 86.00 %) and a mild to moderate severity. Patients with developing dentition (below 14 years old) had a slightly higher prevalence, while severity was higher in older patients. These findings highlight a potential of high fluoride concentrations in aquifers on the Rift Valley floor and relatively low in aquifers located towards the rifts escarpments. The high fluoride correlated positively with high dental fluorosis cases. We therefore recommend low-fluoride groundwater prospecting in the rift escarpments and incorporation of defluoridation methods in high fluoride groundwater areas to reduce its health impacts on the population.

Mineralogical and geochemical analysis of geophagic materials consumed in Baringo, Kenyan Rift Valley: A potential health risk to the population

Gevera P, and Mouri H

Department of Geology, University of Johannesburg, South Africa

Geophagy, the voluntary consumption of earthy materials can be both beneficial and deleterious depending on the mineralogical and chemical composition and the amount of material consumed. In this study, a mineralogical and geochemical investigation of a geophagic rock material consumed in Baringo town in Kenya was conducted to assess its possible health implications. Optical and Scanning Electron Microscope (SEM) as well as X-ray Diffractometer (XRD) were used to determine the mineralogy of the studied samples, which revealed the presence of k-feldspars and quartz as the dominant minerals with minor amphiboles. The material has about 10 to 20% coarse to very coarse (0.38-3.00 mm) and

semi-rounded to angular in shape crystals of quartz, k-feldspars, and amphiboles together with lithic fragments occurring in a fine-grained matrix. This coarse and angular texture may cause abrasion of the dental enamel and the gastro-intestinal tract. X-ray fluorescence (XRF) and Inductively Coupled Plasma Mass Spectrometry (ICP-MS) were used to determine the major and trace elements composition respectively. The results show that, most of these elements are in appreciable values for the material to be consumed for their supplementation, except for silica, iron, manganese, aluminium, chromium, and lead, which are particularly above their recommended daily allowances (RDA). Although the bioavailability and bio-accessibility of elements affect their absorption in the body, the high concentrations of some elements observed in these materials as well as its coarse and angular texture suggest some possible deleterious effects to the health of the consumers in the study area.

Geophagy during pregnancy and possible health effects: A case study from Onangama village, northern Namibia

Kambunga SN¹, Mouri H¹, Candeias C², Hasheela I³, and Nakakuwa F⁴

¹Department of Geology, University of Johannesburg, South Africa, ²Geosciences Department, University of Santiago, Santiago Campus, Portugal, ³Environmental and Engineering Geology Division, Geological Survey of Namibia, Namibia, ⁴General Nursing, Southern Campus, University of Namibia, Namibia

Geophagy, the voluntary consumption of earth materials such as clay is one of the Medical Geology concerns. This study focused on determining the composition of geophagic material consumed mainly by pregnant women in Onangama Village, Northern Namibia and assess their possible health effects. X-ray Fluorescence (XRF), Inductively Coupled Plasma Mass Spectrometry (ICP-MS), X-ray Powder Diffraction (XRD), and Scanning Electron Microscope (SEM) analytical methods were used to determine the geochemistry and mineralogy of the consumed material. A health surveillance on pregnant women from the study area was also conducted.

The mineralogical results revealed quartz, calcite, gypsum, kaolinite, illite, and illite-montmorillonite as the main mineral phases of the studied geophagic materials. The geochemical analysis revealed high concentrations of aluminium, calcium, iron, magnesium, manganese, potassium, sodium, and silica; and trace elements including arsenic, chromium, mercury, nickel and vanadium as well as sulfate, nitrate, and nitrite anions comparing to the Recommended Daily Allowance (RDA) for pregnant women. The prevalence of geophagy in the study area was 88.2% with termite mound soil being the most consumed material. The health data collected from Engela State Hospital on pregnant women revealed limited pregnancy complications and outcomes, low birth weight and other parturition related health issues. Based on the obtained results so far, the studied geophagic materials suggest a potential health risks to pregnant women

Natural Cr(VI) occurrence in ground water: An example from the Bushveld Igneous Complex, South Africa, health impact and removal using Chitosan

Majola LL¹, Mamo M¹, Pillay K¹, and Mouri H²

¹Department of Applied Chemistry, University of Johannesburg, South Africa, ²Department of Geology, University of Johannesburg, South Africa

The presence of Cr(VI) ions in aqueous solution, especially wastewater, has detrimental effects on human and aquatic organisms and this has led to a search for readily available low cost adsorbents. In this study, chitosan modified with cerium oxide was used for the removal Cr(VI) from industrial wastewater. The adsorbent was characterized using Fourier Transform Infrared (FTIR) Spectroscopy, Scanning Electron Microscopy (SEM), Thermal Gravimetric Analysis (TGA), Zetasizer and X-ray Powder Diffraction (XRD). Parameters that were investigated include: adsorbent dosage, pH, initial concentration, contact time and temperature. The results showed that at a pH of 3, there is a maximum removal percentage of 99.89%, with an adsorbent mass of 0.08g at room temperature for 24 hours at a speed of 100 rpm. It was also noted that a higher removal efficiency was achieved with higher temperatures indicating that the adsorption was endothermic. The removal efficiency also increased with increasing initial concentrations and was reduced in the presence of sulphate ions. Further studies, which involve the fitting of kinetic and isotherm models are presently in progress. Also, to avoid secondary pollution caused by disposing the spent adsorbent into landfill sites, the reuse of the spent adsorbent in gas sensing applications are currently in progress





Remediation of Fluoride in groundwater using Rooibos tea waste loaded with Ce/Zr oxides: a case study around the Rustenburg area, South Africa

Mekgoe N¹, Pillay K¹, and Mouri H²

¹Department of Applied Chemistry, University of Johannesburg, South Africa. ²Department of Geology, University of Johannesburg, South Africa

Rooibos tea waste loaded with zirconium and cerium oxide (RBW-Ce-Zr oxide) was developed for fluoride removal from aqueous solution. Fluoride adsorption was studied in a batch system where adsorption was found to be pH dependent with a maximum removal efficiency at 6.13. The experimental data was more satisfactorily fitted with the Langmuir isotherm than with the Freundlich isotherm model. The kinetics of the adsorption process complied with the pseudo-second-order model. $E_a=38.60 \text{ kJmol}^{-1}$, indicating a chemisorption nature of the adsorption of fluoride onto RBW-Ce-Zr oxides. Enthalpy $\Delta H^\circ = +41.21$, ΔG° ranges from -2.813 to $-0.2523 \text{ KJ mol}^{-1}$ and $\Delta S^\circ (-0.1295)$ which supported the endothermic nature. Batch experiments were performed to study the applicability of the adsorbent by using fluoride contaminated water collected around the Pilanesburg area. The experiment of F⁻ adsorption results revealed that RBW-Ce-Zr oxides can be effectively employed as the potential adsorbents in the field of water defluoridation. The optimum dosage of the groundwater study was 0.0815g and the percentage removal was 99.98% and the groundwater the optimum pH was 6.03 and the percentage removal was 83.71% which is around the same pH. It was noted that 0.08 g of RBW-Ce-Zr oxides, effectively reduced the F⁻ concentration to 0.00175 mg/L which is below the standard permissible limit of F⁻ (<1.5 mg/L) in the drinking water.

The uranium and radon gas concentration and impact on human health: A case from abandoned gold mine tailings in the West Rand area, Krugersdorp, South Africa.

Moshupya P¹, Abiye T¹, Mouri H², and Levin M³

¹School of Geosciences, University of the Witwatersrand, Johannesburg, South Africa, ²Geology Department, University of Johannesburg, South Africa, ³Private consultant, P O Box 1731, Faerie Glen, Pretoria 0043, South Africa

The occurrence of uranium and radon gas has long been recognized to cause adverse health impact to the exposed populations. The current study was conducted in the Krugersdorp area, West Rand. The area is dominated by abandoned tailings dams from gold and uranium mines, which could be potential source for toxic metals and gases. In this study sampling of rocks, tailings, construction materials and water was carried out for geochemical and hydrogeological analysis. For characterization of radon, 60 radon monitors (RGMs) were installed in indoor and outdoor environments. The results showed that mine tailings in the area comprises of high uranium level with a maximum of 149.76 ppm and mean value of 48.87 ppm which exceptionally exceed the levels found in rocks. Surface water samples were found to contain uranium levels ranging between 1.93 mg/l and 4.7 mg/l, which are above the recommended levels of 0.015mg/l by WHO (2008). These high concentrations were found to be derived from the adjacent tailings residues. The results further indicated that radon levels range between 31.7 Bq/m³ to 1068.8 Bq/m³ which exceed the typical expected outdoor radon level of about 10 Bq/m³ estimated by UNSCEAR (2000). Significantly high average values of 187.4 Bq/m³ were obtained from gold tailings dams. The levels released from tailings were found to contribute to elevated levels in the background. The distribution was mainly controlled by wind and topographic attributes. In indoor environments radon concentration range up to a maximum of 173.5 Bq/m³ which is above the level recommended by WHO (2009). Subsequently high frequency of death that is related to lung cancer was documented in the area and was correlated with elevated radon levels

Toxic trace constituents in drinking borehole water of rural Greater Giyani area South Africa

Munyangane LP¹, Mouri H², and Kramers, J²

¹Council for Geoscience, South Africa, ²Department of Geology, University of Johannesburg, South Africa

Groundwater water plays an important role in rural Limpopo Province and it accounts for about two-thirds of rural domestic water supply. According to the South African constitution, every citizen has the right to adequate supply to clean and safe drinking water. However, to date, very little groundwater quality assessment has been undertaken throughout the region.

The objectives of our investigation is to assess concentration levels of toxic trace constituents and their spatial distribution patterns in drinking borehole water in the Greater Giyani area Limpopo, South Africa and the potential associated human health risks. Twenty-nine borehole water samples, including 15 community boreholes and 14 primary school boreholes were collected from this area. The samples were analysed for trace constituents such Arsenic (As), Cadmium (Cd), Chromium

(Cr), Selenium (Se), Lead (Pb) using the inductively coupled plasma mass-spectrometry (ICPMS) technique. The average concentrations of As, Cd, Cr, Se, and Pb were 11.3, 0.3, 33.1, 7.1, and 6.0 µg/L in the dry season and 11.0, 0.3, 28.3, 4.2, and 6.6 µg/L in the wet season, respectively. Se, Cr, Cd and Pb levels were generally very low and mostly found below the detection limit, and those boreholes with relatively higher concentrations only slightly exceeded the SANS limit for drinking water. A total of four boreholes exceeded the water quality guideline for arsenic with two of these boreholes containing five times more arsenic than the prescribed limit.

The results obtained from this study suggest that a significant water quality problem mainly with respect to arsenic exists in the rural Greater Giyani area and further imply that a certain proportion of the population in the studied area could be at health risk caused by the exposure to toxic trace constituents.

Distribution of Uranium (U), Molybdenum (Mo) and Mercury (Hg) bearing minerals as potential sources for toxic chemicals in Karoo ground-and-surface waters

Okuhle P¹, de Wit M¹, and Mouri H²

¹AEON, Nelson Mandela University, South Africa, ²Department of Geology, University of Johannesburg, South Africa

Uranium (U), Molybdenum (Mo), and Mercury (Hg) are likely to dissolve in ground-and-surface water during recycling and weathering of rocks and minerals enriched in these elements. Humans exposed to elevated concentrations of these types of chemicals usually suffer from chronic diseases. For example, ingested U has a potential to damage kidneys, causing liver dysfunctionality. Mo at concentrations of below 0.07 mg/l play a vital role to human, animal and plant health, since it acts as a substance for the functioning of a large number of enzymes that speed up chemical reaction entailed in N, C, and S cycling. However, at high concentration Mo can be dangerous. However, only few reports are published about its danger to human health; the main research has been on animals. Mercury is also dangerous to human and animal health; it causes severe gastrointestinal damage, cardiovascular failure, especially when ingested in drinking water at concentration levels exceeding maximum guideline value of 0.006 mg/l as per WHO standards. There are number of exposure pathways of these elements to humans; for instance through drinking of Uranium-contaminated water, eating Uranium-contaminated food or inhalation of Uranium-rich dust or decay products of Uranium like Radon gas. This study focuses on testing the contamination of ground-and-surface water enriched in Uranium (U), Molybdenum (Mo) and Mercury (Hg) and to identify health issues associated with this in the Karoo near Beaufort West. Preliminary sampling was carried out during 17-20 September 2018 in one of my study sites, to collect water samples from open boreholes, wind pumps and dams. A total 12 water samples were collected, PH and conductivity was measured in situ using Ph meter and TLC. Samples were analysed for chemical parameters such as trace element, cation concentrations, Total Dissolved Solids and alkalinity. Average PH values of 8.06 and average conductivity values of 1276 µS/cm where obtained from these samples. Based on these results most of these water samples are alkaline and contain high concentration of ions. Anions where analysed using Ion chromatography, and the results obtained reveal average concentrations of 1.44 mg/l for Fluoride, 59.39 mg/l for Chloride, 11.25 mg/l for Nitrate and 238.70 mg/l for Sulphate. Nitrite and Phosphate where not detected. The majority of these anions are below threshold value of WHO standards, meaning they do not pose high risk on human and animal health. The next step for this study is to collect more samples and analyse trace element and cation concentrations using ICP-MS, to create models to quantify distribution of analysed chemical elements in water. At a later stage, local clinical data and incidences of diseases resulting from excess consumption of chemical elements in drinking water by the surrounding community will be acquired. Conclusively this study will act as baseline study for ahead of anticipated hydraulic fracking and uranium mining in the region.

The possible geological sources of chronic copper poisoning of sheep in some specific farms of the Karoo Basin, South Africa

Pretorius C.¹, Mouri H.¹, Cave M.², Pienaar J.³ and Rose D.¹

¹University of Johannesburg, Faculty of Science, Department of Geology, South Africa, ²British Geological Survey, Keyworth, Nottingham NG12 5GG, UK, ³State Veterinary Beaufort West, Dept. Agriculture Western Cape Blyth Street, Beaufort West 6970, South Africa

Copper (Cu) is an essential trace element for domestic animals, however, higher concentrations can cause poisoning in sheep [1, 2] for example. Chronic toxicity can occur if over than 25 mg/kg of Cu is consumed daily over a period of time [3]. Cu is then accumulated in the liver, and released into the bloodstream when sheep experience stress, due to various factors including transportation, poor nutrition, dosing or handling, change in weather conditions and drought [1]. In South Africa, a form of chronic Cu poisoning, called enzootic icterus occurs in sheep farmed in some specific farms of the main Karoo Basin [4]. The geology of the study area consists of argillaceous rocks [5] and the Karoo igneous intrusions, commonly called the





Karoo dolerites, which intruded through a network of sills, dykes, and discordant sheets [6]. It is suspected that the Karoo dolerites might be the source of excess Cu [4]. However, no detailed research has been conducted in order to prove or disprove such a theory. Our preliminary data on the Karoo dolerites show that these rocks contain Cu concentration ranging between 57.02 and 83.93 mg/kg, which is above the average concentration in earth's crust (55 mg/kg [7]). Whereas other rock types in the area show lower Cu concentrations of 6.19–41.11 mg/kg. Molybdenum (Mo) is also considered as it can affect the uptake of copper when it is combined with sulphur (S) to form an insoluble complex, which prevents the liver from absorbing the Cu [1].

References:

[1] J. W. Spears. Salt and Trace Minerals Newsletter, p. 5, 2011. [2] D. C. Whitehead. Wallingford: CABI Publishing, 369pp. 2000. [3] National Research Council (NRC), Nutrient requirements of sheep, 6th ed., vol. 5. National Academies Press, 1985. [4] G. F. Bath. J. S. Afr. Vet. Assoc. Vol. 50, no. 1, pp. 3–14, 1979. [5] M. R. Johnson et al., Geol. South Afr., pp. 461–499, 2006. [6] A. R. Duncan and J. S. Marsh. Geol. South Afr., pp. 501–520, 2006. [7] A. Kabata-Pendias. 4th ed. Boca Raton: CRC Press, 2011

Possible causes for goiter occurrences in Badagry, Lagos, SW Nigeria: Iodine and other trace elements in drinking water

Sanyaolu OM¹, Mouri H¹, Odukoya A², and Selinus O³

¹ Department of Geology, University of Johannesburg, South Africa, ² Department of Geology, University of Lagos, Nigeria, ³ Linneaus University, Sweden.

Many factors have been advanced to explain the causes of goiter. Among these, the environmental/dietary factors, which include iodine, selenium and goitrogens were the most common causes. In Nigeria, some studies established that the prevalence of endemic goiter is due to iodine deficiency, which occurs mainly in the metamorphic and igneous granitic basement complex. No cases of goiter were reported in the coastal and sedimentary environment due to sufficient level of iodine. However, recent studies from some parts of SW Nigeria revealed occurrences of goiter in these environments. These findings suggest that the occurrence of goiter and its link to such environments (coastal and sedimentary) are still uncertain. Therefore, the purpose of the present study is to analyse iodine and other possible element's concentrations in drinking water and their possible impacts on the prevalence of goiter disease in coastal area of Badagry in Lagos. The geochemical results revealed high concentrations of I, Pb, Hg, As and NO₃ in drinking water samples. These results might suggest that high dietary intake of not only I, but also Pb, As, Hg and NO₃ could have contributed to the goiter prevalence and other thyroid dysfunctions in the study area.

Uptake of heavy metals by vegetable plants grown on potentially contaminated agricultural soils: Evaluating heavy metal accumulation and potential health risk

Sihlahla M¹, Mouri H², Nomngongo PN¹

¹ Department of Applied Chemistry, University of Johannesburg, DFC- Campus, South Africa, ² Department of Geology, University of Johannesburg, APK- Campus, South Africa

Environmental pollution by presence of trace and heavy metals resulting from anthropogenic activities has become a global concern. The use of agrochemicals and untreated water for irrigation of agricultural fields can result in contamination of soil, underground water and agricultural produce (vegetables) by heavy metals, thus posing a threat to human and environmental wellbeing. The aim of the current study was to quantify the concentration of heavy metals in agricultural soils, water and agricultural produce collected from Port St. Johns, Eastern Cape (South Africa). In addition, the potential health risk associated with consumption of vegetables crops contaminated with toxic heavy metals was investigated. The results obtained from the study revealed the presence of some heavy metals in soil, water and vegetables samples (spinach). For instance, metals such as Zn, Se, Ni, Mn, Fe, Cu and Cr were detected in spinach samples and were found to be below maximum permissible level according to World Health Organization (WHO) guidelines. This implied that this agricultural produce was safe for human consumption. Similar results were obtained for soil samples, suggesting that the soil is not heavily contaminated by Zn, Se, Pb, Ni, Mn, Fe and Co). For water samples Fe, Mn, Pb, Se, and Zn were found to be above maximum allowed limit according to Department of Water and Sanitation and WHO guidelines. Different health risk assessment indices were applied to assess the risk posed by these metals such as transfer factor (TF) and health risk index (HRI) among others. The HRI was >1 indicating a potential health risk posed by the metals. The AF for Cd, Mn, Se, Mn and Zn was > 1 indicating that these metals have the ability to translocate from soil to plant and bio-accumulate. The results emphasized the need for pre-treatment of river water for irrigation purposes and routine monitoring of agricultural soil is required in the area to avoid contamination of crops thus reducing the risk exposure of humans to metals

Arsenic in ground water, health impacts and possible remediation: a case study from Mopani District Giyani, South Africa

Tshishonga M1, Gumbo1 J.R., Mouri2 H. and Dowling K.3

1Department of Hydrology and Water Resources, School of Environmental Sciences, University of Venda, Limpopo, South Africa, 2Department of Geology, University of Johannesburg, South Africa, 3Faculty of Science and Technology, Federation University, Australia.

The presence of Arsenic (As) in groundwater is a cause of concern with regard to human health and requires intervention before the water is consumed. Drinking water with As may result in As-related diseases such as skin pigmentation and keratosis (1). For this study, water samples were collected during the wet (February 2018) and dry season (October 2017) from boreholes in Giyani district, South Africa. The boreholes are known to have high levels of Arsenic (2). The three borehole water samples (BH03, 07, 28) were then poured into the ceramic water filters and filtered water was then collected for analysis. The raw and filtered water samples were analysed for pH, electrical conductivity, temperature and turbidity and Arsenic levels using a Inductively Coupled Plasma Mass Spectrometry technique. The average pH, electrical conductivity, water temperature and turbidity of the raw and filtered water samples were: 8.5, 1200 $\mu\text{S}/\text{cm}$, 26.5 $^{\circ}\text{C}$ and 0.8 NTU and 8.5, 1200 $\mu\text{S}/\text{cm}$, 26.5 $^{\circ}\text{C}$ and 0.8 NTU respectively. The average As level in raw water and filtered water samples BH03 was 2.76 $\mu\text{g}/\text{L}$ and 0.36 $\mu\text{g}/\text{L}$ and 3.22 $\mu\text{g}/\text{L}$ and 0.17 $\mu\text{g}/\text{L}$ and the Arsenic levels were reduced by 87% and 95% during wet and dry seasons respectively. The average As level in raw water and filtered water samples BH07 was 12.58 $\mu\text{g}/\text{L}$ and 5.19 $\mu\text{g}/\text{L}$ and 18.44 $\mu\text{g}/\text{L}$ and 3.09 $\mu\text{g}/\text{L}$ and the Arsenic levels were reduced by 59% and 83% during wet and dry seasons respectively. The average As level in raw water and filtered water samples BH28 was 0.88 $\mu\text{g}/\text{L}$ and 7.87 $\mu\text{g}/\text{L}$ and 6.74 $\mu\text{g}/\text{L}$ and 4.86 $\mu\text{g}/\text{L}$ and the Arsenic levels were increased by 794% and reduced by 28% during wet and dry seasons respectively. The As content in raw water sample BH07 was higher than the SANS 241 Arsenic guideline value of 10 $\mu\text{g}/\text{L}$ (SANS, 2011). With sample BH28 there is conflicting As results with data showing an increase in the filtered water during the wet season. This can be due to either leaching of As from clay matrix of the ceramic water filter or an error in As analysis. Further investigation is needed in order to clarify this discrepancy. This study suggests that the ceramic water filters were able to improve the quality of borehole water by reducing the turbidity and the As in contaminated borehole water samples. The filters were manufactured at Mukondeni Pottery, Limpopo and consisted of Mukondeni black clay (Smectite) and sawdust and the heating of clay pot in an oven creates tiny pores that allow passage of water and activated carbon (from the burning of sawdust) is the basis for the removal of As (4).

References:

(1) Mazumder, D. N. G. (2008). Indian Journal of medicine, 28, 436-447. (2) Munyangane, P., Mouri, H., & Kramers, J. (2017). Environmental Geochemistry and Health, 1-19. (3) South Africa National Standard (SANS) 2011). South African National Standard of Drinking water. Part 1: SABS Standard Division. (4) Mulaudzi D. A, Gumbo J. R (2014). Trans-disciplinary E-journal (TEJ). The Inaugural edition. 1 (1): 77-105.





Postgraduate students in PPM who graduated in 2017 and 2018

2017: MSc:

Adeniyi, Elijah Olusola: Thermal impact of dolerite sills on the shale gas potential of Ecca Group mudstone in a drill core from the central Main Karoo basin. Supervisor: Prof. M.O. de Kock; co-supervisors: Prof. NJ Beukes, Fr F-G Ossa Ossa.

Koki, Christa: Investigating geogenic lead contamination and its associated health effects in Kilifi area, Kenya. Supervisor: Prof. H Mouri. Co-supervisor: Prof. L Olaka (Univ. Nairobi).

Lechekoane, Tshwepang: Paleomagnetism and geochemistry of the Mesoarchean Klipwal diamictite, Mozaan Group, Pongola Supergroup, South Africa. Supervisor: Prof MO de Kock; co-supervisors: Prof. A Hofmawnn, Prof. NJ Beukes.

Matiane, Arnold Ripfumelo: Consideration of rare earth elements (ree's) associated with coal and coal ash in South Africa. Supervisor: Prof. NJ Wagner.

Mkhize, Buhle: The variability of particle size distribution measured in 2D versus 3D. Supervisor: Prof. KS Viljoen; co-supervisor: Ms K Duarte (Anglo Research), Ms N Shackleton (Anglo Gold Ashanti).

Monareng, Batobeleng Fisah: Petrography and geochemistry of the pre-Mapedi "bostonite" dykes and sills in the Kalahari Manganese Field, Northern Cape Province. Supervisor: Prof. NJ Beukes; co-supervisors: Prof. M.O de Kock, Mrs L. Blignaut.

Mphaphuli, Maseda (with distinction): Petrographic consideration of the impact of the Tshipise fault on coal quality in the Soutpansberg Coalfield, South Africa. Supervisor: Prof. NJ Wagner; co-supervisor: Mr J. Sparrow (Coal of Africa Ltd).

Ravhure, Livhuwani Given: A multi-pronged approach to to constrain the age of the Molopo Farms Layered Igneous Complex, Northern Cape Province and Southeastern Botswana. Supervisor> Prof. MO de Kock. Co-supervisors: Dr C Vorster, Prof. NJ Beukes.

PhD:

Blignaut, Lauren Cher: A petrographical and geochemical analysis of the Upper and Lower manganese ore bodies from the Kalahari Manganese Deposit, Northern Cape, South Africa – controls on hydrothermal metasomatism and metal upgrading. Supervisor: Prof. KS Viljoen; co-supervisor: Prof. H Tsikos (Rhodes Univ.).

Dzvinamurungu, Thomas: a geometallurgical investigation of the main Mineralized Zone and the peridotitic Chromitite Mineralized Zone at the Nkomati Mine, with a view on the liberation and recovery of pentlandite and chromite. Supervisor: Prof. KS Viljoen.

Lum, Julieta Enone: a mineralogical and geochemical characterization of beryl from Southern Africa. Supervisor: Prof. KS Viljoen; co-supervisor: Prof. B. Cairncross.

Rose, Derek Hugh: A process mineralogical investigation of the Merensky Reef and UG-2 at the Two Rivers platinum mine with emphasis on or echaracterization. Supervisor: Prof. KS Viljoen.

2018: MSc:

de Kock, Marthinus Conrad: Metallogenesis of the Palaeoproterozoic Sishen iron ore deposit, Northern Cape Province, South Africa. Supervisor: Dr AJB Smith, Co-supervisor: Prof. NJ Beukes.

Hlongwani, Nkhensani Caroline (with distinction): Characterization of the upper manganese bed of the Hotazel Formation at KMR mine, Kalahari Manganese Field, Northern Cape Province. Supervisor: Dr AJB Smith; co-supervisors: Prof. NJ Beukes, Dr LC Blignaut.

Masangane, Martha Priscille Nomacala: The timing and nature of post-depositional iron mineralization in in ore from the Wolhaarkop Dome, Northern Cape, South Africa. Supervisor: Dr AJB Smith; co-supervisor: Prof. NJ Beukes.

Nthloro, Boitumela Lena: The timing and nature of of post-depositional iron mineralization at Kolomela Mine, Northern Cape, South Africa. Supervisor: Dr AJB Smith; co-supervisor: Prof. NJ Beukes.

Terblanche, Sullivan: The provenance of the Buffels River complex.: the timing of its formation and the possible source area of its diamonds. Supervisor: Dr HS van Niekerk; co-supervisor: Dr C Vorster.

MSc students registered in PPM ambit in 2017-2018

NAME OF STUDENT	TITLE OF PROJECT	SUPERVISOR	CO-SUPERVISOR	DATE OF FIRST REGISTRATION	STATUS	FULL TIME/PART TIME
Abraham, Rowen	Carbon dioxide adsorption behavior of geological samples from the Karoo Basin, South Africa	Wagner N		2017	Completed 2018	FT
Ahlijah Enoch	Geophagic clay and impact on human health: Case studies from Ghana	Mouri H		Feb-17	Ongoing	FT
Boshoff, Pedro	Case studies of speleogenesis in the Cradle of Humankind UNESCO heritage site and the West Rand Expanse, South Africa: tectonic controls and their Paleoproterozoic component	Kramers JD	Van Niekerk HS	Jul-05	Completed 2017	PT
Breakfast, Mzoli	Mineral prospectivity mapping of the Bushmanland Group of the Namaqua-Natal Mobile Belt, with implications for base metal sulphide deposits	Elburg		1-9-2016	01-04-2019	PT
Brown, Graham	Petrographical, Mineralogical and Geochemical Characterisation of the Iron Formation directly above the Upper and Lower Mn Ore Beds, Main Kalahari Deposit – Alteration Models	Blignaut LC	Smith B, Vafeas N	10th January 2018	Ongoing	FT
De Kock, Martinus Conrad	Metallogenesis of the Palaeoproterozoic Sishen iron ore deposit, Northern Cape Province, South Africa.	Smith AJB	Beukes NJ	02/2014	Graduated in 2018	FT
Ficq, Gabrielle	PGE distribution and Re-Os geochronology of Early Archean ultramafic rock associations from Kaapvaal craton granite-greenstone belts: Clues to the stabilization of Earth's first continents and the evolution of South Africa's platinum endowment	Tappe S		01/2017	Ongoing	FT
Fitzpatrick, S	Paleomagnetism and detrital zircon provenance of the Koras Group, South Africa	Van Niekerk HS	Vorster C	2014	Completed 2017	FT
Francis, Fabien	The stratigraphy, sedimentology and petrography of the Number 2 Coal Seam in the northern portion of the Permian Highveld Coalfield, Karoo Basin, South Africa.	Wagner N		2015	Ongoing	PT



Hlongwani N. Caroline	Characterization of the upper manganese bed of the Hotazel Formation at KMR mine, Kalahari Manganese Field, Northern Cape Province.	Smith AJB	Blignaut LC, Beukes, N.J.	01/2015	Graduated in 2018	FT
Hlungwani, Peace	The geochemistry of the Molopo Farms Complex	Elburg		1-1-2016	Completed 2018	FT
Kambunga Selma	Geophagy during pregnancy and possible health effects: Case studies in northern Namibia	Mouri H		Feb-17	Apr-19	FT
Kekana, Papi	The temporal and spatial variation of coal quality and mineability, with the focus on the Mpumalanga Coalfields	Wagner N		Jan-16	Completed 2018	FT
Khosa, Rivoningo	The determination of erosion rates along the Vaal River in the Vredefort Dome, using cosmogenic nuclide, beryllium-10.	Kramers, J.D.	Makhubela TV			
V. Mbele (iThemba)	Jan-17	Ongoing	FT			
Konyana, Sibusiso	Determination of erosion rates along the Mpumalanga Escarpment using cosmogenic ¹⁰ Be, and weathering geochronology of post-Gondwana soil profiles.	Kramers, J.D.	Makhubela T.V., Van Niekerk HS			
S. Winkler (iThemba)	2017	Ongoing	FT			
Magwaza, Boniswa	Isotopic resetting of zircon: influence of age, temperature and chemical environment	Elburg, M.		1-1-2016	01-04-2018	FT
Majola, Lupita	Natural Cr(VI) occurrence in ground water: Bushveld Igneous Complex, South Africa, risks and remediation	Mouri H		Feb-17	Ongoing	FT
Makukule Xitembiso M.	Using petrography, image analysis and tomography to validate coal washability in southern African coals	Dorland HC	Wagner N	01/2016	12/2017	FT
Masangane, Martha Priscille Nomacola	The timing and nature of post-depositional iron mineralization in ore from the Wolhaarkop Dome, Northern Cape, South Africa.	Smith AJB	Beukes NJ	02/2014	Graduated in 2018	FT
Mashamba, M.Lucas	Geochemical studies of the Brugspruit Stream water and acid mine drainage (AMD) contaminant sources in the Brugspruit catchment area, Emalaheni (Witbank) Coalfield, Mpumalanga	Kramers JD		Jan-13	Completed 2017	PT

Mashiane, Neithel	Rare earth element potential of the Bushveld Complex, Upper Zone	Elburg		9/2016	14-9-2018	FT
McGeer, Bianca	An investigation into whether conditions conducive to the phenomenon of reactive ground are present in the Witbank Coalfield.	Wagner N	S	2017	Ongoing	PT
Mekgoe, Nokuthula	Case studies of remediation of Fluoride in groundwater using Rooibos tea waste loaded with Ce/Zr oxides	Kriveshini, P.	Mouri H	Feb-17	Oct-19	FT
Mgoqi, Aviwe	Effect of regional geology and mining activity on water quality: studies in the eMalahleni (Witbank) and South Rand coalfields	Kramers JD	Dr D. Love (Golder Assoc.)	Jan-15	Completed 2018	FT
Milne, Sarah	The Geology of the Premier Mine, Gauteng	Tappe S		Jan-17	Ongoing	FT
Mokwena, Louisa	The occurrence of chromium and other trace elements in selected South African coals.	Wagner N		2017	2018	Ft
Molekwa, Anna	Reconstruction of the Paleo-Archean shallow water environments: Evidence from Buck Reef Chert Drill Core BARB3	Hofmann A		2015	2017	FT
Morake, Mabueta	Petrography and Geochemistry of Early-Middle Jurassic Mafic Dykes from the H.U. Sverdrupfjella, Antarctica	Knoper MW	Elburg, M. and Kramers, J.	Jul-15	Jul-18	FT
Mpanza, Zama	Constraints on geochemical processes in the mantle below the Premier (Cullinan) diamond mine through the analysis of peridotitic garnets.	Viljoen KS	Tappe S	01/2016	12/2017	FT
Naidoo, Arantxa	Alkaline-carbonatite magmatism of Late Archean age in the North Atlantic craton in east Greenland	Tappe S		2016	Ongoing	FT
Ndlovu, Brian Zwai	A mineralogical and geochemical study of platinum-group minerals and base metal sulphides in the P1 and P2 units of Platreef at the Lonmin Akanani project area, Bushveld Complex, South Africa.	Viljoen, K.S.	Knoper, M.	Jan-16	Jan-18	FT
Nendouhada, Ndivhuho	Lateral comparison of coal composition in Botswana coalfields through the use of coal petrography	Wagner N (Co)		2015	2017	Ft



Ngobeli, R	A comparison between detrital zircon age populations of the Koegas Subgroup of the Ghaap Group and overlying Makganyene Diamictite of the Postmasburg Group, Transvaal Supergroup, Griqualand West.	Vorster C	Beukes NJ	Feb-16	Ongoing	FT
Ntlhoro, Boitumelo	The timing and nature of post-depositional iron mineralization at Kolomela Mine, Northern Cape, South Africa.	Beukes NJ	Smith AJB	2014	Graduated in 2018	FT
O'Kennedy Johan	Paleomagnetism of Jurassic dykes from Dronning Maud Land, Antarctica	Knoper MW		Jul-16	Ongoing	FT
Kabelo, Obakeng	Geochemical and petrographic characterization of coal seams from the Lechana coalfield, eastern Botswana	Wagner N (co-sv)		2016	Graduated 2018	FT
Ormond, Robyn	Structural and geochronological constraints on polyphase deformation of the Zwartkops Hills, central Kaapvaal Craton	Lehmann J		01/2017	Ongoing	FT
Phetla, Shadrack	A petrographic and geochemical characterisation of the upper Mn ore beds above and below the thrust fault in the Main Kalahari Deposit, Northern Cape Province, South Africa	Blignaut, LC	Smith, A.J.B., Vorster, C	01/2018	Ongoing	FT
Pretorius, Carike	The possible geological sources of chronic copper poisoning of sheep in specific areas of the Karoo Basin, South Africa	Mouri H	Rose DH	Feb-17	Ongoing	FT
Sanyaolu Olufunke	Possible causes for goiter occurrences in Badagry, Lagos, SW Nigeria: Iodine and other trace elements in drinking water	Mouri H		Feb-17	Ongoing	FT
Sauer, Megan	Apatite mineralisation in pyroxenites of the Phalaborwa Complex	Elburg, M.		2018	Ongoing	PT
Scheepers GJ	The reconstruction of a paleoenvironment for the Number 4 Lower Coal Seam towards the eastern boundary of the Highveld Coalfield and the associated influence on the coal qualities.	Wagner N		2018	Ongoing	PT
Senzani, Khangesiwe Karen	Investigating Uranium-236 trends in the Mozambican Channel as revealed by Europa Coral	Kramers JD	Dr S. Winkler (iThemba)	Jan-16	Ongoing	PT

Sihlahla Masixole	Evaluating potential health risk from uptake of heavy metals by vegetables grown on potentially contaminated soils	Nomngongo,P	Mouri H	Feb-17	Ongoing	FT
Sito, Welhemina khobi	Petrogenesis and Economic Potential of Mafic-Ultramafic Satellite Intrusions to the Kunene Anorthosite Complex, Angola'	Owen-Smith TM	Tappe, S.	01/2017	Ongoing	FT
Terblanche, Sullivan	The provenance of the Buffels River complex.: the timing of its formation and the possible source area of its diamonds.	Vorster C	Van Niekerk HS	Feb-15	Graduated in 2018	FT
Zardad, Sabiyyah	The Sedimentology of the Rooihoogte Formation of The Transvaal Supergroup in the Carletonville area, South Africa.	Beukes NJ	Smith AJB, Vorster C	2015	2018	PT

PhD students registered in PPM ambit in 2017-2018

NAME OF STUDENT	TITLE OF PROJECT	SUPERVISOR	CO-SUPERVISOR	DATE OF FIRST REGISTRATION	STATUS	FULL TIME / PART TIME
Abobrake, Abusede	Sedimentology and paleomagnetism of KARIN borehole core	De Kock MO		Feb-17	2019	FT
Agra, Naa Afi	Petrogenesis and geochemistry of the Paleoproterozoic Birimian metavolcanic, metasedimentary and intrusive rocks in the Bui belt of Ghana	Elburg MA	Vorster C	1-2-2017	Ongoing	FT
Ahmed U	Radionuclides in coal fired power stations	Wagner N		2018	Ongoing	PT
Badenhorst, Charlotte	Char extracted from coal ash as a replacement for natural graphite -Charphite	Wagner N		2016	Ongoing	FT
Bowden, Laura	Karoo zircon provenance studies	Beukes NJ	Vorster C	Jul-15		FT
Chabalala, Vongani	The Application of Organic Petrology to Gas Exploration in South Africa	Wagner N		2016	2019	PT
Chagondah, Godfrey	Petrogenesis and metallogenesis of Archaean rare element granitic pegmatites in Zimbabwe: implications to exploration	Hofmann A		2016	Ongoing	PT
Coetzee, L.L.	Manganese mineralization in the Avontuur deposit, Hotazel Formation	Beukes, N.J.		01/2018	Ongoing	PT
Costa Giuliana	Evaluation of syn-sedimentary gold deposition in the Wits Basin	Hofmann A		2015	Ongoing	FT



Djeutchou, Cedric	Paleomagnetism of the 1.87-1.84 Ga Black Hills dyke swarm: implications for the Paleoproterozoic geomagnetic field	De Kock MO		Nov-15	Ongoing	FT
Gevera, Patrick	High fluoride and dental fluorosis prevalence: Case studies from the Kenyan Rift and adjacent areas	Mouri, H.		Feb-18	Ongoing	FT
Jodder, Jaganmoy	Unraveling the chronostratigraphy of the Iron Ore Group (IOG) of the Singhbhum craton, India	Hofmann A		2016	Ongoing	FT
Kwayisi, Daniel	The Buem Ophiolite and its implication on the evolution of the Pan-African Dahomeyide Orogen, West Africa	Lehmann J	Elburg MA	Mar-17	Mar-20	FT
Lechekoane, Tshepang	The origin and significance of carbonaceous matter in the Witwatersrand Basin	Hofmann A		2017	Ongoing	FT
Luskin, Casey	Paleomagnetism of the Nsuzi Group	De Kock MO		Mar-16	Ongoing	FT
Makhubela, Tebogo Vincent	Multiple isotope studies relating to cave development and landscape evolution in the Cradle of Humankind and surrounding areas, South Africa.	Kramers JD		Jan-15	Submitted 2018	PT
Mangs, Ayuba	The petrography, mineralogy and geochemistry of coal within the Benue Trough of Nigeria	Wagner N		2017	Ongoing	FT
Mkhatshwa Sindile	A geometallurgical assessment of gold and uranium mineralisation at Randfontein Estates, Sibanye Gold	Viljoen KS	Smith AJB	1/1/2016	31/12/2018	FT
Moitsi, Ernest	Geometallurgy of UG2 at Lonmin Marikana mines	Viljoen KS	Rose DH	1/7/2016	ongoing	FT
Moroeng, Ofentse Marvin	Coal Oxidation – Insights into Elemental and Molecular changes in Coal Macerals	Wagner N			Graduated 2018	PT
Mothloba GB	Geometallurgy of the Big Syncline deposit, Vedanta mines	Smith AJB	Viljoen KS and Rose, DH	02/2017	Ongoing	FT
Muzderengi, Confidence	Supergene gold enrichment in the Giyani Greenstone Belt	Smith, AJB		01/2018	Ongoing	PT
Ncube, Sinikiwe	Petrogenesis of the Kameel Complex and associated mafic intrusions, Northern Cape	Owen-Smith TM		10/2018	Ongoing	FT
Nunoo, Samuel	Deciphering the structural control and ore genesis of the Collette and Josephine deposits, NW Ghana	Hofmann A		2017	Ongoing	FT

Nxumalo, Valerie	Uranium mineralisation and provenance analyses of the Karoo Supergroup in the Springbok Flats Coalfield, South Africa	Kramers JD	Cairncross B and Vorster C	Jan-14	Ongoing	PT
Paprika, Dora	Mesoarchaeon volcanism and associated hydrothermal activity of the Dominion Group, South Africa - implications for Witwatersrand Basin gold	Hofmann A		2017	Ongoing	FT
Shelembe, Refilwe	The alkaline Pilanesberg Complex and the mafic Rustenburg Layered Suite: Sources of potentially harmful elements and their health impact on the regional communities	Mouri, H.	Kramers, J.	Jan-13	Ongoing	PT
Singo, Ndinanye Kenneth	In search of the possible economic potential of defunct mine residue areas for development purposes: case study of Musina copper mine, Giyani Louis Moore gold mine, Zwigodini Nyala magnesite mine, South Africa	Kramers JD		Jan-14	Submitted 2018	PT
Solanki, Anika	The Origin and Evolution of South African Group-2 Kimberlite Magmatism: Insights from Petrology, Geochronology and Diamond Chemistry	Tappe S		Oct-16	Ongoing	FT
Tshiongo-Makgwe, Nkhumeleni	Proposing dry beneficiation methods by using information from petrography, mechanical and micro-hardness of macerals in a selection of South African coals.	Wagner N		2017	Ongoing	FT
Vafeas Nicholas A.	Petrographic and Metallogenic analyses of the carbonated, low-grade manganese ore of the Hotazel Formation and its potential use in flue-gas desulphurisation	Viljoen KS	Blignaut LC	Jun-16	Ongoing	FT
Vines, Marylou	Geology of the "Antimony Line" and associated Sb-deposits of the Murchison greenstone belt, South Africa - Implications for hydrothermal and tectonic processes responsible for antimony and gold mineralization in the Archean.	Hofmann A		2018	Ongoing	FT



Postdoctoral Fellows in PPM 2017-2018

NAME	Research focus	HOST
Ballouard, Christophe	Igneous petrology and geochemistry; Pegmatite-hosted mineral deposits.	Elburg, M.A.
Dietrich, Pierre	Sedimentology, particularly of glacial deposits; Landscape evolution, recent and past environments	Hofmann, A
Ossa Ossa, Frantz-Gerard	Mineralogy in diagenesis and low grade metamorphism; Archaean and Palaeoproterozoic atmosphere and environment	Hofmann, A
Agangi Andrea	Mineral and inclusion trace element chemistry; economic geology	Hofmann, A
Humbert, Fabien	Igneous geochemistry, Petrology, Isotope Geochemistry; structural and palaeomagnetic studies of the Palaeoproterozoic Hekpoort and Ongeluk lavas.	Smith, AJB
Massuyeau, Malcolm	Igneous thermodynamics, Mantle dynamics, with emphasis on the effects of H ₂ O and CO ₂	Viljoen, KS, Tappe, S (co-host)
Sciscio, Lara	Palaeomagnetism and magnetostratigraphy	De Kock, MO

Refereed Journal Publications and Book Chapters, 2017

- Alam, M., Choudhary, A.K., Mouri, H. and Ahmad, T. (2017) Geochemical characterization and petrogenesis of mafic granulites from the Central Indian Tectonic Zone (CITZ). Geological Society, London, Special Publications 449 (1), 207-229
- Andersen, T., Elburg, M. and Erambert, M. (2017) The miaskitic-to-apatitic transition in peralkaline nepheline syenite (white foyaitite) from the Pilanesberg Complex, South Africa. *Chemical Geology* 455, 166-181. doi:10.1016/j.chemgeo.2016.08.020. *SCI* 2015: 3.48.
- Arhin, E., Mouri, H., Kazapoe, R. (2017) Inherent Errors in Using Continental Crustal Averages and Legislated Accepted Values in the Determination of Enrichment Factors (EFs): A Case Study in Northern Ghana. *J Geogr Nat Disast* 7 (204), 2167-0587.1000204.
- Aulbach, S., Jacob, D.J., Cartigny, P., Stern, R.A., Simonetti, S.S., Wörner, G. and Viljoen, K.S. (2017) Eclogite xenoliths from Orapa: Ocean recycling, mantle metasomatism and diamond formation at the western Zimbabwe craton margin. *Geochimica et Cosmochimica Acta*, 213, 574-592.
- Aulbach, S., Woodland, A.B., Vasilyev, P., Galvez, M.E. and Viljoen, K.S. (2017) Effects of low-pressure igneous processes and subduction on Fe³⁺/ΣFe and redox state of mantle eclogites from Lace (Kaaopvaal craton). *Earth and Planetary Science Letters*, 474, 283-295.
- Bolhar, R., Hofmann, A., Kemp, A.I.S., Whitehouse, M.J., Wind, S. and Kamber, B.S. (2017) Juvenile crust formation in the Zimbabwe Craton deduced from the O-Hf isotopic record of 3.8–3.1 Ga detrital zircons. *Geochimica et Cosmochimica Acta*, 215, 432-446.
- Cairncross, B. (2017) Bultfonteinite: The where of mineral names, *Rocks & Minerals*, 92(6), 578-571.
- Cairncross, B. (2017) Leiteite: Connoisseur's choice. *Rocks & Minerals*, 92(3), 264-269.
- Cairncross, B. (2017) Nchwaningite: The where of mineral names, *Rocks & Minerals*, 92(3), 290-292.
- Cairncross, B. (2017) Sugilite: Connoisseur's choice. *Rocks & Minerals*, 92(6), 550-555.
- Cairncross, B. (2017) Tsumcorite: Connoisseur's Choice, *Rocks & Minerals*, 92(5), 454-461.
- Cairncross, B. (2017) Tsumebite: The where of mineral names. *Rocks & Minerals*, 92(5), 466-470.
- Cairncross, B., Beukes, N.J., Moore, T. and Wilson, W.E. (2017) The N'Chwaning mines, Kalahari Manganese Field, Northern Cape Province, South Africa. *Mineralogical Record*, 48(1), 13-114.
- Clemens, J., Elburg, M.A., Harris, C. (2017). Origins of igneous microgranular enclaves in granites: the example of Central

Victoria, Australia. *Contribs. Min. Petrol.* 172: 88. doi:10.1007/s00410-017-1409-2

Clemens, J.D., Stevens, G. and Elburg, M.A. (2017) Petrogenetic processes in granitic magmas and their igneous microgranular enclaves from Central Victoria, Australia: match or mismatch? *Transactions of the Royal Society of South Africa*, 72, 6-32. No SCI rating; DoHET approved local journal.

Da Costa, G., Hofmann, A. and Agangi, A. (2017) Chapter 18 – Provenance of Detrital Pyrite in Archean Sedimentary Rocks: Examples from the Witwatersrand Basin. In: *Sediment provenance- Influences on compositional change from source to sink*. (Edited by Muzumder, R.) Elsevier B.V., Amsterdam, pp.509-531. dx.doi.org/10.1016/B978-0-12-803386-9.00018-6.

De Kock, M.O., Beukes, N.J., Adeniyi, E.O., Cole, D., Götz, A.E., Geel, C. and Ossa Ossa, F.-G. (2017) Deflating the shale gas potential of South Africa's Main Karoo Basin. *South African Journal of Science*, 113 (9-10), Article number 2016-0331, 12pp.

Dirks, P.H.G.M., Roberts, E.M., Hilbert-Wolf, H., Kramers, J.D., Hawks, J., Dosseto, A., Duval, M., Elliott, M., Evans, M., Grün, R., Hellstrom, J., Herries, A.I.R., Joannes-Boyau, R., Makhubela, T.V., Placzek, C.J., Robbins, J., Carl Spandler, C., Wiersma, J., Woodhead, J., Berger, L.R., 2017. The age of *Homo naledi* and associated sediments in the Rising Star Cave, South Africa. *eLife* 2017;6:e24231. 59 pages. DOI: 10.7554/eLife.24231

Dlamini, N., Hofmann, A., Belyanin, G., Xie, H., Kröner, A., Wilson, A. and Slabunov, A. (2017) Supracrustal gneisses in southern Swaziland: a basalt-sandstone assemblage of the upper Mozaan Group deformed in the Neoproterozoic. *South African Journal of Geology*, 120, 477-500.

Dongre, A.N., Chalapathi Rao, N.V., Viljoen, K.S. and Lehmann, B. (2017) Petrology, genesis and geodynamic implication of the Mesoproterozoic-late Cretaceous Timmasamudram kimberlite cluster, Wajrakarur field, Eastern Dharwar craton, southern India. *Geoscience Frontiers*, 8, 541-553.

Elburg, M.A. and Cawthorn, R.G. (2017) Source and evolution of the alkaline Pilanesberg Complex, South Africa. *Chemical Geology*, 455, 148-165. doi:10.1016/j.chemgeo.2016.10.007. SCI 2015: 3.48.

Eroglu, S., van Zuilen, M.A., Taubald, H., Drost, K., Wille, M., Swanner, E.D., Beukes, N.J. and Schoenberg, R. (2017) Depth-dependent $\delta^{13}\text{C}$ trends in platform and slope settings of the Campbellrand-Malmani carbonate platform and possible implications for early earth oxygenation. *Precambrian Research*, 302, 122-139.

Giuliani, A., Tappe, S., Rooney, T.O., McCoy-West, A.J., Yaxley, G.M. and Mezger, K. (2017) The role of intraplate magmas and their inclusions in Earth's mantle evolution. *Chemical Geology*, 455, 1-5.

Glynn S, Master S, Wiedenbeck M, Davis D, Kramers J, Belyanin G, Frei D, Oberthur T (2017) The Proterozoic Choma-Kalomo Block, SE Zambia: Exotic terrane or a reworked segment of the Zimbabwe Craton? *Precambrian Research*, 298, 421-438. doi:10.1016/j.precamres.2017.06.020

Greber, N.D., Dauphas, N., Bekker, A., Ptacek, M.P., Binderman, I.N. and Hofmann, A. (2017) Titanium isotopic evidence for felsic crust and plate tectonics 3.5 billion years ago. *Science*, 22, 1271-1274. DOI: 10.1126/science.aan8086.

Gumsley, A.P., Chamberlain, K.R., Bleeker, W., Söderlund, U., De Kock, M.O., Larsson, E.R. and Bekker, A. (2017) Timing and tempo of the Great Oxidation Event. *Proceedings of the National Academy of Sciences of the United States of America*, 144(8), 1811-1816 (Special mention: PNAS)

Hawks, J., Elliott, M., Peter Schmid, Steven E Churchill, Darryl J de Ruiter, Eric M Roberts, Hannah Hilbert-Wolf, Heather M Garvin, Scott A Williams, Lucas K Delezenne, Elen M Feuerriegel, Patrick Randolph-Quinney, Tracy L Kivell, Myra F Laird, Gaokgathe Tawane, Jeremy M DeSilva, Shara E Bailey, Juliet K Brophy, Marc R Meyer, Matthew M Skinner, Matthew W Tocheri, Caroline VanSickle, Christopher S Walker, Timothy L Campbell, Brian Kuhn, Ashley Kruger, Steven Tucker, Alia Gurto, Nompumelelo Hlophe, Rick Hunter, Hannah Morris, Becca Peixotto, Maropeng Ramalepa, Dirk van Rooyen, Mathabela Tsikoane, Pedro Boshoff, Paul HGM Dirks, Lee R Berger (2017) New fossil remains of *Homo naledi* from the Lesedi Chamber, South Africa. *eLife* 6:e24232

Hofmann, A., Pitcairn, I. and Wilson, A. (2017) Gold mobility during Palaeoproterozoic submarine alteration. *Earth and Planetary Science Letters*, 462, 47-54.

Humbert, F., Sonnette, L., De Kock, M.O., Robion, P., Hornig, C.S., Cousture, A. and Wabo, H. (2017) Palaeomagnetism of the early Palaeoproterozoic, volcanic Hekpoort Formation (Transvaal Supergroup) of the Kaapvaal craton, South Africa. *Geophysical Journal International*, 209, 842-865.

Huthmann, F., Yudovskaya, M.A., Elburg, M.A., Kinnaird, J.A. (2017). The Sr isotope stratigraphy of the far northern Bushveld Complex. *S. Afr. J. Geol.* 120, 497-508; doi: 10.25131/gssajg.120.4.497

Jacobs, J., Opås, B., Elburg, M.A., Läufer, A., Estrada, S., Ksienzyk, A.K., Damaske, D. and Hofmann, M. (2017) Cryptic sub-ice geology revealed by a U-Pb zircon study of glacial till in Dronning Maud Land, East Antarctica. *Precambrian Research*, 294, 1-14





- Kramers, J.D. and Dirks, P.H.G.M., 2017. The age of fossil StW573 ('Little Foot'): Reply to comments by Stratford et al. (2017). *South African Journal of Science*, 113(7/8), Art. #a0222, 3 pp. <http://dx.doi.org/10.17159/sajs.2017/a0222>.
- Kramers, J.D. and Dirks, P.H.G.M., 2017. The age of fossil StW573 ('Little Foot'): An alternative interpretation of $^{26}\text{Al}/^{10}\text{Be}$ burial data. *South African Journal of Science*, 113(3/4), Art. #2016-0085, 8 pages. <http://dx.doi.org/10.17159/sajs.2017/20160085>
- Kuhn, B.F., Werdelin, L. Steininger, C. (2017) Fossil Hyaenidae from Cooper's Cave and the palaeoenvironmental implications. *Palaeobiodiversity and Palaeoenvironments* 97(2): 355-365.
- Latypov, R., Chistyakova, S. and Kramers, J., 2017. Arguments against syn-magmatic sills in the Bushveld Complex, South Africa. *South African Journal of Geology*, 120, 565-574. DOI: 10.25131/gssajg.120.4.565
- Lehmann J, Schulmann K, Lexa O, Štípská P, Hasalova P, Belyanin G, Corsini M. (2017) Detachment folding of partially molten crust in accretionary orogens: new magma-enhanced vertical mass and heat transfer mechanism. *The Geological Society of America Bulletin*, 9, 889-909. doi:10.1130/L670.1
- Lehmann, J., Schulmann, K., Lexa, O., Závada, P., Štípská, P., Hasalová, P., Belyanin, G. and Corsini, M. (2017) Detachment folding of partially molten crust in accretionary orogens: A new magma-enhanced vertical mass and heat transfer mechanism, *Lithosphere*, 9, 889-909
- Lemelle, L., Simionovici, A., Schoonjans, T., Tucoulou, R., Enrico, E., Salome, M., Hofmann, A. and Cavalazzi, B. (2017) Analytical requirements for quantitative X-ray fluorescence nano-imaging of metal traces in solid samples. *Trends in Analytic Chemistry*, 91, 104-111.
- Makhubela, T.V., Kramers, J.D., Belyanin, G.A., Dirks, P.H.G.M. and Roberts, E.M., 2017. Proterozoic $^{40}\text{Ar}/^{39}\text{Ar}$ ages from cave deposits of the Malapa, Sterkfontein and Dinaledi fossil sites, Cradle of Humankind, South Africa. *South African Journal of Geology*, 120, 21-44. Doi: 10.25131/gssajg.120.1.21
- Masiala Ngoy, J., Daramola, M.O., Chitsiga, T.L, Falcon, R. and Wagner, N. (2017) CO₂ Adsorption using water-soluble polyaspartamide. *South African Journal of Chemical Engineering*, 23,139-144.
- Munyangane, P., Mouri, H. and Kramers, J. (2017) Assessment of some potential harmful trace elements (PHTEs) in the borehole water of Greater Giyani, Limpopo Province, South Africa: possible implications for human health. *Environmental geochemistry and health* 39 (5), 1201-1219
- Nxumalo, V., Kramers, J.D., Mongwakedsi, N. and Przybylowicz, W.J., 2017. Micro-PIXE characterisation of uranium occurrence in the coal zones and the mudstones of the Springbok Flats Basin, South Africa. *Nuclear Inst. and Methods in Physics Research, B*, 404, 114-120 <http://dx.doi.org/10.1016/j.nimb.2016.10.034>.
- Osler, K., Dheda, D., Ngoy, J., Wagner N.J. and Daramola, M.O. (2017) Synthesis and evaluation of carbon nanotubes composite adsorbent for CO₂ capture: a comparative study of CO₂ adsorption capacity of single-walled and multi-walled carbon nanotubes. *International Journal of Coal Science & Technology*, 4, 41-49.
- Owen-Smith, T.M., Ashwal, L.D., Sudo, M. & Trumbull, R.B. (2017). Age and petrogenesis of the Doros Complex, Namibia, and implications for early plume-derived melts in the Paraná-Etendeka LIP. *Journal of Petrology*, 58(3), 423-442. doi:10.1093/petrology/egx021
- Pickel W., Kus J., Flore D., Kalaitzidis S., Christanis K., Cardott B.J., Misch-Kennan M., Rodrigues S., Hentshel A., Hamor-Vido M., Crosdale P., Wagner, N. and ICCP. (2017) Classification of liptinite – ICCP System 1994. *International Journal of Coal Geology*, 169, 40-61.
- Pienaar, D., Guy, B. M., Pienaar, C., and Viljoen, K. S. (2017) A geometallurgical characterization study of the Crystalkop Reef at the Great Noligwa Mine, Klerksdorp Goldfield, South Africa. *South African Journal of Geology*, 120, 303-322.
- Siahi, M., Hofmann, A., Master, S., Mueller, C.W. and Gerdes, A. (2017) Carbonate ooids of the Mesoarchaeon Pongola Supergroup, South Africa. *Geobiology*, 15, 750-766.
- Smart, K.A., Cartigny, P., Tappe, S., O'Brien, H. and Klemme, S. (2017) Lithospheric diamond formation as a consequence of methane-rich volatile flooding: An example from diamondiferous eclogite xenoliths of the Karelian craton (Finland) *Geochimica et Cosmochimica Acta*, 206, 312-342.
- Smart, K.A., Tappe, S., Simonetti, A., Simonetti, S.S., Woodland, A. and Harris, C. (2017) Tectonic significance and redox state of eclogite and pyroxenite components in the Slave cratonic mantle lithosphere, Voyageur kimberlite, Arctic Canada. *Chemical Geology*, 455, 98-119.
- Smith, A.J.B., Beukes, N.J., Gutzmer, J., Czaja, A.D., Johnson, C.M. and Nhleko, N. (2017) Oncoidal granular iron formation in the Mesoarchaeon Pongola Supergroup, southern Africa: Textural and geochemical evidence for biological activity during iron deposition. *Geobiology*, 15, 731-749.

- Southwood, M. and Cairncross, B. (2017) The minerals of Palabora mine. *Rocks & Minerals*, 92, 426-452.
- Suárez-Ruiz, I., Valentim, B., Borrego, A.G., Bouzinos, A., and Wagner, N. (2017) Development of a petrographic classification of fly-ash components from coal combustion and co-combustion. (An ICCP Classification System, Fly-Ash Working Group – Commission III.) *International Journal of Coal Geology*, 183, 188-203
- Tappe, S., Brand, N.B., Stracke, A., van Acken, D., Liu, C.-Z., Strauss, H., Wu, F.-Y., Luguët, A. and Mitchell, R.H. (2017) Plates or plumes in the origin of kimberlites: U/Pb perovskite and Sr-Nd-Hf-Os-C-O isotope constraints from the Superior craton (Canada). *Chemical Geology*, 455, 57-83.
- Tappe, S., Romer, R.L., Stracke, A., Steenfelt, A., Smart, K.A., Muehlenbachs, K. and Torsvik, T.H. (2017) Sources and mobility of carbonate melts beneath cratons, with implications for deep carbon cycling, metasomatism and rift initiation. *Earth and Planetary Science Letters*, 466, 152-167.
- Yang, H., Cairncross, B., Gu, X., Yong, T. and Downs, R.T. (2017) Strontioruizite, IMA 2017-045. *CNMNC Newsletter No. 39*, October 2017, page 1280; *Mineralogical Magazine*, 81, 1279-1286.

Conference Proceedings, 2017

- Abraham, R. and Wagner, N.J. (2017) Carbon dioxide adsorption behaviour of geological samples from the Karoo Basin, South Africa. *Fossil Fuel Foundation: Conference on Sustainable Development of South Africa's Energy Sources*, 29-30 November 2017, Johannesburg, South Africa.
- Agangi, A., Hofmann, A., Hegner, E. and Teschner, C. (2017) The Mesoarchaean Dominion Group and the onset of intracontinental volcanism on the Kaapvaal craton. *Abstract Volume, 4th International Geoscience Symposium "Precambrian World 2"*, 3-10 March 2017, Fukuoka, Japan.
- Andersen, T. and Elburg, M. (2017) Accessory Ba minerals as indicators of crystallization conditions in alkaline igneous rocks. *Conference on Accessory Minerals*, 13-17 September 2017, Vienna, Austria.
- Andersen, T. and Elburg, M. (2017) Controls on the HFSE Mineralogy of Alkaline Rocks: Peralkalinity vs. Volatiles. *Goldschmidt 2017 Conference Abstracts*, 13-18 August, Paris, France.
- Andersen, T., Elburg, M. and Erambert, M. (2017) Eudialyte or no Eudialyte - Contrasting trends of apatitic crystallization in nepheline syenite of the Pilanesberg Complex, South Africa. *Igneous and Metamorphic Studies Group (IMSG) meeting*, 15-18 January 2017, Johannesburg, South Africa.
- Andreoli, M.A.G., Di Martino, M., V. Pischedda, R. L. Gibson, S. Huotari, A. Kallonen, G. Belyanin, R. Erasmus, A. Ziegler, H. Mouri, T. Ntsoane, R. van der Merwe, M.D.S. Lekgoathi, Z. Jinnah, J. Kramers, R. Serra, G. P. Sighinolfi, I. Stengel, L.D. Kock, D. Block, L. Chown, M. Bamford, K. Rumbold and D. Billing (2017). 1 Polymetallic and carbonaceous debris in palaeosol from the Libyan Desert Glass strewn field, SW Egypt: evidence for a cometary impact. *Lunar and Planetary Science Conference 48*, Abstract 1045.
- Asael, D., Planavsky, N., Bellefroid, E., Hofmann, A., and Reinhard, C. (2017). Sulfur non-mass dependent anomalies in modern river water of Archean catchment. *Goldschmidt 2017 Conference Abstracts*, 13-18 August, Paris, France.
- Badenhorst, C. and Wagner, N.J. (2017) Char extracted from coal ash as a replacement for natural graphite – Charphite. *Fossil Fuel Foundation: Conference on Sustainable Development of South Africa's Energy Sources*, 29-30 November 2017, Johannesburg, South Africa.
- Bellot, N., Debaille, V. and Hofmann, A. (2017) Cerium Stable Isotopes as a Redox Tracer in Early Earth Environments. *Goldschmidt 2017 Conference Abstracts*, 13-18 August, Paris, France.
- Beukes, N.J. and de Kock, M.O. (2017) Experiences gained from the CIMERA-KARIN scientific drilling project on the shale gas potential of the southern Main Karoo Basin. *American Association of Petroleum Geologists Conference on "Exploration and development of unconventional hydrocarbons: Understanding and mitigating geotechnical challenges through conventional wisdom"*. Abstract series. Article 90305. 20-23 June, 2017. Cape Town, South Africa.
- Beukes, N.J. and de Kock, M.O. (2017) Questioning the existence of an economic producible shale gas resource in the southern Main Karoo Basin based on results of the CIMERA-Karin drilling project. *Fossil Fuel Foundation: Conference on Sustainable Development of South Africa's Energy Sources*, 29-30 November 2017, Johannesburg, South Africa.
- Bindeman, I., Zakharov, D., Palandri, J., Greber, N., Dauphas, N., Retallack, G., Lackey, J. Hofmann, A. and Bekker, A. (2017) Shift in the hydrologic cycle and rapid growth of subaerial continental crust at ~2.5 Ga based on triple oxygen isotope systematics of shales. *Geological Society of America Abstracts with Programs*. Vol. 49, No. 6, doi: 10.1130/abs/2017AM-294858.
- Brüske, A., Schuth, S., Albut, G., Schoenberg, R., Beukes, N.J., Hofmann, A., Nägler, T. and Weyer, S. (2017) Constraints on metal mobilization in Archean and early Proterozoic marine sediments from uranium isotopes. *Goldschmidt 2017 Conference Abstracts*, 13-18 August, Paris, France.





- Burger, E.P., Roberts, R.J., Grantham, G.H., Elburg, M., Ueckermann, H. and le Roux P (2017) Evidence For multiple granitoid sheet Sources In HU Sverdrupfjella, Antarctica. Igneous and Metamorphic Studies Group (IMSG) meeting, 15-18 January 2017, Johannesburg, South Africa.
- Burness, S., Smart, K.A., Stevens, G. and Tappe, S. (2017) The role of sulphur during partial melting of eclogite in the cratonic mantle: constraints from experiments and mantle xenoliths. 11th International Kimberlite Conference, 18-22 September 2017, Gaborone, Botswana.
- Burness, S., Smart, K.A., Stevens, G., Tappe S., Sharp, Z.D. and Gibbons, J. (2017) S-bearing metasomatism of mantle eclogites: constraints from the Kaapvaal craton and experiments. Goldschmidt 2017 Conference Abstracts, 13-18 August, Paris, France.
- Chabalala, V. and Wagner N.J. (2017) The Application organic petrology to shale gas exploration in the Karoo Basin, South Africa. International Committee for Coal and Organic Petrology (ICCP) Symposium, 3-9 September 2017, Bucharest, Romania.
- Chabalala, V. and Wagner N.J. (2017) The application organic petrology to shale gas exploration in the Karoo Basin, South Africa. Fossil Fuel Foundation: Conference on Sustainable Development of South Africa's Energy Sources, 29-30 November 2017, Johannesburg, South Africa.
- Clemens, J., Stevens, G., and Elburg, M.A. (2017) Magmatic enclaves in granitic rocks: Paragons or parasites? European Geosciences Union (EGU) General Assembly, 23-28 April 2017, Vienna, Austria.
- De Kock, M.O. and Beukes, N.J. (2017) Results from the CIMERA-KARIN scientific drilling project and implications for the shale gas potential of the southern main Karoo basin. Conference: The shale gas industry in South Africa: towards a science action plan. Academy of Science in South Africa (ASSAf). 31 August – 1 September 2017, Port Elizabeth, South Africa.
- De Kock, M.O. and Gumsley, A.P. (2017) Geospatial mapping of South Africa's large igneous province (LIP), sill and dyke record. Igneous and Metamorphic Studies Group (IMSG) meeting, 15-18 January 2017, Johannesburg, South Africa.
- Elburg, M.A., Andersen, T., Mahlaku, S.M., Cawthorn, R.G. and Kramers, J. (2017). A potassic magma series in the Pilanesberg Alkaline Complex? Goldschmidt 2017 Conference Abstracts, 13-18 August, Paris, France.
- Elburg, M.A., Cawthorn, R.C. and Andersen, T. (2017) Whole rock geochemistry of the Pilanesberg Complex: Reflecting on controlling mineralogy? Igneous and Metamorphic Studies Group (IMSG) meeting, 15-18 January 2017, Johannesburg, South Africa.
- Hlungwani, R.P. and Elburg, M.A. (2017) The Geochemistry Of The Layered Molopo Farms Complex, South Africa: Preliminary Results. Igneous and Metamorphic Studies Group (IMSG) meeting, 15-18 January 2017, Johannesburg, South Africa.
- Hofmann, A. (2017). Early Earth Surface Processes 3.5 to 3.0 Ga ago. Abstract Volume, 4th International Geoscience Symposium "Precambrian World 2", 3-10 March 2017, Fukuoka, Japan.
- Humbert, F. and Elburg, M.A. (2017) Large Igneous Provinces (LIP) and the Subcontinental Lithosphere of the Kaapvaal Craton (South Africa) from the Mesoarchean to the Present. Goldschmidt 2017 Conference Abstracts, 13-18 August, Paris, France.
- Hunt, J.P., Hatton, C., De Kock, M.O. and Bleeker, W. (2017) Plume activity related to the Kaapvaal craton and implications for Rhyacian plate reconstructions and ore deposits. Society for Geology Applied to Mineral Deposits (SGA) 14th Biennial Meeting, 20-23 August 2017, Quebec City, Canada.
- Huthmann, F.M., Kinnaird, J.A., Yudovskaya, M.A., McCreesh, M., Elburg, M.A., Frei, D. and Botha, T. (2017) The Waterberg Project – Atypical Bushveld Magmatism And Mineralization. Igneous and Metamorphic Studies Group (IMSG) meeting, 15-18 January 2017, Johannesburg, South Africa.
- Izon, G., Ono, S., Beukes, N.J. and Summons, R.E. (2017) New quadruple sulphur isotope records from the Duitschland/Rooihooigte Formations(s): (Re) defining the structure of the Great Oxidation event. Astrobiology Science Conference (AbSciCon), Abstract 3181. 24-28 April, 2017, Mesa, Arizona, USA.
- Jacobs, J., Opås, B., Elburg, M.A., Läufer, A., Estrada, S., Ksienzyk, A.K., Damaske, D. and Hofmann, M. (2017) Cryptic sub-ice geology revealed by a U-Pb zircon study of glacial till in Dronning Maud Land, East Antarctica. European Geosciences Union (EGU) General Assembly, 23-28 April 2017, Vienna, Austria.
- Kabelo, O., Wagner, N. and Shindo, K. (2017) Petrographic characterization of a Permian coal deposit, south-eastern Kalahari belt, Moiyabana area, eastern Botswana. Fossil Fuel Foundation: Conference on Sustainable Development of South Africa's Energy Sources, 29-30 November 2017, Johannesburg, South Africa.
- Lehmann, J., Schulmann, K., Lexa, O., Závada, P., Štípská, P., Hasalová, P., Belyanin, G. and Corsini, M. (2017) Detachment folding of partially molten crust in accretionary orogens: A new magma-enhanced vertical mass and heat transfer mechanism. Igneous and Metamorphic Studies Group (IMSG) meeting, 15-18 January 2017, Johannesburg, South Africa.

- Levitt, N.P., Eiler, J.M., Beukes, N.J. and Johnson, C.M. (2017) Application of clumped isotope thermometry to Archean carbonates: thermal histories and potential biomarker preservation. Astrobiology Science Conference (AbSciCon), Abstract 3522. 24-28 April, 2017. Mesa, Arizona, USA.
- Lum, J., Viljoen, F., Cairncross, B. and Frei, D. (2017). The correlation of colour, chemistry and crystallochemistry in emerald: A case study from the Leydsdorp area, South Africa. Abstract. Geological Society of America Annual Meeting, 22-25 October 2017, Seattle, USA.
- Magwaza, B. and Elburg, M.A. (2017) Isotopic resetting of zircon: Influence of age, temperature and chemical environment, preliminary results. Igneous and Metamorphic Studies Group (IMSG) meeting, 15-18 January 2017, Johannesburg, South Africa.
- Makukule, X.M., Dorland, H.C. and Wagner, N.J. (2017) The usefulness of petrographic information for the coal industry. . Proceedings of the Southern African Coal Processing Society (Editor: De Korte, J.), 22 – 24 August 2017, Secunda, South Africa.
- Makukule, X.M., Dorland, H.C. and Wagner, N.J. (2017) Using Petrography and Image analysis to validate washability of southern African coals. Fossil Fuel Foundation: Conference on Sustainable Development of South Africa's Energy Sources, 29-30 November 2017, Johannesburg, South Africa.
- Mangs, A.D., Wagner, N.J., Lar, U.A, Fube, A.A., Sallau, A.K. and Longpia, B.C. (2017) An overview of the coal geology within the Benue Trough, Nigeria. Fossil Fuel Foundation: Conference on Sustainable Development of South Africa's Energy Sources, 29-30 November 2017, Johannesburg, South Africa.
- Maponga, O., Wagner, N.J. and Falcon, R.M.S. (2017) Assessment of coals from the Hwange Coal Basin, Zimbabwe, with specific focus on coking properties. Fossil Fuel Foundation: Conference on Sustainable Development of South Africa's Energy Sources, 29-30 November 2017, Johannesburg, South Africa.
- Master, S., Armstrong, R.A., Belyanin, G., Kramers, J.D. and Wade, S. (2017). Neoproterozoic and Late Palaeozoic magmatic and tectono-metamorphic events in the Velingara Impact Structure and Southern Mauritanides (Senegal) and the Southern Soutouffides (Mauritania): new U-Pb and 40Ar-39Ar ages. Abstract, WACMA1, the First West African Craton and Margins International Workshop, 24-29 April 201, Dakhla, Morocco.
- Master, S., Madonsela, J., Kramers, J.D., Belyanin, G., Bolhar, R. and Shirazi, R. (2017). Palaeocene-Eocene magmatism related to Neo-Tethys closure, Alborz Mountains, Iran. Igneous and Metamorphic Studies Group (IMSG) meeting, 15-18 January 2017, Johannesburg, South Africa.
- Moroeng, M.O., Wagner, N.J. and Roberts, R.J. (2017) Geochemistry of South African coal – Implications for the formation inertinite macerals in the Witbank Coalfield. Fossil Fuel Foundation: Conference on Sustainable Development of South Africa's Energy Sources, 29-30 November 2017, Johannesburg, South Africa.
- Ormond, R.J., Lehmann, J. and Belyanin, G.A. (2017) The structural geology, metamorphism and geochronology of the Zwartkops Hill. Igneous and Metamorphic Studies Group (IMSG) meeting, 15-18 January 2017, Johannesburg, South Africa.
- Owen-Smith, T., Hayes, B., Bybee, G., Lehmann, J., Ashwal, L., Hill, K. and A. Brower, A. (2017) Magma mush dynamics in the Kunene Anorthosite Complex, Angola. Igneous and Metamorphic Studies Group (IMSG) meeting, 15-18 January 2017, Johannesburg, South Africa.
- Schiera, K., Baua, M., Münkerb, C., Beukes, N.J. and Viehmann, S. (2017) Stromatolite bioherms record absence of high-temperature hydrothermal fluids from shallow "Transvaal seawater" shortly before the Great Oxidation Event. GeoBremen Conference, Bremen, Germany, 24-29 September 2017. Abstract Volume.
- Smart, K.A., Tappe, S. and Stern, R.A. (2017) Evidence for the deep carbon cycle from Archean placer diamond. Third Deep Carbon Observatory (DCO) International Science Meeting, 23-25 March 2017. St. Andrews, Scotland. Invited Talk.
- Smart, K.A., Tappe, S., Simonetti, A., Simonetti, S.S., Woodland, A.B. and Harris, C. (2017) The redox state of mantle eclogites. Goldschmidt 2017 Conference Abstracts, 13-18 August, Paris, France.
- Smith, A.J.B., Beukes, N.J., Gutzmer, J., Johnson, C., Czaja, A., Nhleko, N., De Beer, F. and Hoffman, J. (2017) Assessing the grain morphology and sedimentology of a Mesoarchean granular iron formation from southern Africa using 3D X-ray computed tomography (μ XCT). IMGRAD (Imaging with Radiation) Conference, 14-15 September 2017. Johannesburg, South Africa.
- Smith, A.J.B., Beukes, N.J., Gutzmer, J., Johnson, C.M., Czaja, A.D. and De Beer, F.C. (2017) Insights into oncoidal morphology and sedimentology of a Mesoarchean granular iron formation from southern Africa using 3D X-ray computed tomography (μ XCT). Goldschmidt 2017 Conference Abstracts, 13-18 August, Paris, France.
- Tappe, S., Smart, K.A. and Stern, R.A. (2017) Cycling of the elements of life within the Archean crust-mantle system. Goldschmidt 2017 Conference Abstracts, 13-18 August, Paris, France. (Keynote)
- Tappe, S., Smart, K.A., Stern, R.A., Massuyeau, M. and de Wit, M. (2017) Evolution of kimberlite magmatism on the dynamic Earth. 11th International Kimberlite Conference, 18-22 September 2017, Gaborone, Botswana.





Tlou Sebola, M.-J., Wagner, N.J., Drennen, G. (2017) Weathering of coals from the Waterberg and Limpopo Coalfields, South Africa. Fossil Fuel Foundation: Conference on Sustainable Development of South Africa's Energy Sources, 29-30 November 2017, Johannesburg, South Africa.

Warke, M.R., Edwards, N.P., Schröder, S., Wogelius, R.A., Manning, P.L., Bergmann, U., Kimball-Linares, K., Garwood, R., and Beukes, N.J. (2017) Synchrotron-based XRF mapping of Neoproterozoic stromatolites: trace element distribution in microbialites. Goldschmidt 2017 Conference Abstracts, 13-18 August, Paris, France.

Wilmith, D.T., Corsetti, F.A., Berelson, W.M., Beukes, N.J., Awramik, S.M. and Petryshyn, V.A. (2017) Gas production with Archean stromatolites: evidence for ancient microbial metabolisms. Geological Society of America, Annual Conference 22-25 October 2017, Seattle, USA, Conference Abstracts, 249-2.

Zheng, X.-Y., Satkoski, A.M., Beard, B., Reddy T.R., Beukes, N.J. and Johnson, C. (2017) Tracing of the coupled Si and Fe cycle in the Archean ocean. Geological Society of America, Annual Conference 22-25 October 2017, Seattle, USA, Conference Abstracts, 249-11.

Refereed Journal Publications and Book Chapters, 2018

Adeniyi, E. O., Ossa Ossa, F. O., Kramers, J. D., de Kock, M. O., Belyanin, G., & Beukes, N. J. (2018). Cause and timing of the thermal over-maturation of hydrocarbon source rocks of the Ecca Group (Main Karoo Basin, South Africa). *Marine and Petroleum Geology*, 91, 480-500.

Agangi, A., Hofmann, A. and Elburg, M.A. (2018). A review of Palaeoarchean felsic volcanism in the eastern Kaapvaal craton: linking plutonic and volcanic records. *Geoscience Frontiers* 6, 667-688. doi 10.1016/j.gsf.2017.08.003.

Albut, G., Babechuk, M.G., Kleinhanns, I.C., Bengler, M., Beukes, N.J., Steinhilber, B., Smith, A.J.B., Kruger, S.J. and Schoenberg, R. (2018). Modern rather than Mesoarchean oxidative weathering responsible for the heavy stable Cr isotopic signatures of the 2.95 Ga old Ijzermijn iron formation (South Africa). *Geochimica et Cosmochimica Acta*, 228, 157-189.

Andersen, T., Elburg, M.A. and Erambert, M. (2018). Contrasting trends of apatitic crystallization in nepheline syenite in the Pilanesberg Alkaline Complex, South Africa. *Lithos* 312-313, 375-388.

Andersen, T., Elburg, M.A., Van Niekerk, H.S. and Ueckermann, H. (2018). Successive sedimentary recycling regimes in southwestern Gondwana: Evidence from detrital zircons in Neoproterozoic to Cambrian sedimentary rocks in southern Africa. *Earth-Science Reviews* 181, 43-60.

Andersen, T., Kristoffersen, M. and Elburg, M.A. (2018). Visualizing, interpreting and comparing detrital zircon age and Hf isotope data in basin analysis – a graphical approach. *Basin Research* 30, 132-147; doi: 10.1111/bre.12245

Avice, G., Marty, B., Burgess, R., Hofmann, A., Philippot, P., Zahnle, K. and Zakharov, D. (2018). Evolution of atmospheric xenon and other noble gases inferred from Archean to Paleoproterozoic rocks. *Geochimica et Cosmochimica Acta*, 232, 82-100.

Baiyegunhi, C., Liu, K., Wagner, N., Gwavava, O. and Oloniyi, T.L. (2018). Geochemical evaluation of the Permian Ecca Shale in Eastern Cape Province, South Africa: implications for shale gas potential. *Acta Geologica Sinica*, 92:3, 1193 – 1217. ISSN 03755444. <https://doi.org/10.1111/1755-6724.13599>.

Belyanin GA, Kramers JD, Andreoli MAG, Greco F, Gucsik A, Makhubela TV, Przybylowicz WJ, Wiedenbeck M (2018) Petrography of the carbonaceous, diamond-bearing stone "Hypatia" from southwest Egypt: A contribution to the debate on its origin. *Geochimica et Cosmochimica Acta*, 223, 462-492. doi:10.1016/j.gca.2017.12.020

Bindeman, I.N., Zakharov, D.O., Palandri, J., Greber, N.D., Dauphas, N., Retallack, G.J., Hofmann, A., Lackey, J.S. and Bekker, A. (2018). Rapid emergence of subaerial landmasses and onset of a modern hydrologic cycle 2.5 billion years ago. *Nature*, 557, 545-548.

Birski, Ł., Wirth, R., Slaby, E., Wudarska, A., Lepland, A., Hofmann, A. and Schreiber, A. (2018). (Ca-Y)-phosphate inclusions in apatite crystals from Archean rocks from the Barberton Greenstone Belt and Pilbara Craton: First report of natural occurrence. *American Mineralogist*, 103(2), 307-313.

Burron, I., da Costa, G., Sharpe, R., Fayek, M., Gauert, C., and Hofmann, A. (2018). 3.2 Ga detrital uraninite in the Witwatersrand Basin, South Africa: Evidence of a reducing Archean atmosphere. *Geology*, 46, 295-298.

Cairncross, B. (2018). Hausmannite: Connoisseur's choice. *Rocks & Minerals*. 93(3), 244-249.

Cairncross, B. (2018). Hydrocerussite. Connoisseur's choice. *Rocks & Minerals*, 93(2), 150-156.

Cairncross, B. (2018). Iowaite: the where of mineral names. *Rocks & Minerals*. 93(3), 271-273.

- Cairncross, B. (2018). Mountainite: The where of mineral names, *Rocks & Minerals*, 93(3), 276-278.
- Cairncross, B. (2018). Namibite: The where of mineral names. *Rocks & Minerals*, 93(2), 184-187.
- Cairncross, B. (2018). Okorusu fluorite mine, Namibia. *Mineralogical Record*, 49(3), 375-398.
- Cairncross, B. (2018). Skorpionite: the where of mineral names. *Rocks & Minerals*, 93(6), 562-564.
- Cairncross, B. and du Plessis, H. (2018). Stilbite and associated minerals from Lesotho. *Rocks & Minerals*, 93(4), 306-319.
- Cairncross, B., Kramers, J. and Villa, I.M. (2018) Thabazimbi mine cave, Limpopo Province, South Africa: an unusual cave system and its chronology. *South African Journal of Geology*.
- Chitsiga, T.L., Daramola, M.O., Wagner, N. and Ngoy, J.M. (2018). Parametric effect of adsorption variables on CO₂ adsorption of amine-grafted polyaspartamide composite adsorbent during post-combustion CO₂ capture: a response surface methodology approach. *Int. J. Oil, Gas and Coal Technology*, vol 17:3, 321 – 336. ISSN 17533309.
- Dongre, A., Viljoen, K.S. and Rathodi, A. (2018) Mineralogy and geochemistry of micro-dolerite dykes from the central Deccan Traps flood basaltic province, India, and their geodynamic significance. *Mineralogy and Petrology*, 112(2): 267-277.
- Eickmann, B., Hofmann, A., Wille, M., Bui, T. H., Wing, B. A. and Schoenberg, R. (2018). Isotopic evidence for oxygenated Mesoarchean shallow oceans. *Nature Geoscience*, 11, 133-138.
- Eroglu, S., Schoenberg, R., Pascarelli, S., Beukes, N. J., Kleinhanns, I. C., & Swanner, E. D. (2018). Open ocean vs. continentally-derived iron cycles along the Neoproterozoic Campbellrand-Malmani Carbonate platform, South Africa. *American Journal of Science*, 318(4), 367-408.
- Gevera, P. and Mouri, H. (2018) Natural occurrence of potentially harmful fluoride contamination in groundwater: an example from Nakuru County, the Kenyan Rift Valley. *Environmental earth sciences* 77 (10), 365
- Gevera, P., Mouri, H. and G Maronga, G. (2018) Occurrence of fluorosis in a population living in a high-fluoride groundwater area: Nakuru area in the Central Kenyan Rift Valley. *Environmental geochemistry and health*, 1-12
- Greco, F., Cavalazzi, B., Hofmann, A. and Hickman-Lewis, K. (2018). 3.4 Ga biostructures from the Barberton greenstone belt of South Africa: new insights into microbial life. *Bollettino della Societa Paleontologica Italiana*, 57(1), 59-74.
- Hoehnel, D., Reimold, W. U., Altenberger, U., Hofmann, A., Mohr-Westheide, T., Özdemir, S. and Koeberl, C. (2018). Petrographic and Micro-XRF analysis of multiple Archean impact-derived spherule layers in drill core CT3 from the northern Barberton Greenstone Belt (South Africa). *Journal of African Earth Sciences*, 138, 264-288.
- Humbert, F., de Kock, M.O., Altermann, W., Elburg, M.A., Lenhardt, N., Smith, A.J.B. and Masango, S. (2018). Petrology, physical volcanology and geochemistry of a Paleoproterozoic large igneous province: The Hekpoort Formation in the southern Transvaal sub-basin (Kaapvaal Craton). *Precambrian Research* 315, 232-256. <https://doi.org/10.1016/j.precamres.2018.07.022>.
- Humbert, F., Elburg, M.A., Ossa-Ossa, F., de Kock, M.O. and Robin, P. (2018). Variolites of the Paleoproterozoic Hekpoort Formation (Transvaal sub-basin, Kaapvaal craton): Multistage undercooling textures? *Lithos* 316-317, 48-65
- Huthman, F.M., Yudovskaya, M., Elburg, M.A. and Kinnaird, J.A. (2017 – only came out in 2018) The Sr isotopic stratigraphy of the far northern Bushveld Complex. *South African Journal of Geology*, 120, 499-510.
- Jacobs, J., Paoli, G., Rocchi, S., Ksienzyk, A.K., Sirevaag, H. and Elburg, M.A. (2018). Alps to Apennines zircon roller coaster along the Adria microplate margin. *Scientific Reports* 8:2704 | DOI:10.1038/s41598-018-20979-w.
- Joy, S., Patranabis-Deb, S., Saha, D., Jelsma, H., Maas, R., Sodelund, U., Tappe, S., van der Linder, G., Banerjee, A. and Krishnan, U. (2018). Depositional history and provenance of cratonic "Purana" basins in southern India: A multiple geochronology approach to the Proterozoic Kaladgi and Bhima basins. *Geological Journal*, <https://doi.org/10.1002/gj.3415>. First published 21 Dec 2018.
- Joy, S., Van der Linde, G., Choudhury, A.K., Deb, G.K. and Tappe, S. (2018) Reassembly of the Dharwar and Bastar cratons at ca. 1 Ga: Evidence from multiple tectonothermal events along the Karimnagar granulite belt and Khammam schist belt, southern India. *Journal of Earth Systems*, August 2018, 127:76. (Open access) <https://doi.org/10.1007/s12040-018-0988-2>.
- Kaavera J, Rajesh HM, Tsunogae T, Belyanin GA (2018) Marginal facies and compositional equivalents of Bushveld parental sills from the Molopo Farms Complex layered intrusion, Botswana: Petrogenetic and mineralization implications. *Ore Geology Reviews*, 92, 506–528. doi:10.1016/j.oregeorev.2017.12.001
- Kitt, S., Kisters, A., Buick, I. and Kramers, J. (2018). Structural, geochronological and P-T constraints on subduction-accretion processes in a Pan-African accretionary wedge – The Deep Level Southern Zone of the Damara Belt in Namibia. *Precambrian Research*, 310, 39-62. DOI: 10.1016/j.precamres.2018.02.012
- Kröner, A., Nagel, T.J., Hoffmann, J.E., Liu, X., Wong, J., Hegner, E., Xie, H., Kasper, U., Hofmann, A. and Liu, D. (2018). High-temperature metamorphism and crustal melting at ca. 3.2 Ga in the eastern Kaapvaal craton, southern Africa. *Precambrian Research*, 317, pp.101-116.





- Latypov, R. M., Chistyakova, S.Y. and Kramers, J. (2018). Reply to discussion of "Arguments against synmagmatic sills in the Bushveld Complex, South Africa" by Roger Scoon and Andrew Mitchell (2018). *South African Journal of Geology* 121(2): 211-216. doi: 10.25131/sajg.121.0014.
- Luo, G., Junium, C. K., Izon, G., Ono, S., Beukes, N. J., Algeo, T. J., ... & Summons, R. E. (2018). Nitrogen fixation sustained productivity in the wake of the Palaeoproterozoic Great Oxygenation Event. *Nature communications*, 9(1), 978
- McCarthy, T. S., Corner, B., Lombard, H., Beukes, N. J., Armstrong, R. A. and Cawthorn, R. G. (2018). The pre-Karoo geology of the southern portion of the Kaapvaal Craton, South Africa. *South African Journal of Geology* 2018, 121(1), 1-22.
- Moroeng, M., Wagner, N.J., Brand, D.J. and Roberts, R.J. (2018). A Nuclear Magnetic Resonance study: Implications for coal formation in the Witbank Coalfield, South Africa. *International Journal of Coal Geology* 188, 145-155. ISSN 01665162.
- Moroeng, O., Keartland, J.M., Roberts, R.J. and Wagner, N.J. (2018). Characterization of coal using Electron Spin Resonance: implications for the formation of inertinite macerals in the Witbank Coalfield, South Africa. *International Journal of Coal Science and Technology*, 3, 385-398. ISSN 20958293.
- Moroeng, O., Wagner, N.J., Hall, G. and Roberts, R.J. (2018). Using $\delta^{15}\text{N}$ and $\delta^{13}\text{C}$ and nitrogen functionalities to support a fire-origin for certain inertinite macerals in a No. 4 Seam Upper Witbank coal, South Africa. *Organic Geochemistry* 126, 23-32 ISSN 2052-4129.
- Ossa Ossa, F. O., Eickmann, B., Hofmann, A., Planavsky, N. J., Asael, D., Pambo, F. and Bekker, A. (2018). Two-step deoxygenation at the end of the Paleoproterozoic Lomagundi Event. *Earth and Planetary Science Letters*, 486, 70-83.
- Ossa Ossa, F.O., Hofmann, A., Wille, M., Spangenberg, J.E., Bekker, A., Poulton, S.W., Eickmann, B. and Schoenberg, R. (2018). Aerobic iron and manganese cycling in a redox-stratified Mesoarchean epicontinental sea. *Earth and Planetary Science Letters*, 500, 28-40.
- Rajesh HM, Belyanin GA, Safonov OG, Vorster C, Van Reenen DD (2018) Garnet-bearing low-Sr and high-Sr Singelele leucogranite: A record of Neoproterozoic episodic melting in collisional setting and Paleoproterozoic overprint in the Beit Bridge complex, southern Africa. *Lithos*, 322, 67-86. <https://doi.org/10.1016/j.lithos.2018.10.004>
- Rajesh HM, Belyanin GA, Van Reenen DD (2018) Three tier transition of Neoproterozoic TTG-sanukitoid magmatism in the Beit Bridge Complex, Southern Africa. *Lithos*, 296-299, 431-451. doi:10.1016/j.lithos.2017.11.018
- Rajesh HM, Safonov OG, Basupi TO, Belyanin GA, Tsunogae T (2018) Complexity of characterizing granitoids in high-grade terranes: An example from the Neoproterozoic Verbaard granitoid, Limpopo Complex, Southern Africa. *Lithos*, 318-319, 399-418. <https://doi.org/10.1016/j.lithos.2018.08.019>
- Rose, D.H., Viljoen, K.S. and Mulaba-Bafubandi, A. (2018). A mineralogical perspective on the recovery of platinum-group elements from Merensky Reef and UG2 at the Two Rivers platinum mine on the eastern limb of the Bushveld Complex in South Africa. *Mineralogy and Petrology* 112 : 881-902. DOI: 10.1007/s00710-018-0594-7.
- Safonov OG, van Reenen DD, Yapaskurt VO, Varlamov DA, Mityaev AS, Butvina VG, Golunova MA, Belyanin GA, and Smit CA (2018) Thermal and Fluid Effects of Granitoid Intrusions on Granulite Complexes: Examples from the Southern Marginal Zone of the Limpopo Complex, South Africa. *Petrology*, 26 (6), 617-639.
- Safonov, O.F., Yapaskurt, V.O., Elburg, M., van Reenen, D.R., Tatarinova, D.S., Varlamov, D.A., Golunova, M.A. and Smit, C.A. (2018). P-T conditions, mechanism and timing of the localized melting of metapelites from the Petronella shear-zone and relationships with granite intrusions in the Southern Marginal Zone of the Limpopo Belt, South Africa. *Journal of Petrology*, 59, 695-734.
- Sarkar, T., Dubinina, E.O., Harris, C. Maier, W.D., Mouri, H. (2018) Petrogenesis of ultramafic rocks of komatiitic composition from the Central Zone of the Limpopo Belt, South Africa: Evidence from O and H isotopes. *Journal of African Earth Sciences* 147, 68-77
- Schier, K., Bau, M., Münker, C., Beukes, N., & Viehmann, S. (2018). Trace element and Nd isotope composition of shallow seawater prior to the Great Oxidation Event: Evidence from stromatolitic bioherms in the Paleoproterozoic Rooinekke and Nelani Formations, South Africa. *Precambrian Research*, 315, 92-102.
- Siahi, M., Hofmann, A., Master, S., Wilson, A. and Mayr, C. (2018). Trace element and stable (C, O) and radiogenic (Sr) isotope geochemistry of stromatolitic carbonate rocks of the Mesoarchaeic Pongola Supergroup: Implications for seawater composition. *Chemical Geology*, 476, 389-406.
- Simonson, B. M., Beukes, N. J., & Biller, S. (2018). Extending the paleogeographic range and our understanding of the Neoproterozoic Monteville impact spherule layer (Transvaal Supergroup, South Africa). *Meteoritics & Planetary Science*, 1-24.

- Sun, J., Tappe, S., Kostrovitsky, S.I., Liu, C-Z, Skuzovatov, S.Y. and Wu, F-Y. (2018). Mantle sources of kimberlites through time: A U-Pb and Lu-Hf isotope study of zircon megacrysts from the Siberian diamond fields. *Chemical Geology*, 479, 228-240.
- Tappe, S., Dongre, A., Liu, C-Z and Wu, Fu-Y. (2018). 'Premier' evidence for prolonged kimberlite pipe formation and its influence on diamond transport from deep Earth. *Geology*, 46, 843-846.
- Tappe, S., Smart, K.A., Torsvik, T., Massuyeau, M. and de Wit, M. (2018). Geodynamics of kimberlites on a cooling Earth: Clues to plate tectonic evolution and deep volatile cycling. *Earth and Planetary Science Letters*, 484, 1-14.
- Topper, T. P., Greco, F., Hofmann, A., Beeby, A., and Harper, D. A. (2018). Characterization of kerogenous films and taphonomic modes of the Sirius Passet Lagerstätte, Greenland. *Geology*, 46, 359-362
- Vafeas, N.A., Blignaut, L.C. and Viljoen, K.S. (2018). Mineralogical characterisation of the thrust manganese ore above the Blackridge Thrust Fault, Kalahari Manganese Field: The footprint of the Mukulu Enrichment. *Island Arc*, DOI: 10.1111/iar.12280.
- Vafeas, N.A., Blignaut, L.C., Meffre, S. and Viljoen, K.S. (2018). New evidence for the early onset of supergene alteration along the Kalahari unconformity. *South African Journal of Geology*, 121(2), 175-188. DOI: <https://doi.org/10.25131/sajg.121.0012>.
- Vafeas, N.A., Viljoen, K.S. and Blignaut, L.C. (2018). Characterisation of fibrous cryptomelane from the todorokite-cryptomelane mineral assemblage at the Sebilo mine, Northern Cape Province, South Africa. *The Canadian Mineralogist*, 56, 1-12.
- Viljoen, K.S., Perritt, S.H. and Chinn, I.L. (2018). An unusual suite of eclogitic, websteritic and transitional websteritic-Iherzolitic diamonds from the Voorspoed kimberlite in South Africa: Mineral inclusions and infrared characteristics. *Lithos*, 320-321, 416-434. <https://doi.org/10.1016/j.lithos.2018.09.034>
- Wabo, H., Maré, L. P., Beukes, N. J., Kruger, S. J., Humbert, F. and de Kock, M. O. (2018). Mineral transformations during thermal demagnetization of sideritic jasper mesobands in jaspilites of the ~ 3.25 Ga Fig Tree Group in the Barberton Greenstone Belt, Kaapvaal craton (South Africa). *South African Journal of Geology* 2018, 121(2), 131-140.
- Wagner, N.J. and Matiane, A. (2018). Rare earth elements in select Main Karoo Basin (South Africa) coal and coal ash samples. *International Journal of Coal Geology*. Vol 196, 82-92. ISSN 01665162.
- Wang, X., Planavsky, N.J., Hofmann, A., Saupe, E.E., De Corte, B.P., Philippot, P., LaLonde, S.V., Jemison, N.E., Zou, H., Ossa Ossa, F.O., Tsikos, H. and Rybacki, K. (2018). A Mesoarchean shift in uranium isotope systematics. *Geochimica et Cosmochimica Acta*, 238, 438-452.
- Wilmeth, D. T., Corsetti, F. A., Beukes, N. J., Awramik, S. M., Petryshyn, V., Spear, J. R., & Celestian, A. J. (2019). Neoproterozoic lacustrine stromatolite deposits in the Hartbeesfontein Basin, Ventersdorp Supergroup, South Africa: Implications for oxygen oases. *Precambrian Research*, 320, 291-302.

Conference Proceedings, 2018

- Abraham, R. and Wagner, N.J. (2018). Carbon dioxide adsorption behaviour of geological samples from the Karoo Basin, South Africa. *Geocongress 2018*, 17 – 20 July, 2018, University of Johannesburg, South Africa.
- Agangi, A., Hofmann, A., Paprika, D. and Bekker, A. (2018). Terrestrial life colonised Mesoarchean volcanic caldera lakes on the Kaapvaal craton. *Geocongress 2018*, 17 – 20 July, 2018, University of Johannesburg, South Africa.
- Ali, L., Khattak, S., Mouri, H., Tariq, M. and Mehmood, M. (2018) Geological Control of High Fluoride Concentrations in Drinking Water and its Health Impacts: A Case Study From the District Swabi, Khyber Pakhtunkhwa Pakistan. *EGU General Assembly Conference Abstracts* 20, 11712
- Andersen, T. and Elburg, M.A. (2018). Contrasting behaviour of Zr and Ti in highly alkaline magmas: The White and Green Foyaite in the Pilanesberg complex, South Africa. *Geocongress 2018*, 17 – 20 July, 2018, University of Johannesburg, South Africa.
- Andersen, T. and Elburg, M.A. (2018). The South African detrital zircon record: Recycling of clastic sediments since the late Mesoproterozoic. *Geocongress 2018*, 17 – 20 July, 2018, University of Johannesburg, South Africa
- André, L., Abraham, K., Foley, S. and Hofmann, A. (2018). Heavy $\delta^{30}\text{Si}$ in Archean Granitoids as Evidence for Supracrustal Components in their Sources. *Goldschmidt Conference 2018*, 12-17 August, Boston, USA.
- Aulbach, S., Woodland, A., Prokopyi, V. and Viljoen, F. (2018). Redox state of deeply subducted ancient oceanic crust. *Abstracts Goldschmidt 2018*, 12-17 August, Boston, U.S.A.
- Badenhorst, C., Wagner, N., Valentim, B. and Viljoen, F. (2018). Fifty Shades of Grey: The extraction of char from a variety of coal ash for consideration as synthetic graphite. *70th Annual Meeting of the International Committee for Coal and Organic Petrology*, 23 – 29 September, Brisbane, Australia, p. 21.
- Badenhorst, C., Wagner, N.J., Viljoen, F. and Valentim, B. (2018). Char extracted from coal ash as a replacement for natural graphite – Charphite. *Geocongress 2018*, 17 – 20 July, 2018, University of Johannesburg, South Africa.





- Ballouard, C., Elburg, M.A., Tappe, S. and Knoper, M. (2018). Magmatic-hydrothermal evolution of LCT pegmatites from the Orange River pegmatite belt, South Africa: Implications for rare metal and Li metallogeny. *Geocongress 2018*, 17 – 20 July, 2018, University of Johannesburg, South Africa.
- Beukes, N.J. and McCarthy, T.S. (2018) Stratigraphy and sedimentology of the Transvaal Supergroup in the Philippolis outlier below Karoo cover in the southern Free State: Implications for original basin size and geometry. *Geocongress 2018*, 17 – 20 July, 2018, University of Johannesburg, South Africa.
- Bindeman, I., Zakharov, D., Greber, Nn, Dauphas, N., Retallack, G., Hofmann, A., Lackey, J.S. and Bekker, A. (2018). Triple oxygen isotopes in shales through time: Rapid emergence of subaerial landmasses at 2.5Ga. *Goldschmidt Conference 2018*, 12-17 August, Boston, USA.
- Blignault, L., Viljoen, K., Tsikos, H. and Elburg, M. (2018). Boron isotope and REE signatures and their sources in high grade manganese ores of the Kalahari manganese field, South Africa. *International Mineralogical Association 22nd Meeting*. 13-17 August 2018, Melbourne, Australia.
- Blignaut, C., Viljoen, K.S., Elburg, M. and Tsikos, H. (2018). Boron isotope and REE signatures and their sources in manganese ores of the Kalahari Manganese field. *Goldschmidt Conference 2018*, 12-17 August, Boston, USA.
- Brüske, A., Albut, G., Schuth, S., Schoenberg, R., Beukes, N., Hofmann, A. T. Nägler, T. and Weyer, S. (2018). The onset of oxidative weathering traced by uranium isotopes. *Goldschmidt Conference 2018*, 12-17 August, Boston, USA.
- Brüske, A., Albut, G., Schuth, S., Schoenberg, R., Beukes, N., Hofmann, A. T. Nägler, T. and Weyer, S. (2018) Tracing the onset of oxidative weathering with uranium isotopes. *GeoBonn*.
- Bybee, G. M., Owen-Smith, T. M., Hayes, B. and Lehmann, J. (2018). Large, long-lived magmatic systems built by crystal-rich slurries – insights from Proterozoic anorthosites. *Wager and Brown Workshop 2018*, 13th International Platinum Symposium, Polokwane, South Africa.
- Bybee, G. M., Owen-Smith, T. M., Hayes, B., Lehmann, J., Brower, A., Ashwal, L., Corfu, F. and Hill, C. M. (2018). Age and Magmatic Architecture of the Kunene Anorthosite Complex (Angola). *Geocongress 2018*, 17 – 20 July, 2018, University of Johannesburg, South Africa.
- Cairncross, B. and James, K. (2018). Dr David Draper (1849-1929) and the Johannesburg Geological Museum. *Abstract. Geocongress 2018*, 17 – 20 July, 2018, University of Johannesburg, South Africa.
- Djeutchou, C., Wabo, H. and De Kock, M.O. (2018). New paleomagnetic results from mafic dykes in the Badplaas area in the Mpumalanga Province. *Geocongress 2018*, 17 – 20 July, 2018, University of Johannesburg, South Africa.
- Djeutchou, C., De Kock, MO and Wabo, H. (2018). New key paleomagnetic pole for the 1.8 Ga Kaapvaal craton: implications for Paleoproterozoic apparent polar wander and paleogeographic reconstructions. *American Geophysical Union Fall Meeting*, Washington D.C., USA, 10-14 December 2018.
- Elburg, M.A. and Andersen, T. (2018). Controls on peralkalinity in the Pilanesberg Complex. *Geocongress 2018*, 17 – 20 July, 2018, University of Johannesburg, South Africa.
- Elburg, M.A., Kristoffersen, M. and Andersen, T. (2018). Contrasting quality of detrital zircon in samples from the Witwatersrand Supergroup. *Geocongress 2018*, 17 – 20 July, 2018, University of Johannesburg, South Africa.
- Ficq, G., Tappe, S., Bolhar, R., Wilson, A. and Harris, C. (2018). Age, origin and alteration of Archaean mafic-ultramafic layered intrusions in the Barberton Greenstone Belt: New evidence from Stolzburg. *Geocongress 2018*, 17 – 20 July, 2018, University of Johannesburg, South Africa.
- Geel, C., Bordy, E.M., Nolte, S., Schulz, H-M. and Beukes, N. (2018) Geochemical and petrophysical analysis of the Permian lower Ecca Group, Karoo Basin, South Africa. *Geocongress 2018*, 17 – 20 July, 2018, University of Johannesburg, South Africa.
- Gevera, P., Mouri, H. and Maronga G., (2018) High fluoride and dental fluorosis prevalence: A case study from Nakuru area, The Kenyan Rift Valley. *EGU General Assembly Conference Abstracts 20*, 1422
- Hayes, B., Lehmann, J., Bybee, G. M. and Owen-Smith, T.M. (2018) Manufacturing xenocrysts by squeezing melt out of syn-tectonic granitoids. *10th Igneous and Metamorphic Studies Group Conference (IMSG 2018)*, 14 – 17 January, Cape Town, South Africa.
- Hofmann A., Anhaeusser C., Dixon J., Kröner A., Saha L., Wilson A. and Xie H. (2018). Archaean granitoid-greenstone geology of the south-eastern part of the Kaapvaal Craton. *Geocongress 2018*, 17 – 20 July, 2018, University of Johannesburg, South Africa.

- Humbert, F. and Elburg, M.A. (2018). Geochemical comparisons of Mesoarchean to Present mafic igneous units in the Kaapvaal craton. Geocongress 2018, 17 – 20 July, 2018, University of Johannesburg, South Africa.
- Huthmann, F., Yudovskaya, M., Kinnaird, J.A., McCreesh, M., McDonald, I. and Elburg, M. (2018). The Waterberg Pd-Pt Deposit: A comprehensive overview. 13th International Platinum Symposium, Polokwane, South Africa. 30th June – 6th July, 2018.
- Izon, G., Ono, S., Beukes, N. and Summons, R. (2018) (Re)defining the Structure of the Great Oxidation Event. Goldschmidt Conference 2018, 12-17 August, Boston, USA.
- Jacobs, J., Läufer, A., Ruppel, A., Elvevold, S., Eagles, G., Jokat, W. and Elburg, M.A. (2018). United plates of Dronning Maud Land revealed by connecting geology & geophysics. Scientific Committee on Antarctic Research (SACR) Open Science Conference 2018, 15-26 June, Davos, Switzerland.
- Jacobs, J., Läufer, A., Ruppel, A., Elvevold, S., Eagles, G., Jokat, W. and Elburg, M.A. (2018): Connecting geology and geophysics (CGG): Delineation and characterisation of major tectonic provinces in Dronning Maud Land, East Antarctica, and significance for Gondwana assembly. European Geosciences Union General Assembly 2018, 8-13 April 2018, Vienna, Austria.
- Jodder J., Hofmann A., Xie H., Wilson A. and Butler M (2018). Decoding the Palaeoarchean record of the Daitari greenstone belt, India: a quest for early life. Geocongress 2018, 17 – 20 July, 2018, University of Johannesburg, South Africa.
- Kambunga, S., Mouri, H., Candeias, C. and Hasheela, I., (2018) Geophagy during pregnancy and its possible health impact, case study: Onangama village, northern Namibia. EGU General Assembly Conference Abstracts 20, 1141
- Kramers, J.D. (2018). Palaeoclimatic data and thoughts on H. sapiens migration. Second UJ Palaeo-Research symposium, Johannesburg, 1st November 2018.
- Kramers, J.D., Belyanin, G.A., Przybyłowicz, W. and Andreoli, M.A.G. (2018). The Hypatia stone, a space-time capsule with the fingerprint of an interstellar cloud. Geocongress 2018, 17 – 20 July, 2018, University of Johannesburg, South Africa.
- Kristoffersen, M., Elburg, M.A., Watkeys, M. and Andersen, T. (2018). The curious case of the missing Archaean. Geocongress 2018, 17 – 20 July, 2018, University of Johannesburg, South Africa.
- Kuhn, B.F., Gommery, D., Kgasi, L. (2018) The carnivore guild of Bolt's Farm, South Africa: Carnivore biodiversity in the Plio-Pleistocene. 5th International Palaeontological Congress, Paris, France.
- Kuhn, B.F., Randolph-Quinney, P. (2018) The southern boundary of Australopithecus africanus: are the Buxton-Norlim Limeworks a false boundary for early hominins? 5th International Palaeontological Congress, Paris, France.
- Kwayisi, D., Lehmann, J. and Elburg, M. (2018) Geology of the Buem Ophiolite: A record of accretionary tectonics during the Pan-African orogeny. American Geophysical Union Fall Meeting, Washington D.C., USA, 10-14 December 2018.
- Kwayisi, D., Lehmann, J. and Elburg, M.A. (2018). The Buem Ophiolite and Its Implication to the evolution of the Pan-African Dahomeyide Orogen, West Africa. Geocongress 2018, 17 – 20 July, 2018, University of Johannesburg, South Africa.
- Lehmann, J., Bybee, G. M., Hayes, B., Owen-Smith, T. M. and Brower, A. (2018). Emplacement mechanisms of the Kunene Anorthosite Complex, Angola, in the frame of the Kibaran orogenic system. Geocongress 2018, 17 – 20 July, 2018, University of Johannesburg, South Africa.
- Lehmann, J., Bybee, G.M., Hayes, B. and Owen-Smith, T.M. (2018). A Mesoproterozoic cordilleran orogen recorded by the Kunene Anorthosite Complex in Angola. American Geophysical Union Fall Meeting, Washington DC, USA, 10-14 December 2018.
- Lehmann, J., Bybee, G.M., Hayes, B. and Owen-Smith, T.M. (2018). Emplacement mechanisms of the Kunene Anorthosite Complex, Angola, in the frame of the Kibaran orogenic system. Crustaman Conference, Prague, Czech Republic, August 2018.
- Luskin, C., De Kock, M.O., and Wabo, H. (2018). Paleomagnetic results of the Mesoarchean Pongola Supergroup Nsuze Large Igneous Province and a primary Post-Pongola Pole, Kaapvaal Craton, Southern Africa. American Geophysical Union Fall Meeting, Washington D.C., USA, 10-14 December 2018.
- Luskin, C., De Kock, M.O. and Wabo, H. (2018). Paleomagnetic results of volcanics of the Pongola Supergroup, Kaapvaal Craton. Geocongress 2018, 17 – 20 July, 2018, University of Johannesburg, South Africa.
- Luskin, C., De Kock, M.O., Djetchou, C. and Wabo, H. (2018). Multiplot: A program for visualizing and diagramming paleomagnetic data. Geocongress 2018, 17 – 20 July, 2018, University of Johannesburg, South Africa.
- Mangs, A.D., Wagner, N.J. and Lar, U.A. (2018). The petrography, mineralogy and geochemistry of coal within the Benue Trough of Nigeria. Geocongress 2018, 17 – 20 July, 2018, University of Johannesburg, South Africa.
- Maponga, O., Falcon, R. and Wagner, N. (2018). The importance of the Karoo System to Zimbabwe's economy with particular reference to the Hwange Coal Basin, Zimbabwe. Geocongress 2018, 17 – 20 July, 2018, University of Johannesburg, South Africa.





- Mashiane, M., Elburg, M. Billay, A., Mutele, L. (2018). Potential for critical metals in the Upper Zone of the Rustenburg Layered Suite. Geocongress 2018, 17 – 20 July, 2018, University of Johannesburg, South Africa.
- Massuyeau, M.G.J., Tappe, S. and Viljoen, F. (2018). A thermodynamic model with CO₂ and H₂O for the lithosphere-asthenosphere boundary beneath thick continental roots. Abstracts 16th International Conference on Experimental Mineralogy, Petrology and Geochemistry, 17 – 21 June 2018, Clermont-Ferrand, France, p. 94.
- Mkhathshwa, S., Viljoen, K.S., Guy, B. and Smith, A. (2018). A process mineralogical characterisation of the UE1A, A1, A5 and E9EC reefs at Cooke mine, Randfontein, South Africa. Geocongress 2018, 17 – 20 July, 2018, University of Johannesburg, South Africa.
- Mokwena, L., Wagner, N., and Kolker, A. (2018). The occurrence of chromium and other trace elements in selected South African coals. Geocongress 2018, 17 – 20 July, 2018, University of Johannesburg, South Africa.
- Moroeng, M.O., Wagner, N.J. and Roberts, R.J. (2018). Using geochemistry to understand the origin of certain inertinite macerals in a South African coal from the Witbank Coalfield. Geocongress 2018, 17 – 20 July, 2018, University of Johannesburg, South Africa.
- Moshupya, P. Abiye, T., Mouri, H. and Levin, M. (2018) The uranium and radon gas concentration and impact on human health: A case from abandoned gold mine tailings in the West Rand area, Krugersdorp, South Africa EGU General Assembly Conference Abstracts 20, 4661
- Mouri, H. (2018) The relevance of Medical Geology in Africa: some examples. EGU General Assembly Conference Abstracts 20, 1769
- Ngobeli, R., Vorster, C., Beukes, N., Frei, D. and Elburg, M. (2018). Detrital zircon ages as young as 2,22Ga in the Makganyene Diamictite versus a 2,42Ga baddeleyite age of the conformably overlying Ongeluk Lava, Postmasburg Group, Transvaal Supergroup: Urgent resolution required. Geocongress 2018, 17 – 20 July, 2018, University of Johannesburg, South Africa.
- Nunoo, S. and Hofmann, A. (2018). Gold mineralization within the Collette and Kjersti deposits of the Julie belt, northwest Ghana. Geocongress 2018, 17 – 20 July, 2018, University of Johannesburg, South Africa.
- Nxumalo, V., Vorster, C., Kramers, J. and Cairncross, B. (2018). Preliminary detrital zircon age data from the Karoo Supergroup of the Springbok Flats Basin, South Africa: An extensive provenance study. Geocongress 2018, 17 – 20 July, 2018, University of Johannesburg, South Africa.
- Okereafor, G., Makhatha, E., Mouri, H. and Mavumengwana, V. (2018) Assessment of the impacts of mine tailings from a South African Gold Mine: An example from Blesbokspruit Conservation Trust, Springs, Ekurhuleni. EGU General Assembly Conference Abstracts 20, 18362
- Ormond, R., Lehmann, J., Belyanin, G. (2018). How and when did the Johannesburg Dome form? American Geophysical Union Fall Meeting, Washington D.C., USA, 10-14 December 2018.
- Owen-Smith, T. M., Bybee, G. M., Hayes, B., and Lehmann, J. (2018) Proterozoic massif-type anorthosites—the archetype of long-lived magmatic systems. American Geophysical Union Fall Meeting, Washington D.C., USA, 10-14 December 2018.
- Owen-Smith, T.M. and Ashwal, L.D. (2018). Multiple mingling magma mushes? Petrogenesis of the Doros Gabbroic Complex, Namibia. Wager & Brown Workshop, Polokwane, South Africa, 27-30 June 2018.
- Owen-Smith, T.M., Bybee, G.M., Hayes, B., Lehmann, J. and Mothabela, N. (2018). Proterozoic massif-type anorthosites—the archetype of long-lived magmatic systems. American Geophysical Union Fall Meeting, Washington DC, USA, 10-14 December 2018.
- Owen-Smith, T.M., Keiding, J.K. and Trumbull, R.B. (2018). Olivine-hosted melt inclusions from the Doros Complex, Namibia: Insights (and pitfalls) for interpreting parental magma compositions. 10th Annual Meeting of the Igneous and Metamorphic Study Group, University of the Western Cape, South Africa, 14-17 January 2018.
- Paprika D., Agangi A. and Hofmann A. (2018). The Mesoarchaeon Dominion Group in the Ottosdal area, South Africa. Geocongress 2018, 17 – 20 July, 2018, University of Johannesburg, South Africa.
- Pretorius, C., Mouri, H., Cave, M. and Pienaar, J. (2018) The possible geological sources of chronic copper poisoning of sheep in some specific farms of the Karoo Basin, South Africa. EGU General Assembly Conference Abstracts 20, 19831
- Randolph-Quinney, P., Kuhn, B., Kruger, A., Sinclair, A.G.M. (2018) Landscape archaeology of the Makapansgat region, Limpopo, South Africa: historical approaches and future directions. 15th Congress of the Pan-African Archaeological Association, Rabat, Morocco.

- Sanyaolu, O., Mouri, H., Odukoya, A., and Selinus, O. (2018). A possible geogenic cause of goiter occurrence in the coastal environment of SW Nigeria: a case study from, Badagry, Lagos. EGU General Assembly Conference Abstracts 20, 1151
- Sauer, M. and Elburg, M. (2018). Apatite mineralisation of the Northern Pyroxenite, Phalaborwa Complex, South Africa: Petrogenetic processes. Geocongress 2018, 17 – 20 July, 2018, University of Johannesburg, South Africa.
- Singo, N.K.(2) and Kramers, J.D. (2018). Discovery of white asbestos (chrysotile) in unrehabilitated dumps and soils at the abandoned Nyala magnesite mine, Limpopo Province. Proceedings of the 6th International Mining and Industrial Waste Management Conference, 29, 30 & 31st October, 2018, Polokwane, Limpopo, 6pp.
- Sito, W.M., Owen-Smith, T.M., Bybee, G.M. and Tappe, S. (2018). New age and compositional constraints on mafic to ultramafic intrusions of SW Angola and implications for the geology of the region. Geocongress 2018, 17 – 20 July, 2018, University of Johannesburg, South Africa.
- Sito, W.M., Owen-Smith, T.M., Bybee, G.M. and Tappe, S. (2018). New age and compositional constraints on mafic to ultramafic intrusions of SW Angola and implications for the geology of the region. American Geophysical Union Fall Meeting, Washington DC, USA, 10-14 December 2018.
- Sito, W.M., Owen-Smith, T.M., Bybee, G.M. and Tappe, S. (2018). The petrology and economic potential of mafic-ultramafic satellite intrusions to the Kunene Anorthosite Complex. 10th Annual Meeting of the Igneous and Metamorphic Study Group, University of the Western Cape, South Africa, 14-17 January 2018. [Oral]
- Sluzhenikin, M.A., Costin, S.F., Shatagin, G., Dubinina, K.N., Grobler, E.O., D.F., Ueckermann, H. and Kinnaird, J.A. (2018). Assimilation by ultramafic melts of the Bushveld Complex, and its consequences to petrology and mineralization. Society of Economic Geologists: Metals, Mineral and Society 2018 Conference. 22 -25 September, Keystone, Colorado, USA.
- Smart, K.A., Cartigny, P., Tappe, S., O'Brien, H. and Klemme, S. (2018). Reduced volatile sources for Karelian diamonds linked to punctuated ultramafic magmatism. Goldschmidt Conference 2018, 12-17 August, Boston, USA.
- Smart, K.A., Tappe, S., Ishikawa, A., Pfänder, J.A., Stracke, A. (2018). Remelting of the fossil Ontong Java Plateau plume head, with clues to Archean continent formation. American Geophysical Union Fall Meeting, Washington D.C., USA, 10-14 December 2018.
- Smith, A.J.B. and Beukes, N.J. (2018). Free oxygen and microbial activity in Mesoarchean oceans: a sequence stratigraphic case study of the iron-rich units of the Witwatersrand-Pongola basin of southern Africa. European Geosciences Union General Assembly 2018, 8-13 April 2018, Vienna, Austria.
- Smith, A.J.B. and Beukes, N.J. (2018). Free oxygen in Mesoarchean oceans: geological evidence from the iron-rich units of the Witwatersrand-Pongola basin of southern Africa. Geocongress 2018, 17 – 20 July, 2018, University of Johannesburg, South Africa.
- Smith, A.J.B., Beukes, N.J., Gutzmer, J., Johnson, C.M., Czaja, A.D., De Beer, F., Hoffman, J. and Nhleko, N. (2018). Assessing a Mesoarchean granular iron formation from southern Africa using 3D X-ray computed tomography (μ XCT). Geocongress 2018, 17 – 20 July, 2018, University of Johannesburg, South Africa.
- Solanki, A.M., Tappe, S., Stracke, A., Magna, T. and Wilson, A. (2018). The kimberlite – MARID metasoma link: New conflicting evidence. American Geophysical Union Fall Meeting, Washington D.C., USA, 10-14 December 2018.
- Tappe, S., Smart, K.A., Torsvik, T., Massuyeau, M., Stracke, A., Budde, G. and Kleine, T. (2018). A plate tectonic origin of kimberlites on a cooling Earth. American Geophysical Union Fall Meeting, Washington D.C., USA, 10-14 December 2018.
- Vilakazi, N., Kgasi, L., Gommery, D., Sénégas, F., Brink, J., Thackeray, F., Kuhn, B. (2018) Bolt's farm Cave System (Cradle of Humankind-South Africa) from 1936 to 2018. 5th International Palaeontological Congress, Paris, France.
- Wabo, H., De Kock, M.O., Vorster, C. and Beukes, N.J. (2018). New geochronological and paleomagnetic results from some sediments of Kaladgi and Bhima sub-basins in India: Implication for timing of deposition. American Geophysical Union Fall Meeting, Washington D.C., USA, 10-14 December 2018.
- Wabo, H., Mare, L.P. and Beukes, N.J. (2018). Application of magnetic geothermometer in Archean rocks: An example from the Barberton Greenstone Belt in South Africa. Geocongress 2018, 17 – 20 July, 2018, University of Johannesburg, South Africa.
- Wagner, N., Phenyra, R., Moroeng, M. and Tabane, X. (2018). Understanding the distribution of sulphur in the No. 2 and 4 Seams of the Ntshovelo Colliery, Witbank Coalfield. Geocongress 2018, 17 – 20 July, 2018, University of Johannesburg, South Africa.
- Wilmeth, D.T., Corsetti, F.A., Berelson, W.M., Beukes, N. J., Awramik, S. M., Petryshyn, V.A., Spear, J.R. and Celestian, A. J. (2018) Rapid rates of oxygenic photosynthesis within Neoproterozoic stromatolites. Abstract #318717. Geological Society of America 130th Annual Meeting, 4 – 7 November, 2018, Indianapolis, USA.
- Wilson A. and Hofmann A. (2018). The Pongola Supergroup Large Igneous Province. Abstract. Geocongress 2018, 17 – 20 July, 2018, University of Johannesburg, South Africa.





SUPPORT STAFF IN PPM AND GEOLOGY



Lisborn Mangwane and Baldwin Tshivhahuvhi: Technical assistants, thin section laboratory.



Daniel Selepe: Technical assistant, field vehicle maintenance.



Thuso Ramaliba: Laboratory Assistant, thin section laboratory.



Herbert Gugwane: Technical assistant, rock preparation laboratory.



Diana Khoza: Finance and transport.



Hennie Jonker: Finance and field schools.



Herbert Leteane: Technical assistant.



Elaine Minnaar: Departmental Secretary.

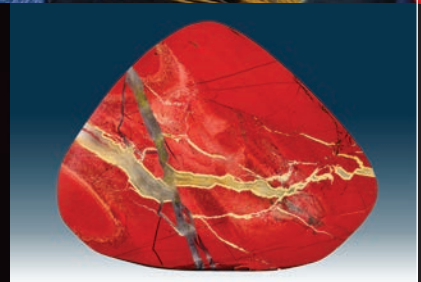
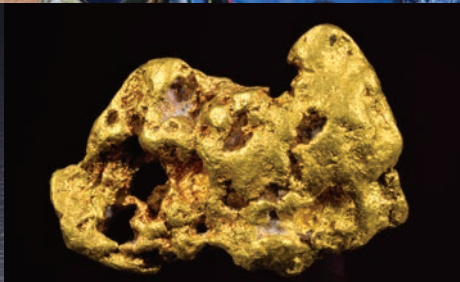
PPM RESEARCH COLLOQUIUM

Date: Friday, 29 March 2019

Venue: Lecture room 215 in C1 Lab Building, Auckland Park Kingsway Campus

Programme of talks to be announced

Time: 9.00 to 16.00 with lunch break, finger lunch will be provided.



SPECTRUM

SPECTRUM, the Central Analytical Facility of the Faculty of Science at UJ, was established in 1999 to serve as a one-stop state-of-the-art unit, managed and staffed to ensure an accessible analytical service not only for UJ staff and students but also for outside cooperation and clients.

SPECTRUM offers comprehensive solutions for a broad range of applications, utilizing modern high-technology equipment. This includes PANalytical X'Pert Pro X ray diffraction (XRD) and Magix Pro X ray fluorescence (XRF) instruments, a Tescan Vega3 scanning electron microscope (SEM) with EDX detector for semiquantitative chemical analysis, a JEOL 733 microprobe, a Spectro ARCOS ICP optical emission spectrometer (OES), a Perkin Elmer NexION 350 ICP quadrupole mass spectrometer (ICP-QMS) for solution analysis, a Varian Unity Inova NMR system, and Zeiss Axioplan 2 compound and Zeiss Discovery stereo microscopes.



Argon extraction and mass spectrometer



Electron microprobe



Laser ablation ICP-MS



Laser ablation multicollector ICP-MS

SPECIALIZED GEOSCIENCE APPLICATIONS AT SPECTRUM

Other than the more general instrumentation at SPECTRUM mentioned above, the facility also houses five units (two of them unique in Africa) geared specifically to Geoscience applications, among them the needs of PPM:

- A FEI Quanta 600F field emission Mineral Liberation Analyzer (MLA). This instrument is the one mainly used in geometallurgical research.
- A CAMECA SX100 electron microprobe with 4 wavelength dispersive spectrometers (WDS) and an energy dispersive spectrometer (EDS), used extensively for in situ micrometer-scale quantitative chemical analysis of minerals in a broad spectrum of projects.
- A ThermoFischer X-Series II ICP quadrupole mass spectrometer coupled to a New Wave UP-213 Nd YAG laser ablation system, as well as a Nu Instruments Nu Plasma II multicollector ICP mass spectrometer, coupled to a Resolution 199 nm excimer laser ablation system, are dedicated to in situ isotope and chemical analysis of minerals on a microscopic scale. The quadrupole system is particularly suited to rapid series of uranium-lead zircon age determinations, for instance in sediments, and trace element geochemical profiling. The multicollector system enables high-precision uranium-lead dating of zircon and other uranium-bearing minerals, as well as high precision isotope ratio analyses on strontium, neodymium, hafnium and many other elements, from both laser ablation and samples in solution.
- A MAP-215 noble gas mass spectrometer coupled to an ultra-high vacuum gas extraction system using a continuous 1064 nm Nd-YAG laser as a heat source. This is the only functional unit of its kind in Africa and is chiefly used for both $^{40}\text{Ar}/^{39}\text{Ar}$ and (in conjunction with the solution ICP-QMS system) U-Th-He geochronology.
- A paleomagnetic laboratory, likewise unique in Africa. This is equipped with a SQUID magnetometer and a fully automated snake chain sampling system, allowing for rapid and accurate measurements of samples for paleomagnetic studies.



SQUID magnetometer with sample magazine



Solution ICP-MS



X ray diffraction



X ray fluorescence

**For further information and cost of services please contact: Dr Willie Oldewage,
Tel: 011 559 2274; Fax: 011 559 3361; e-mail: willieho@uj.ac.za**